

1994

# Cooperative binding by a self-assembled receptor: metal in a structural and functional role

Jin-ho Lee  
*Iowa State University*

Follow this and additional works at: <https://lib.dr.iastate.edu/rtd>

 Part of the [Biochemistry Commons](#), [Inorganic Chemistry Commons](#), and the [Organic Chemistry Commons](#)

## Recommended Citation

Lee, Jin-ho, "Cooperative binding by a self-assembled receptor: metal in a structural and functional role " (1994). *Retrospective Theses and Dissertations*. 10493.  
<https://lib.dr.iastate.edu/rtd/10493>

This Dissertation is brought to you for free and open access by the Iowa State University Capstones, Theses and Dissertations at Iowa State University Digital Repository. It has been accepted for inclusion in Retrospective Theses and Dissertations by an authorized administrator of Iowa State University Digital Repository. For more information, please contact [digirep@iastate.edu](mailto:digirep@iastate.edu).

## INFORMATION TO USERS

This manuscript has been reproduced from the microfilm master. UMI films the text directly from the original or copy submitted. Thus, some thesis and dissertation copies are in typewriter face, while others may be from any type of computer printer.

**The quality of this reproduction is dependent upon the quality of the copy submitted.** Broken or indistinct print, colored or poor quality illustrations and photographs, print bleedthrough, substandard margins, and improper alignment can adversely affect reproduction.

In the unlikely event that the author did not send UMI a complete manuscript and there are missing pages, these will be noted. Also, if unauthorized copyright material had to be removed, a note will indicate the deletion.

Oversize materials (e.g., maps, drawings, charts) are reproduced by sectioning the original, beginning at the upper left-hand corner and continuing from left to right in equal sections with small overlaps. Each original is also photographed in one exposure and is included in reduced form at the back of the book.

Photographs included in the original manuscript have been reproduced xerographically in this copy. Higher quality 6" x 9" black and white photographic prints are available for any photographs or illustrations appearing in this copy for an additional charge. Contact UMI directly to order.



University Microfilms International  
A Bell & Howell Information Company  
300 North Zeeb Road, Ann Arbor, MI 48106-1346 USA  
313/761-4700 800/521-0600



Order Number 9503578

**Cooperative binding by a self-assembled receptor: Metal in a structural and functional role**

Lee, Jin-ho, Ph.D.

Iowa State University, 1994

**U·M·I**  
300 N. Zeeb Rd.  
Ann Arbor, MI 48106



Cooperative binding by a self-assembled receptor:  
metal in a structural and functional role

by

Jin-ho Lee

A Dissertation Submitted to the  
Graduate Faculty in Partial Fulfilment of the  
Requirements for the Degree of  
DOCTOR OF PHILOSOPHY

Department: Chemistry  
Major: Organic Chemistry

Approved:

Signature was redacted for privacy.

---

In Charge of Major Work

Signature was redacted for privacy.

---

For the Major Department

Signature was redacted for privacy.

---

For the Graduate College

Iowa State University  
Ames, Iowa

1994

## **DEDICATION**

To my wife Eunkyung, my parents and parents-in-law

## TABLE OF CONTENTS

ABBREVIATIONS	iv
INTRODUCTION	i
RESULTS AND DISCUSSION	17
Design and Synthesis of Receptor	17
Molecular design of receptor	17
Synthesis of 4,4'-(hydroxyphosphinylidene) bis-L-phenylalanine (PBP)	20
Qualitative Binding Study with Carrier-mediated Transport	23
Structural Studies of Receptor	36
Potentiometric titration	36
Protonation constants of $H_4PBP^+$	38
Stability constants of $Co^{2+}$ complexes with $PBP^{-3}$	44
Paramagnetic susceptibility	50
Electrospray mass spectroscopy	54
Fluorescence spectra	60
Quantitative Binding Studies with $^1H$ NMR.	62
Other Properties of Receptor	75
Enantioselectivity in host-guest complexation	75
Circular Dichroism spectra	77
Catalytic effect of $Co_2PBP_2$ on the hydrolysis of esters	82
CONCLUSION	87
EXPERIMENTAL SECTION	90
REFERENCES	105
ACKNOWLEDGMENTS	113



**ABBREVIATIONS**

$\chi$	mass susceptibility
CAC	critical aggregation concentration
cal'd	calculated
Co <sub>2</sub> PBP <sub>2</sub>	bis[4,4'-(hydroxyphosphinylidene) bis-L-phenylalanine] cobalt(II)]
conc.	concentrated
d	doublet (NMR)
dd	doublet of doublet (NMR)
DSS	2,2-dimethyl-2-silapentane-5-sulfonate
EDTA	ethylenediamine tetraacetate
EM	effective molarity
Et <sub>2</sub> O	diethyl ether
EtOAc	ethyl acetate
EtOH	ethyl alcohol
HLADH	horse liver alcohol dehydrogenase
HOAc	acetic acid
HPLC	high performance liquid chromatography
J	coupling constant (NMR)
K <sub>ai</sub>	macroscopic protonation constant
K' <sub>ai</sub>	microscopic protonation constant
K <sub>D</sub>	dissociation constant
K <sub>i</sub>	macroscopic stability constant
K' <sub>i</sub>	microscopic stability constant

m	multiplet (NMR)
M2PBP2	bis[4,4'-(hydroxyphosphinyldene) bis-L-phenylalanine} transition metal(II)]; transition metal: Mn <sup>2+</sup> , Fe <sup>2+</sup> , Co <sup>2+</sup> , Ni <sup>2+</sup> , Cu <sup>2+</sup> , Zn <sup>2+</sup> , Cd <sup>2+</sup> .
MEK	methyl ethyl ketone
MeOH	methyl alcohol
Me <sub>6</sub> tren	tris(2-dimethylaminoethyl)amine
μ <sub>M</sub>	effective magnetic moment
mp	melting point
MS	mass spectrometry
NAD	nicotinamide adenine dinucleotide
NMR	nuclear magnetic resonance
PBP	4,4'-(hydroxyphosphinyldene) bis-L-phenylalanine
Ph <sub>3</sub> P	triphenylphosphine
q	quartet (NMR)
s	singlet (NMR)
sat'd	saturated
t	triplet (NMR)
t-Boc	tert-butyloxycarbonyl
THF	tetrahydrofuran
TLC	thin layer chromatography
TMS	tetramethyl silane
tren	tris(aminoethyl)amine

## INTRODUCTION

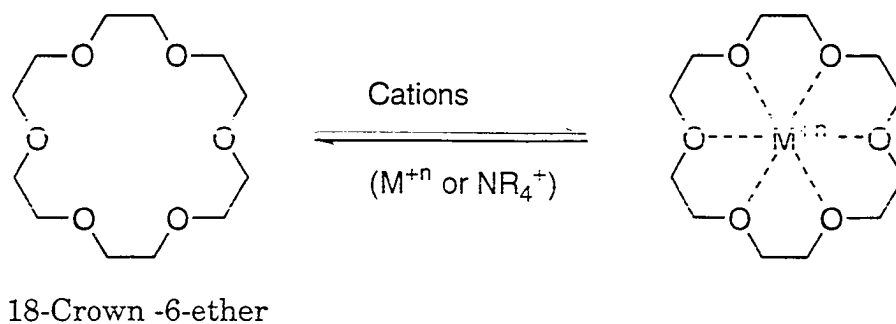
Supramolecular chemistry is the chemistry of the intermolecular bond and involves a study of the structure and function of the complexes formed by association of two or more chemical species. It has developed very rapidly and it has three basic aspects: molecular recognition, supramolecular reactivity and catalysis, and transport processes. It is an interdisciplinary field of science covering the chemical, physical and biological features of chemical species held together and organized by means of intermolecular non-covalent bonding interactions. It projects roots into organic chemistry and the synthetic procedures for receptor construction, into coordination chemistry and metal ion-ligand complexes, into physical chemistry and the experimental and theoretical studies of molecular interactions, and into biochemistry and the biological processes that all start with substrate binding and recognition.

The selective binding of a substrate (guest) by a molecular receptor (host) to form a supermolecule involves molecular recognition. It requires the design of receptors possessing steric and electronic features complementary to those of the substrate to be bound, together with a rigidity/ flexibility balance suitable for the function to be performed. The chemistry of molecular receptors and recognition has become a field of intense activity<sup>1-8</sup>. A great variety of receptor molecules has been designed for effecting the recognition of numerous and very diverse types of substrates (spherical, tetrahedral, linear or branched, charged or neutral, organic, inorganic, or biological, etc.).

Molecular recognition through an inclusion complex began with the use of cyclodextrins.  $\alpha$ -Cyclodextrin is a natural molecule composed of six D-glucose

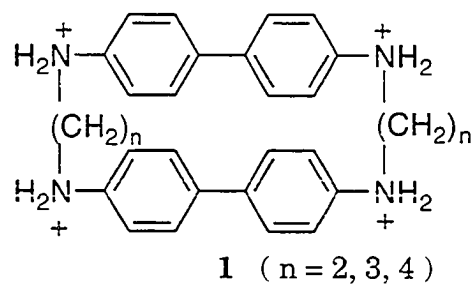
units linked in a 1 $\alpha$ , 4-relationship to form a ring. It functions as a host through the use of its relatively inflexible doughnut shaped structure where the outside has hydrophilic hydroxyl groups while the inside cavity is hydrophobic in nature. Hydrophobic interactions seem to be the most probable driving force for inclusion complex formation. The application of cyclodextrins to biomimetic chemistry was originated by Cramer<sup>9</sup>, followed by Bender<sup>10, 11</sup>, Breslow<sup>12-15</sup>, Tabushi<sup>16-18</sup> and others.<sup>19-22</sup>

Studies in the field of synthetic receptor was triggered by the fundamental discovery of synthetic crown ethers by Pederson<sup>23, 24</sup> and established by remarkable works of Lehn et al.<sup>25-29</sup> and Cram et al.<sup>30-34</sup> and others.<sup>35, 36</sup> They established that efficient and selective receptors for a variety of substrates can be prepared when appropriate amounts of preorganization<sup>34</sup> and complementary between receptors and substrates are designed into synthetic receptors.

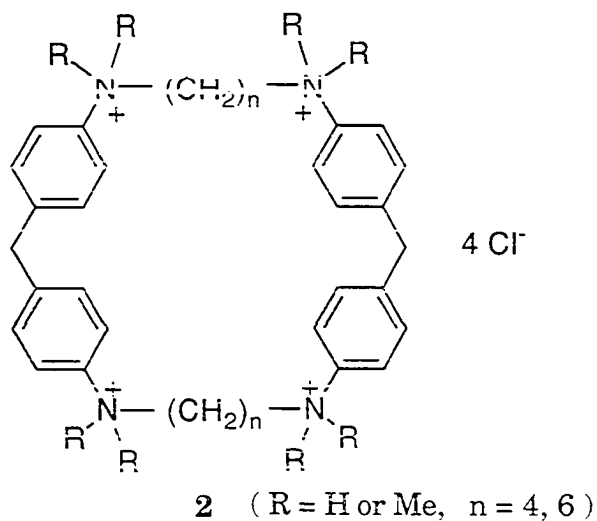


Cyclophane is a water soluble macrocyclic synthetic receptor where solvophobic forces play a major role in binding substrates. Stetter's cyclophanes **1** were the first that were thought to encapsulate benzene or dioxane in the cavity.<sup>37</sup> However X-ray analysis showed that guest intercalated between the cyclophanes in the crystal.<sup>38</sup> The probable reason for the small tendency of

macrocycles to encapsulate lipophilic substrates in spite of matching sizes is the collapse of lipophilic elements in a host which then interferes with the formation of an inclusion complex.



The substitution of biphenyl spacer with diphenylmethane protects against the collapse of hydrophobic cavity by providing a rigid concave shape to the cavity. Koga designed cyclophanes **2** which show complex formation with aromatic guests.<sup>39, 40</sup>



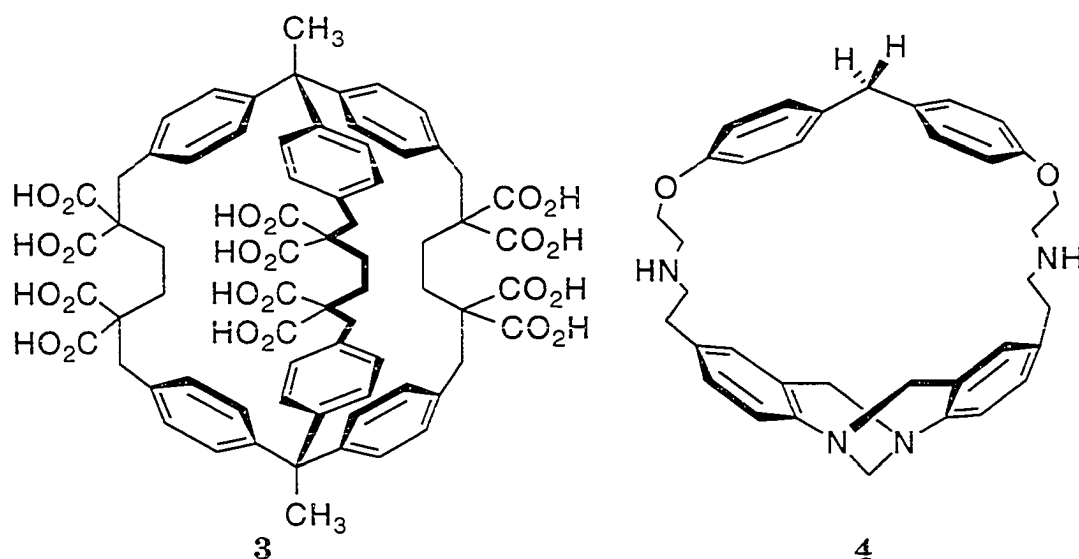
He provided the evidence for the formation of an inclusion complex by means of both  $^1\text{H}$  NMR spectroscopy and X-ray analysis. According to an X-ray crystal structure of the durene-cyclophane complex, durene was completely encapsulated by a hydrophobic cavity of the cyclophane. This critical observation provided the first direct evidence that such cyclophanes do bind guests by encapsulation. In addition, Koga's work established  $^1\text{H}$  NMR spectroscopy as the method for studying the inclusion complexation in solution. The  $^1\text{H}$  NMR method provides not only information about the complex structures but also the thermodynamic parameters of complexation.

The design of efficient cyclophane receptors is guided by two principles that are valid throughout the entire molecular recognition field: (i) the principle of stereoelectronic complementarity between host and guest and (ii) the principle of preorganization of a binding site prior to complexation. The latter, demonstrated by Cram,<sup>34</sup> states that preorganization of a host prior to complexation is an essential factor in controlling association strength. If a host's binding site is not organized, a structural reorganization must occur upon complexation of the guest. This reorganization can cost part of or all of the binding free energy.

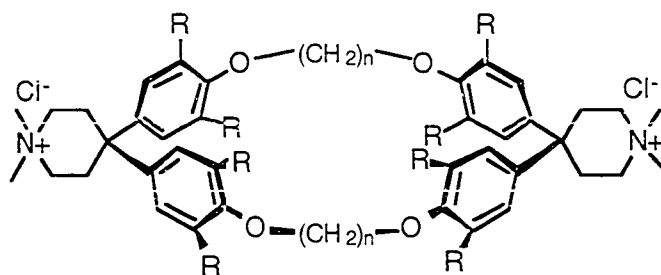
Cyclophanes capable of forming stable inclusion complexes with apolar organic molecules in water possess cavities shaped by lipophilic walls. To generate the cavity binding sites, two or more spacers are connected by bridges having adjustable chain lengths. The length of the bridges between the spacers allows one to adjust the size of the cavity. Water-solubility of the receptors is achieved by introducing a suitable number of charged centers. These are either located in the cavity periphery or at a more remote distance from the binding site.

Four protonated or quaternary ammonium centers at the cavity's

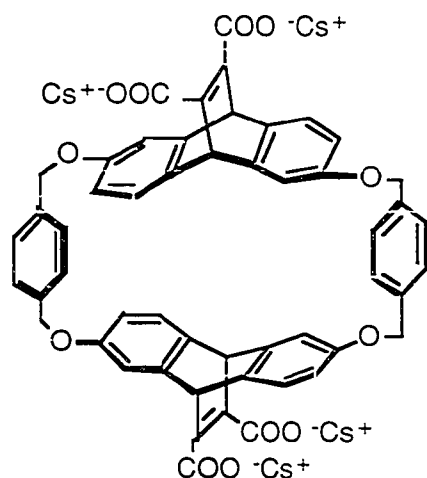
periphery provide water solubility for Koga's cyclophanes **2**. Water solubility is also provided by attaching carboxylate residues to the bridges between two triphenylmethane units in Vögtle's cyclophane **3**.<sup>41</sup> Wilcox introduced derivatives of Tröger's base into macrocycles **4**<sup>42, 43</sup> as rigid chiral spacers. Similar to diphenylmethane units, spacers derived from Tröger's base give flat open binding sites for aromatic rings.



The cationic centers can stabilize complexes of aromatic substrates by participation in effective cation- $\pi$  interactions.<sup>44,45</sup> However, the solvated charged centers in the periphery of the binding sites in the above cyclophanes reduce the driving forces for complexation that result from the desolvation of apolar surfaces.<sup>46</sup> The perturbation of the hydrophobic binding sites by strongly hydrated charged centers has been removed by locating the ionic centers remote from the cavity. Diederich et al. introduced quaternary ammonium centers in a spiro-type arrangement to obtain cyclophanes **5**.<sup>47, 48</sup> and Dougherty et al. used 9,10-bridged 9,10-dihydroanthracene which provide rigid spacers and place the carboxylates at sites remote from the cavity of **3**.<sup>44, 45</sup>



**5** ( R = H or CH<sub>3</sub> )



**6**

The separation of the hydrophilic charged groups and the hydrophobic cavity allows meaningful investigations into the nature and strength of apolar host-guest binding interactions. Also, these studies have established the cation- $\pi$  interaction as one of the driving forces for the complex formation.

The intermolecular interaction in supramolecular chemistry involves several attractive forces: hydrophobic, electrostatic, hydrogen bonding, van der Waals, and charge transfer interactions.<sup>46</sup> Even though determining the predominant interaction in a given host-guest complex is difficult, quantifying non-covalent interactions is important in understanding molecular recognition



processes as well as biological processes.

The most important host-guest interaction in aqueous solution consists of the attraction between lipophilic regions in the host and guest molecules. The hydrophobic effect is caused by the entropy gain through release of water molecules. Prior to association of the lipophilic particles, water solvates the particle surfaces in the form of highly organized solvation shells.<sup>49</sup> While the solvophobic effects increase the stability of supramolecular associations, they lead to a simultaneous reduction in the selectivity of interactions between host and guest molecules.

Electrostatic forces play a central role in molecular association not only with respect to inorganic systems but also in biological phenomena. It also provide a suitable basis for developing organic host-guest complexes. Positive charges are capable of associating with the partially negatively charged  $\pi$ -faces of arenes. The best known example is the edge-to face arene-arene interaction.<sup>50-52</sup> Dougherty et al. have established the dominant influence of cation- $\pi$  interactions in host-guest complexation.<sup>45</sup>

The characteristic feature of the hydrogen bonding interaction is its high directionality. It provides high substrate selectivity and chiral recognition to the host-guest complexation through well designed multiple complementary hydrogen donor-acceptor sites.<sup>8, 53-58</sup>

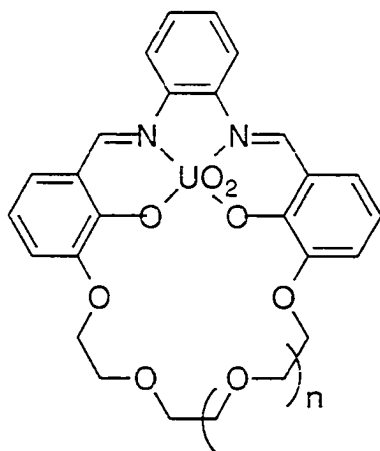
In addition to the understanding of the intermolecular interactions, cyclophanes have been designed as enzyme mimics. The enzyme is a highly efficient catalyst where the mechanisms are generated through the cooperative action of functional groups. The cooperativity in the specific active sites provides catalytic mechanisms such as transition-state binding and stabilization, acid-

base catalysis, nucleophilic and electrophilic catalysis and desolvation. The potential of water-soluble cyclophanes to act as enzyme-like catalysts and to accelerate reactions in supramolecular complexes has been increasingly investigated.<sup>59-62</sup> Although these designed systems are not yet comparable to enzymes in their catalytic efficiency and selectivity, a variety of interesting results have been obtained which demonstrate the potential for future developments in the area of catalytic cyclophanes.

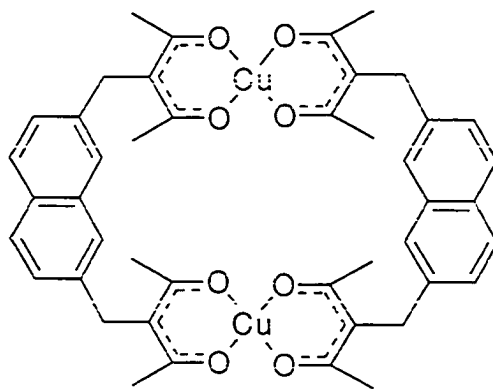
Metal coordination by macrocyclic ligands constitutes the principal activity for early studies on macrocyclic complexes of transition-metal ions. Later, host-guest chemistry extended to the formation of inclusion complexes of a variety of guests within the void or cavity of the host molecule. The union of host-guest chemistry with macrocyclic ligand chemistry has expanded inclusion chemistry to the mimics of metalloenzymes.

Metal ions are known to play important roles in defining the three dimensional structure of native metalloproteins such as DNA-binding zinc finger proteins.<sup>63</sup> Also, they are essential for binding of substrates in metalloenzymes and often activate the complexed guest for subsequent chemical transformation. Therefore, metal ions have been used in designing receptor molecules for neutral guests. Moreover, such metal ions can activate the guest for further chemical transformation in a manner similar to reactions catalyzed by metalloenzymes.

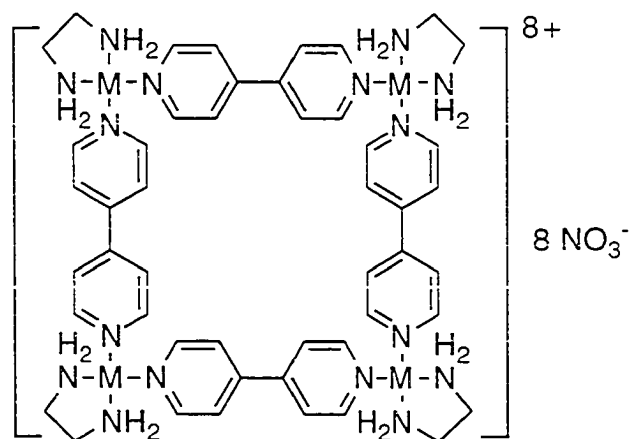
Reinholdt et al. designed receptors by combining a macrocyclic polyether cavity with cyclic ligands which coordinated the metal cation.<sup>64-67</sup> Receptors **7** form inclusion complexes with urea through the coordination of carbonyl oxygen to uranyl cation( $\text{UO}_2^{2+}$ ) and the hydrogen bonding of the  $\text{NH}_2$  group of the guest with the macrocyclic polyether cavity.

**7** ( $n = 1, 2, 3, 4, 5$ )

A cofacial binuclear transition metal complex based on bis ( $\beta$ -diketone) ligands has been used as receptor **8**.<sup>68, 69</sup> It forms inclusion complexes with Lewis bases such as pyrazine and 1,4-diazabicyclo[2.2.2]octane (Dabco) through the coordination of bases to copper ions. The binding affinity largely depends on the basicity of the guest.

**8**

Polynuclear Pd or Pt complexes wherein metal ions are bridged by 4,4'-bipyridine behave as macrocycles which recognize organic molecules in an aqueous phase.<sup>70, 71</sup> The square-planar geometry of Pd(II) and Pt(II) complexes **9** has been utilized in designing these macrocycles.

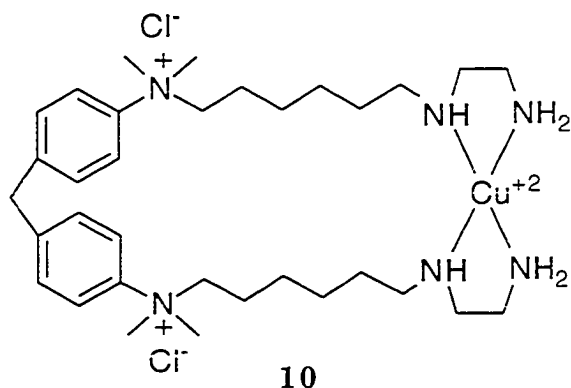


**9** ( M = Pd (II) or Pt (II) )

Macrocycles **9** form inclusion complexes through a hydrophobic interaction as well as a charge transfer interaction between electron-deficient pyridines and electron-rich aromatic guests regardless of the metal ions used. This argument is supported by the observation that complexation of aromatic compounds is preferred over aliphatic compounds and by the substituent effect observed for the complexation of aromatic compounds (  $1,3,5\text{-(MeO)}_3\text{C}_6\text{H}_3 > 1,4\text{-(MeO)}_2\text{C}_6\text{H}_4 > 1,4\text{-(MeOCH}_2)_2\text{C}_6\text{H}_4 \sim 1,4\text{-(HOCH}_2)_2\text{C}_6\text{H}_4$  for increasing  $K_{\text{assoc.}}$  value ).

The characteristic of allosteric systems is that the occupation of spatially separated binding sites by different or identical effector molecules leads to a mutual influence of the binding sites. An artificial system with significant allosteric effects, eg. between an ionic and a lipophilic binding site has been

reported by Schneider et al.<sup>72</sup> The occupation of a polar site by metal ion leads to the closing of a hydrophobic pocket to give **10**. In aqueous medium a hydrophobic binding site is formed in which a lipophilic guest molecule is complexed.

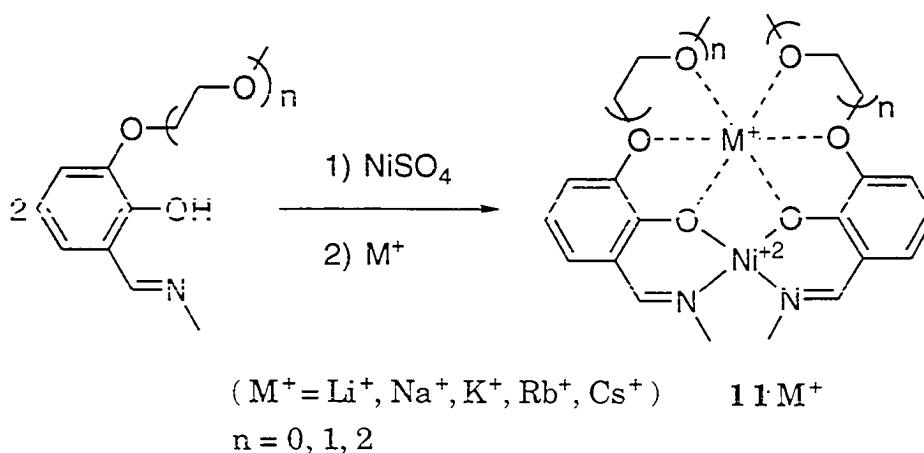


Although macrocycle **10** binds dansyl amide much weaker than Koga's macrocycle **2** ( $n=6$ ), binding studies indicate at least a tenfold to hundred fold stronger complexation of lipophilic substrates in the presence of metal ion than without any metal ions. This allosteric system bears the characteristics of a heterotropic, positive, and especially strong cooperativity. A related molecule was prepared by Desheyes.<sup>73</sup>

A distinctive feature of many biological supramolecules is that they are formed by self-assembly of their subunits. Self-assembly consists of the spontaneous generation of a well-defined, discrete supramolecular architecture from a given set of components under specific conditions. Depending on the nature of the molecules involved, the self-assembly can be organic or inorganic. In the assembly of supermolecules from metal ions and ligands, the latter must contain the steric program that is read by the metal ion following the algorithm represented by their coordination geometry. The self-assembly of a given

superstructure involves three stages: recognition between the components, correct orientation so as to allow growth, and termination of the process leading to a discrete, finite, supramolecular species.<sup>72</sup>

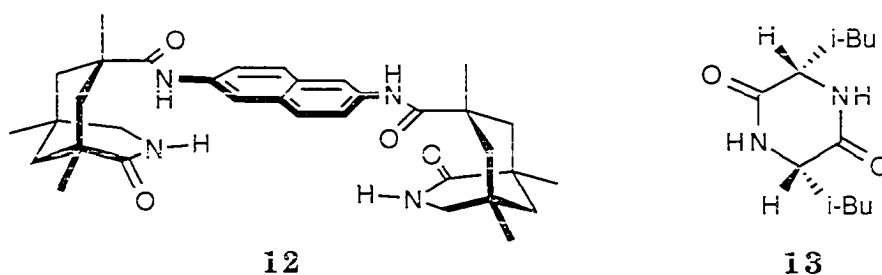
Large supramolecules have been prepared through molecular self-assembly.<sup>74</sup> Also, metal ions have been used as a template to assemble secondary structures in simple model proteins.<sup>75-78</sup> Receptors have been constructed by using self-assembly.<sup>79-81</sup> However, the evidence of the inclusion complex by the self-assembled receptor has been reported only with Schepartz's receptor **11**.<sup>79(a)</sup> Linear polyethers were self-assembled to the cation binding receptors **11** by dimerizing imines in the presence of Ni<sup>2+</sup>. Subsequent structural studies demonstrated that the binding was not in the predicted mode, however.<sup>79(b)</sup>



The development of supramolecular chemistry has been discussed with a focus on cyclophanes. The attempt to understand the extraordinary properties of biological systems stimulates the desire to generate similar properties in designed

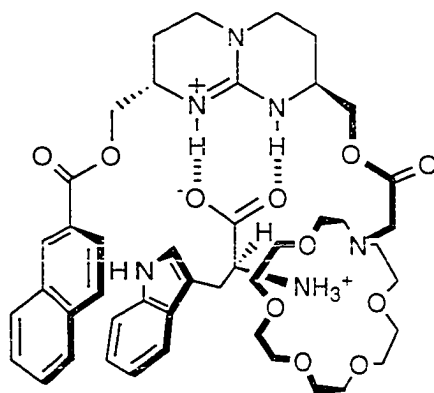
systems. Molecular recognition is one of the aspects involved. Much of the substrate selectivity of the synthetic receptors depends on the cavity size while the cavity shape, charge and degree of substrate saturation also contribute to the selectivity. Multiple interactions during the complexation provide the host with the high guest selectivity observed. It is known how the complexing ability of one binding site is influenced by a second adjacent binding site and its solvation pattern. The understanding of multiple interactions in supramolecular chemistry could result in the rational design of optically active receptors with enantioselectivity.

The high directionality of the hydrogen bond is frequently used in the designing of enantioselective receptors. The series of cleft type chiral receptors which contain convergent lactams and use hydrogen bonding as the host-guest interaction have been designed by Rebek et al.<sup>82</sup> Receptor (+)-**12** binds cyclo-(L-leucyl-L leucine) **13** with  $K_{\text{assoc.}} = 82000 \text{ M}^{-1}$ , while enantiomer (-)-**12** binds it with  $K_{\text{assoc.}} = 840 \text{ M}^{-1}$ . High binding affinity is obtained when the guest is held by the four hydrogen bonds with the receptor.



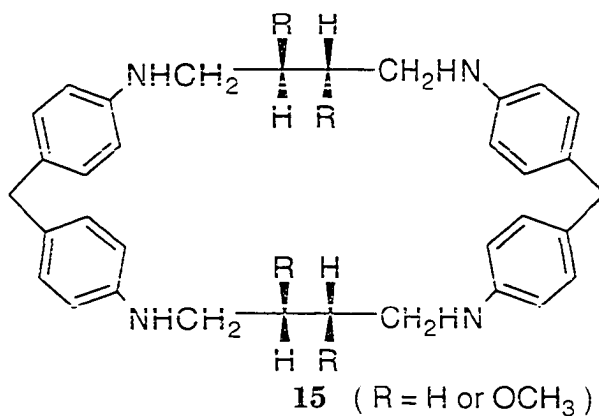
Mendoza et al. designed a receptor which binds aromatic amino acids with high enantioselectivity.<sup>83</sup> Three interactions are proposed for the chiral recognition as shown in **14**: the carboxylate undergoes hydrogen bonding with the

guanidinium unit, the aromatic side-chain undergoes  $\pi$ -stacking with the naphthalene unit, and the ammonium group binds with the crown ether.



14

In aqueous solution, hydrogen bonding interactions become ineffective. The enantioselective recognition in aqueous solution is challenging because it deals with non-directional intermolecular interaction. The first examples of this type are receptors **15** which utilized L-tartaric acid as a chiral source.<sup>84, 85</sup>

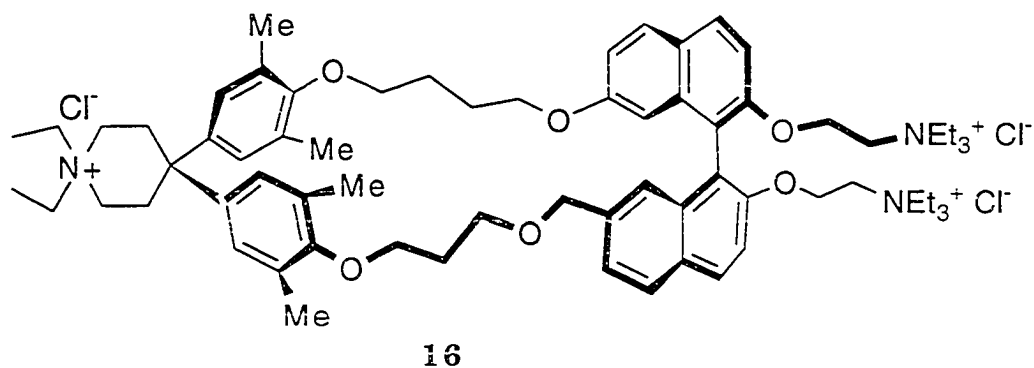


Even though association constants are not determined, the enantioselectivity has been suggested by the  $^1\text{H}$  NMR signals of the two enantiomers being shifted to a different degree. Further evidence of the



enantioselectivity of these hosts was given when asymmetric reductions of achiral arylglyoxylic acids were performed on their inclusion complexes using  $\text{NaBH}_4$ .<sup>85</sup>

Diederich and co-workers have designed a number of chiral cyclophanes and examined their enantioselectivity in substrate binding.<sup>48</sup> Most of the designed receptors have not showed binding or enantioselectivity because of the small cavity size or the insufficient preorganization of the cavity. However, receptors **16** using binaphthyl derivatives as chiral sources show enantioselective recognition ( $\Delta\Delta G = 0.33 \text{ kcal mol}^{-1}$ ).<sup>86</sup> The binaphthyl spacers have been found to provide wide enough cavities for the inclusion complex while maintaining chiral discrimination.



Most of the previous supramolecular chemistry using synthetic receptors was aimed mainly towards mimicking enzymes. Even though many reports with interesting results had been reported and provided valuable information in understanding the supramolecular chemistry, the complexity of enzymes interferes with the mimicking of its behaviors. Therefore, most enzyme mimicking dealt with only parts of enzyme properties. In addition, synthetic receptors designed for enzyme mimics have been prepared with non-biologically related compounds.

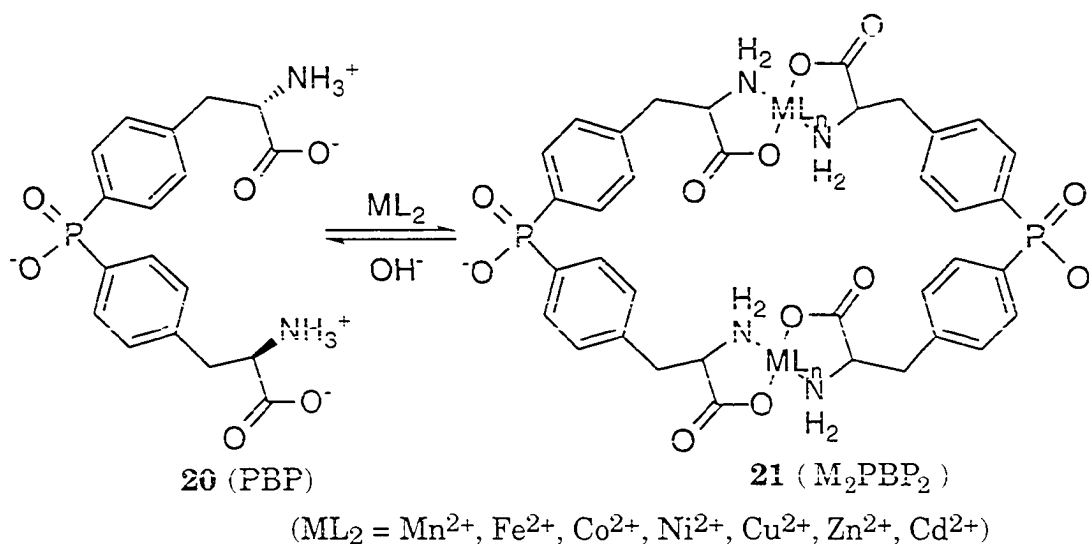
We designed a receptor which was expected to demonstrate many features analogous to those of enzymes. The receptor was designed to form by self assembly of derivatized L-phenylalanines and was expected to be water soluble with a hydrophobic binding site. With several functionalities such as a hydrophobic cavity and transition metal, the receptor was expected to demonstrate substrate selectivity with multipoint interactions and catalytic activity. These expected properties have been found, using several methods to study the designed receptor.

## RESULTS AND DISCUSSION

### Design and Synthesis of Receptor

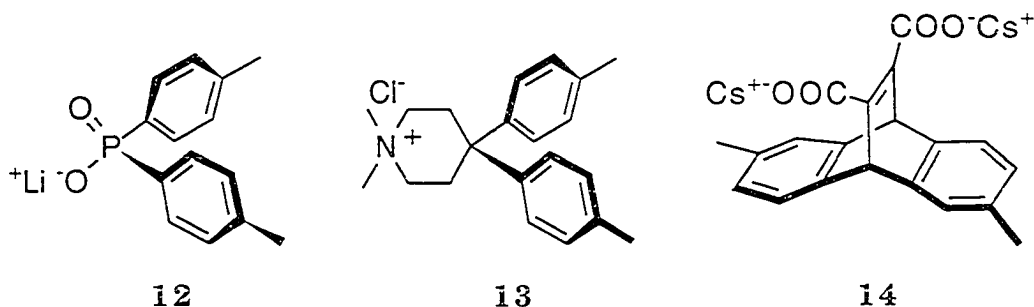
#### Molecular design of receptor

We designed water soluble receptor (**21**) to self-assemble from PBP **20** as shown in Scheme 1. The novel aspects of this design are incorporation of the naturally occurring amino acid L-phenylalanine **15**, use of transition metals as integral parts of the structure, and the self assembly itself. The concave shape of diarylphosphinates provides the preorganized building block 4,4'-(hydroxyphosphinylidene)bis-L-phenylalanine (PBP, **20**). In the presence of a transition metal ion in aqueous solution, PBP dimerizes to the macrocycle  $M_2PBP_2$  **21** through the metal-amino acid interaction. This is a self-assembly process because the macrocyclization occurs spontaneously by the complexation between ligands and metals.



Scheme 1. Self-assembly of the receptor in the presence of transition metal.

In designing a water soluble receptor which has a hydrophobic cavity, we proposed the diarylphosphinate as a spacer in the macrocycle. The diarylphosphinate spacer **12** has several advantages over diphenylmethane derivatives. First, it provides a concave shape to the macrocycle as those the non-planar diphenylmethane spacer, which prevents the collapse of the hydrophobic cavity.<sup>38, 39</sup> Second, the anionic phosphinate functionality provides the macrocycle with water solubility. Researchers have introduced water solubility to related macrocycles by modifying the methylene group of the diphenylmethane spacer such as spiro piperidinium **13**,<sup>59</sup> and 9,10-bridged 9,10-dihydroanthracene **14**.<sup>44</sup> While those modifications need several difficult synthetic steps, the connection of diaryl group by phosphinate is relatively simple.



Third, the Schwabacher group has established supramolecular character in macrocycles containing diarylphosphinate spacers, enabling the newly developed method for the synthesis of the phosphinate ester<sup>87, 88</sup> to be used in designing a variety of receptors with various size and functionalities.<sup>89-90</sup> Fourth, a compound which possesses either a negative charge adjacent to the phosphorus atom, as in the phosphinate anion, or a positive charge positioned on the phosphorus atom, as in the quaternary phosphonium salt, can be obtained from the common phosphinate ester intermediate by hydrolysis<sup>89</sup> or by reduction and

alkylation<sup>90</sup>, respectively.

The metal-amino acid interactions have been one of the most extensively studied fields among the possible model systems involving metal ions and biologically important ligands. The reason for this is that proteins are composed of amino acids and the properties of proteins are modified by having metal ions attached to them. Various metal ions in metalloenzymes play an important role in the binding of organic molecules and in the catalysis of different acid-base and redox processes in biological system. Therefore, the receptor construction through the amino acid-metal interaction is a mimicking of biological systems.

Construction of the receptor **21** through self-assembly using metal-amino acid complexation provides very interesting features. Complexes of transition metals with amino acids exist in a variety of geometries depending upon the metal used. This diversity of complex structure suggests that we can easily modify the size and the shape of the binding cavity by changing the metal. While the preparation of covalently linked macrocycles needs the macrocyclization step which is normally carried out by a dilution method with low yields, the macrocycle **21** was prepared in high yield simply by mixing metal and PBP in basic solution.

The supramolecular chemistry of the macrocycle **21** was studied with carrier mediated transport experiments and <sup>1</sup>H NMR titration. Also, structural and functional properties of macrocycle M<sub>2</sub>PBP<sub>2</sub> were investigated in several ways. Except for discussion of potentiometric titration, PBP and M<sub>2</sub>PBP<sub>2</sub> will be used without specifying charge for naming of the free PBP and macrocyclic M<sup>2+</sup> complex with PBP, respectively.

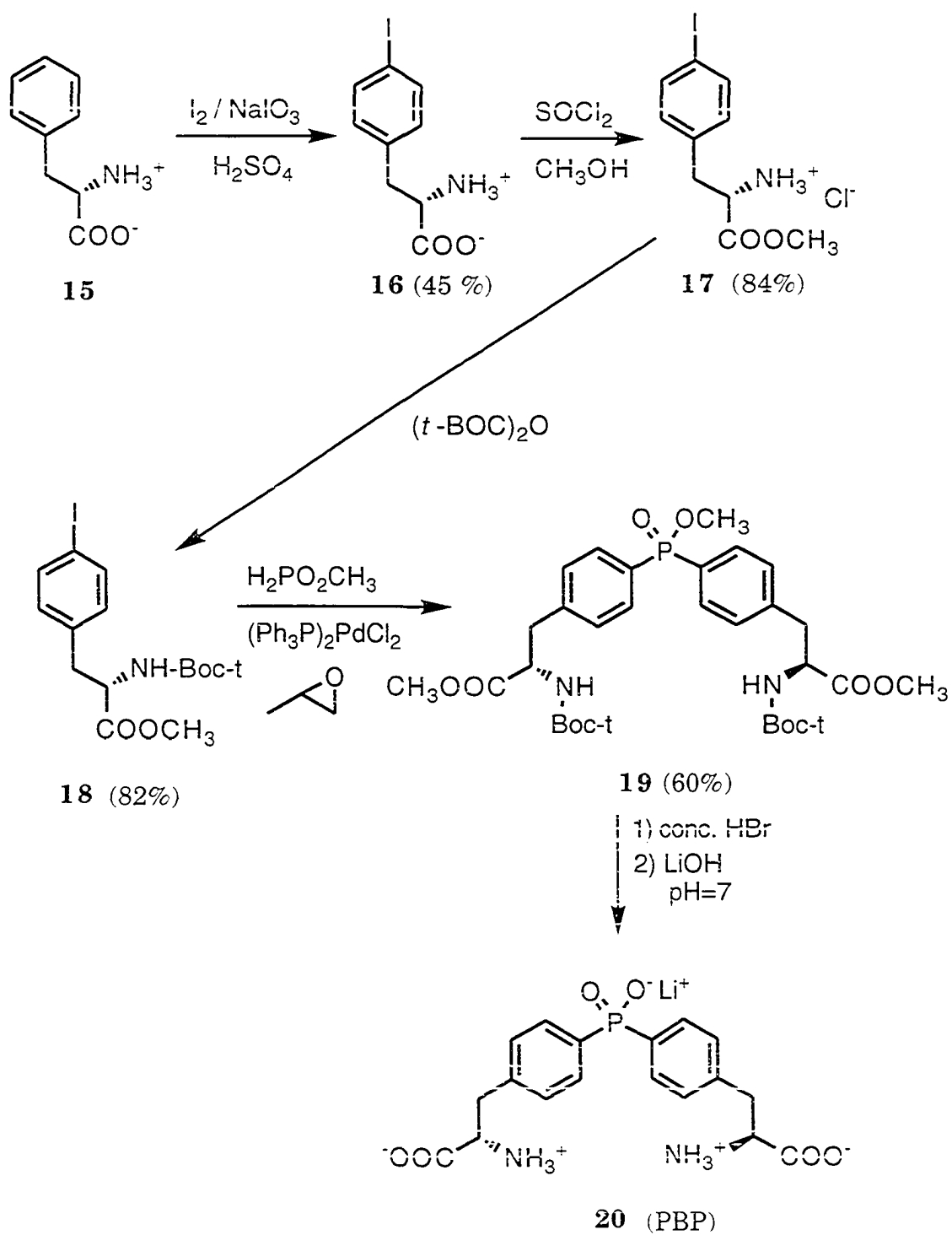
### Synthesis of 4,4'-(hydroxyphosphinylidene)bis-L-phenylalanine (PBP)

PBP was synthesized as shown in Scheme 2, and isolated as salt **20**. Compound **19** had been prepared by Haiyan Lei Grady in the Schwabacher laboratory, however in each step, modifications were made to the reported procedure<sup>87-88</sup> to improve the yields or to simplify the reaction procedure.

Iodination of phenylalanine at the para position was performed at low temperature instead of using the vigorous refluxing described. The temperature of the reaction mixture was increased slowly to 80 °C. This gave more reproducible results. The relatively low yield might be caused by the purification steps. The recrystallization of the product from acetic acid was good for obtaining pure product but it was not optimized for high yield.

The esterification step was the same as the reported procedure. However, the product was purified by recrystallization from EtOH, which did not cause ester exchange. This method provided analytically pure product, not obtained by H. Lei Grady.

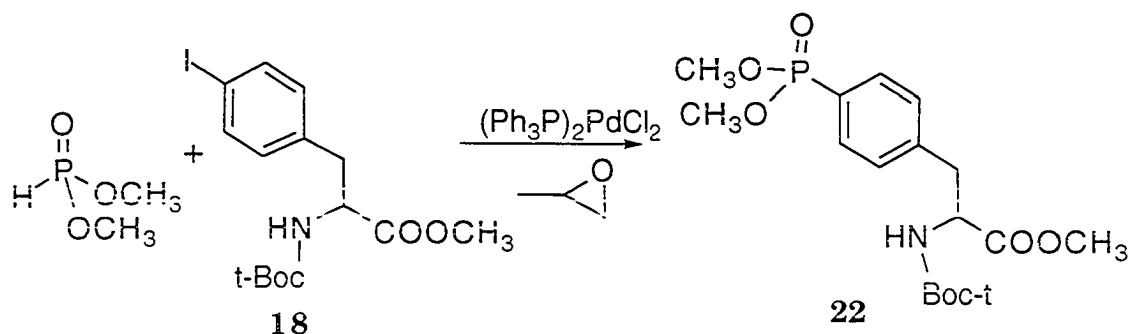
The key step is the conversion of protected *p*-iodophenylalanine **18** into the protected PBP **19** through the palladium catalyzed coupling reaction. N-t-Boc-4-iodo-L-phenylalanine methyl ester **18** was coupled with methyl phosphinate in the presence of bis(triphenylphosphine)palladium dichloride as a catalyst precursor and propylene oxide as a HI scavenger. This coupling reaction has been developed in our group.<sup>87, 88</sup> Despite the coupling reaction procedure being well established, the purification of the product becomes the trouble spot because one side product has very similar physical properties to those of the desired product in both protected and deprotected form.



Scheme 2. Synthetic scheme for preparation of PBP.

those of the desired product in both protected and deprotected form.

The main side product is thought to be the monoarylated 4-(dimethoxyphosphonylidene)-L-(N-t-Boc)phenylalanine methyl ester **22**. The presence of this side product was detected by two doublet corresponding protons of  $\text{CH}_3\text{O-P}$  by  $^1\text{H}$  NMR: doublet at 3.75 ppm vs doublet at 3.74 ppm for **19**,  $J = 11$  Hz for both, while the other protons had same chemical shift and two peaks at  $^{31}\text{P}$  NMR: 21.91 ppm vs . 33.88 ppm for **18**. The formation of this side product is explained by Scheme 3. The coupling reaction of **18** with methyl phosphonate produces compound **22**. Methyl phosphonate was a side product in preparation of methyl phosphinate by treatment of anhydrous phosphinic acid with trimethyl orthoformate.<sup>91</sup> Compounds **19** and **22** had very similar  $R_f$  values even in two eluting systems ( $R_f = 0.3$  with EtOAc, and  $R_f = 0.26$  with  $\text{CH}_2\text{Cl}_2 : \text{CH}_3\text{CN} / 2:1$ ).



Scheme 3. Synthetic route for the formation of the main side product.

The coupling reaction is performed in two steps rather than reported one step coupling: coupling to monoaryl phosphinate followed by coupling to diaryl phosphinate. Usually the amount of compound **22** was relatively small and it could be removed by two successive flash chromatography purifications including the use of gradient eluting methods. At first, most of the other side products are



removed by flash chromatography with EtOAc as an eluting solvent. This is then followed by a second flash chromatography with a CH<sub>2</sub>Cl<sub>2</sub> and CH<sub>3</sub>CN mixture. In the second purification, eluent composition is changed in a step gradient starting from a 4:1 mixture and ending with a 1:1 mixture of CH<sub>2</sub>Cl<sub>2</sub> and CH<sub>3</sub>CN. While on a small scale this gave pure **19**, on a large scale preparation, the amount of compound **22** was not negligible and it could not be removed by flash chromatography even after several repeated purifications. As a result, purification was carried out after deprotection.

Deprotection of the t-Boc group and hydrolysis of the methyl ester of carboxylate and phosphinate in compound **19** were performed in one step by refluxing with concentrated HCl or HBr, followed by evaporation of the excess acid, and neutralization with LiOH. The use of HBr is preferred because the solubility of LiBr in organic solvents is higher than that of LiCl. The final product **20** is purified by fractional precipitation from a water and acetone (1:2) mixture. At least 6 repeated precipitations, as followed by <sup>31</sup>P NMR ( $\delta = 23.82$  ppm for **20**,  $\delta = 13.73$  ppm for the hydrolyzed form of **22**), were needed to obtain analytically pure product **20**; the recovery was 23%.

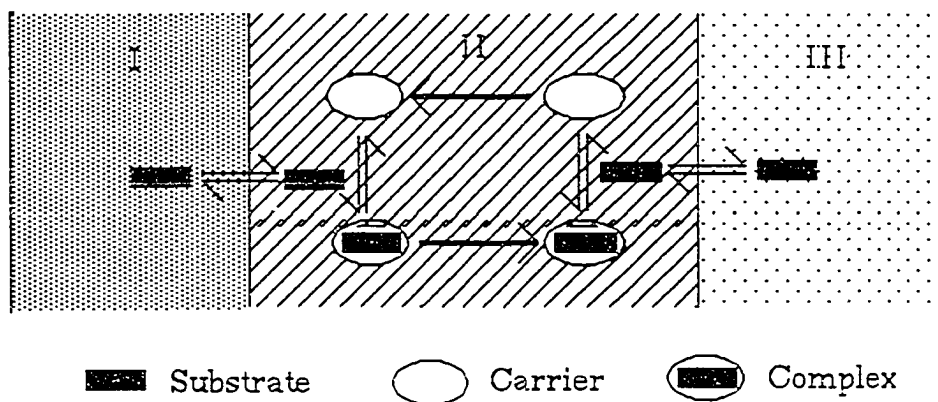
### **Qualitative Binding Study with Carrier-mediated Transport**

Carrier-mediated transport experiments were performed to investigate the supramolecular character of metal-PBP complexes. This provided a simple way to screen various metal ions to determine which were most worth intensive study.

The organic chemistry of transport processes and carrier molecules has developed recently,<sup>92</sup> although the physico-chemical features and the biological

importance of transport processes have been well known. Synthetic receptor molecules which are soluble in membranes and show selectivity in substrate binding can behave as carrier molecules. They bind substrate selectively and induce selective transport by making membranes permeable to the bound species. Transport represents one of the basic functional features of supramolecular species in addition to recognition and catalysis.

Carrier-mediated transport is the carrier facilitated transfer of a substrate across a membrane. The carrier is the transport catalyst where the active species is the carrier-substrate supermolecule. It is a four-step cyclic process: association, dissociation, forward and back diffusion (Scheme 4).<sup>1</sup>



Scheme 4. Schematic diagram of carrier mediated transport.<sup>1</sup>

Extensive studies of carrier-mediated transport have focused on the transport of inorganic and organic cations through lipophilic membranes.<sup>2</sup> However, little information is available about the transport of lipophilic substrates through an aqueous phase by simple synthetic carriers.<sup>92-94</sup> Diederich et al. observed for the first time the molecular carrier-mediated acceleration of the transport of lipophilic arenes through an aqueous phase along a

concentration gradient.<sup>92</sup> The guest selectivity in the transport acceleration shows that the highest acceleration is measured for the arenes with the lowest distribution constant  $K_D$  and the highest association constant  $K_A$  of the complex formed with the host in the aqueous phase. However, the molecular understanding of carrier-mediated transport through aqueous solutions is not fully elucidated. In particular, the relationship between the rate of transport and the stability constant of the carrier-complex needs to be determined.

The carrier-mediated transport experiment was performed with iso-octane solutions of arenes and an aqueous solution of  $M_2PBP_2$ . Transport rates of lipophilic arenes through aqueous phase have been observed using the H-shaped tube.<sup>94</sup> In the beginning of transport experiments, a normal U-shaped tube with one stirring bar in the middle of the tube was used.<sup>92</sup> However, the transport rates were very slow and inconsistent from one set of experiments to another. The H-shaped tube (Figure 1) which was originally designed by Murakami et al.<sup>94</sup> was made and it gave better consistency in transport experiments. We found, using pH indicators and the addition of base, that effective mixing of the whole tube took place in seconds using a tube of the Murakami design, whereas hours were required using a simple U-shaped tube. Arenes are dissolved in iso-octane and the carrier is added to the aqueous phase which separates the source and the receiving phases. Transport rates are obtained by measuring the concentration of an arene in the receiving phase.

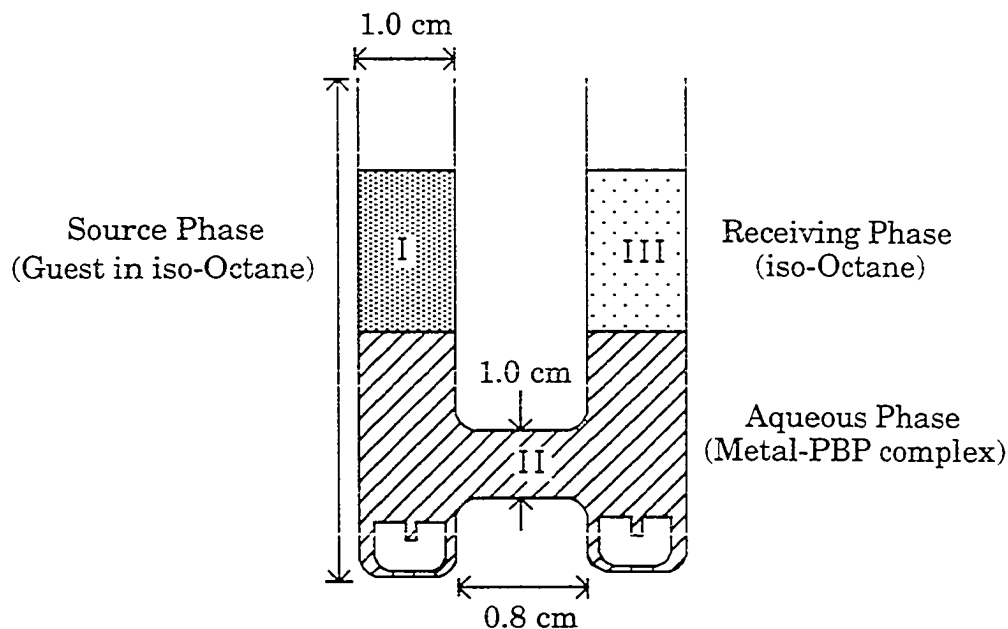


Figure 1. H-Shaped tube used for transport experiments.

Transport rates are highly dependent on the conditions used such as the relative position of the magnetic stirring motor to the H-shaped tube and the vigorousness of agitation of the aqueous phase. The results of 17 repeated transport experiments at a constant, but arbitrary stirring rate, show that the transport rate of  $1.0 \times 10^{-2}$  M pyrene in iso-octane through aqueous phase without the carrier molecule is  $1.20 \times 10^{-7}$  M/h with 18% error. As a result, the evaluation of carrier facilitated transport rate by comparing the absolute transport rates from different sets of transport experiments would not be appropriate. Higher reproducibility was obtained by measuring the relative rate which was the ratio of the facilitated rate to the nonmediated background rate. The carrier molecule was added to the aqueous phase after the background rate was measured and the

facilitated rate was then measured without disturbing the stirring apparatus. The ratio of transport rate before and after the addition of the carrier molecule can then be calculated.

The carrier metal-PBP complexes are prepared in aqueous solution through self-assembly by mixing equimolar amounts of metal salt with PBP solution.  $\text{Co}^{2+}$  solution or PBP solution alone does not accelerate the transport rate of pyrene. Addition of equivalent amount of  $\text{Co}^{2+}$  to  $3.52 \times 10^{-3} \text{ M}$  PBP solution enhances the transport rate 27 times (Figure 2).

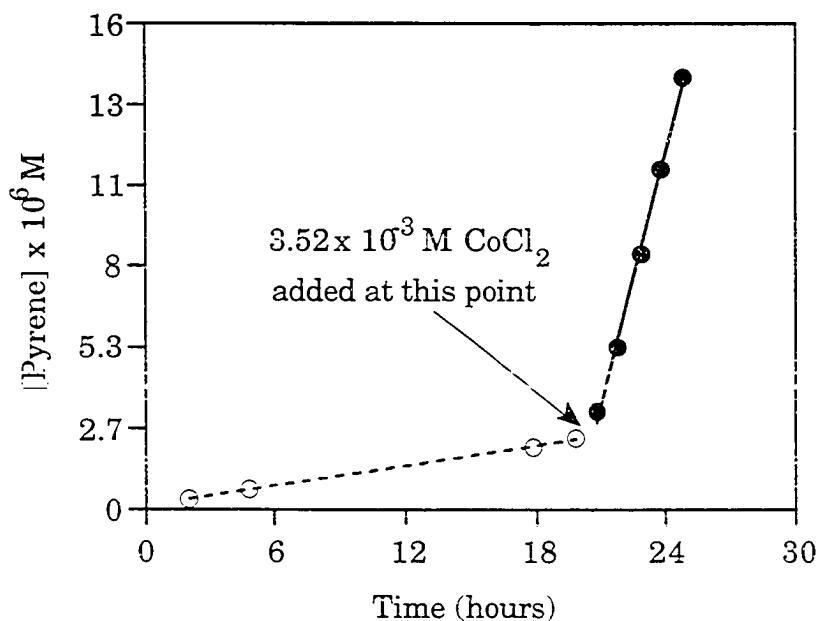


Figure 2. Transport of pyrene through aqueous layer: acceleration by  $\text{Co}^{2+}$ /PBP complex. Transport rate at  $[\text{PBP}] = 3.52 \times 10^{-3} \text{ M}$  (○), and accelerated rate after addition of  $3.52 \times 10^{-3} \text{ M}$   $\text{Co}^{2+}$  (●).

Also, addition of an equivalent amount of PBP solution to  $1.86 \times 10^{-3}$  M  $\text{Co}^{2+}$  solution enhances the transport rate by 13 times (Figure 3). The binding ability of the self-assembled  $\text{Co}^{2+}$  complex is destroyed by addition of EDTA, which sequesters the metal; pyrene transport rate returns to the background rate. These transport rate results provide the evidence that  $\text{Co}^{2+}$  and PBP form a complex which is responsible for the rate enhancement. Consistent with this interpretation, addition of  $7.1 \times 10^{-4}$  M N-methyl quinolinium iodide to the  $\text{Co}^{2+}$  and PBP mixture ( $8.1 \times 10^{-4}$  M each) causes a 46% decrease in the pyrene transport rate, presumably by competing for well-defined binding sites.

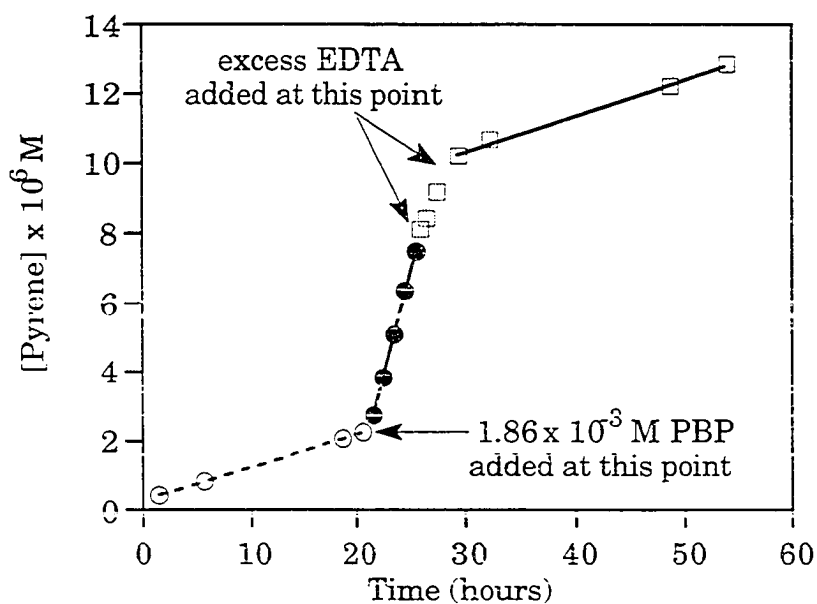


Figure 3. Transport of pyrene through aqueous layer: scavenging of  $\text{Co}^{2+}$  with EDTA removes the acceleration effect of  $\text{Co}^{2+}$ /PBP complex. Background rate (○,  $[\text{Co}^{2+}] = 1.86 \times 10^{-3}$  M), acceleration by addition of PBP (●,  $[\text{PBP}] = 1.86 \times 10^{-3}$  M), transport rate after addition of excess EDTA (□).

However, addition of the equivalent amount of  $\text{Co}^{2+}$  to  $9.6 \times 10^{-4}$  M tyrosine solution does not affect the pyrene transport rate (Figure 4). These results imply that the pyrene carrier in  $\text{Co}^{2+}$  and PBP solution is not the simple  $\text{Co}^{2+}$ -amino acid complex.

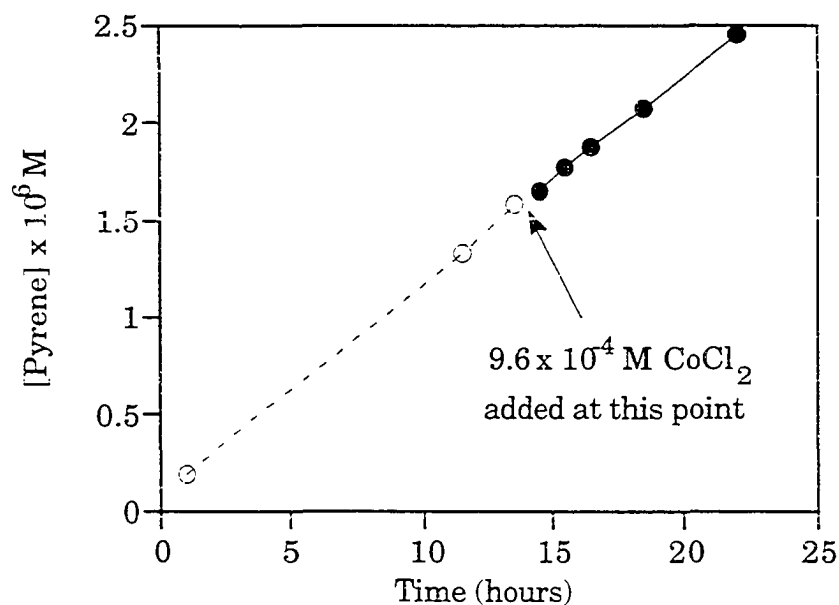


Figure 4. Transport of pyrene through aqueous phase:  $\text{Co}^{2+}$ / tyrosine complex does not facilitate transport. Background rate (○, [tyrosine] =  $9.6 \times 10^{-4}$  M), transport rate after addition of  $\text{Co}^{2+}$  (●, [ $\text{Co}^{2+}$ ] =  $9.6 \times 10^{-4}$  M).

Addition of an equivalent amount of  $\text{Cu}^{2+}$  to a  $1.86 \times 10^{-3}$  M of PBP solution does not affect the pyrene transport rate (Figure 5). This result suggests that the  $\text{Cu}^{2+}$  complex with PBP does not make a suitable binding site for pyrene and that the geometry of the metal complex may determine the size or shape of the binding site.

Aqueous solutions of  $1.0 \times 10^{-3}$  M each in metal salt and PBP were screened for their ability to transport pyrene. As shown in Table 1,  $\text{Co}^{2+}$  and  $\text{Ni}^{2+}$  are highly effective while  $\text{Fe}^{2+}$ ,  $\text{Mn}^{2+}$ ,  $\text{Cu}^{2+}$ ,  $\text{Zn}^{2+}$ , and  $\text{Cd}^{2+}$  are much less so in the transport of pyrene through an aqueous phase.

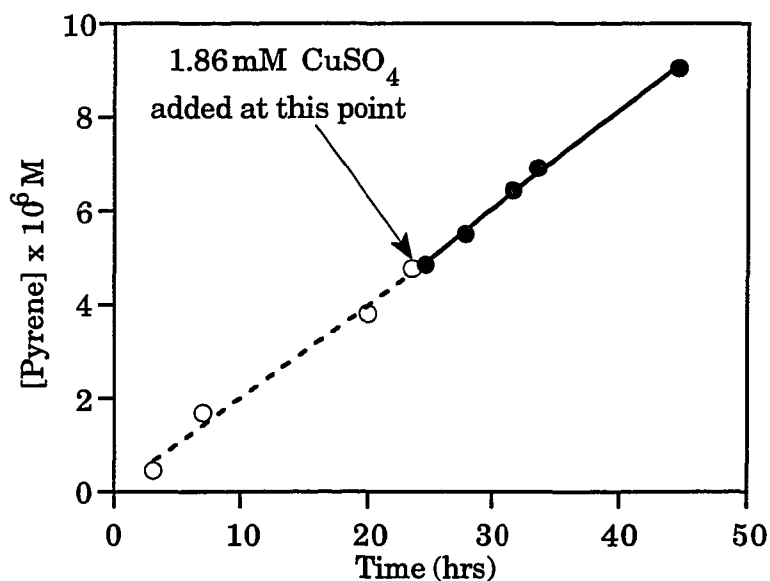


Figure 5. Transport of pyrene through aqueous phase:  $\text{Cu}^{2+}$ / PBP complex does not facilitate transport. Background rate in the presence of PBP (○,  $[\text{PBP}] = 1.86 \times 10^{-3}$  M), transport rate after addition of  $\text{Cu}^{2+}$  (●,  $[\text{Cu}^{2+}] = 9.6 \times 10^{-4}$  M).

Examination of CPK models suggests that certain isomers of octahedral or five-coordinated metal complexes would be appropriate for pyrene binding and that square planar (e.g.,  $\text{Cu}^{2+}$ ) complexes would not be, but the peculiarity of  $\text{Co}^{2+}$  and  $\text{Ni}^{2+}$  could not be explained yet.



The transport rate depends on the amount of pyrene dissolved in the aqueous phase, which in turn depends on the concentration of host and on the binding constant of the host for pyrene. The concentration of host complex is related to the concentration of  $M(\text{amino acid})_2$ , which has been estimated

Table 1. Transport of Pyrene Mediated by Metal/PBP Complexes<sup>a</sup>

	Mn <sup>2+</sup>	Fe <sup>2+</sup>	Co <sup>2+</sup>	Ni <sup>2+</sup>	Cu <sup>2+</sup>	Zn <sup>2+</sup>	Cd <sup>2+</sup>
relative rate <sup>b</sup>	1.15	1.12	9.96	9.92	1.07 <sup>c</sup>	1.43	1.33 <sup>c</sup>
% of $\bar{M}\bar{L}_2$ complex <sup>d</sup>	5.0	48.0	51.0	79.0	99.0 <sup>c</sup>	70.0	37.0 <sup>c</sup>

<sup>a</sup> Transport of pyrene from a  $1.01 \times 10^{-2}$  M isooctane solution through a 24 °C, pH  $\geq 9.5$ , aqueous layer  $9.6 \times 10^{-4}$  M in 1:1 PBP and metal salt, except as noted.

<sup>b</sup> Rates are relative to background rate measured without metal ( $\pm 20\%$ ).

<sup>c</sup>  $[M^{2+}] = [PBP] = 1.86 \times 10^{-3}$  M.

<sup>d</sup> Calculated fraction of metal at this concentration and pH 9.5 that would exist as  $M(\text{Phe})_2$  complex.

from known stability constants for metal complexes of phenylalanine; these are displayed in Table 1. They are minimal estimates of  $ML_2$  formation in the macrocyclic case. More than those amounts are expected to present as  $M_2PBP_2$  complex because of its cyclic nature, i.e. effective molarity. The transport rate does not correlate with stability, which suggests that transport rate is dependent not only on the amount of host complex formed but also on the geometry of the complex.

The stoichiometry of the  $\text{Co}^{2+}$ /PBP complex which is responsible for the transport acceleration is determined by the method of continuous variations (or Job' plot). Changes in acceleration of transport are plotted according to variations of  $\text{Co}^{2+}$  to PBP-1 ratio while keeping the sum of the total  $\text{Co}^{2+}$  and PBP-1 concentration constant (Figure 6).

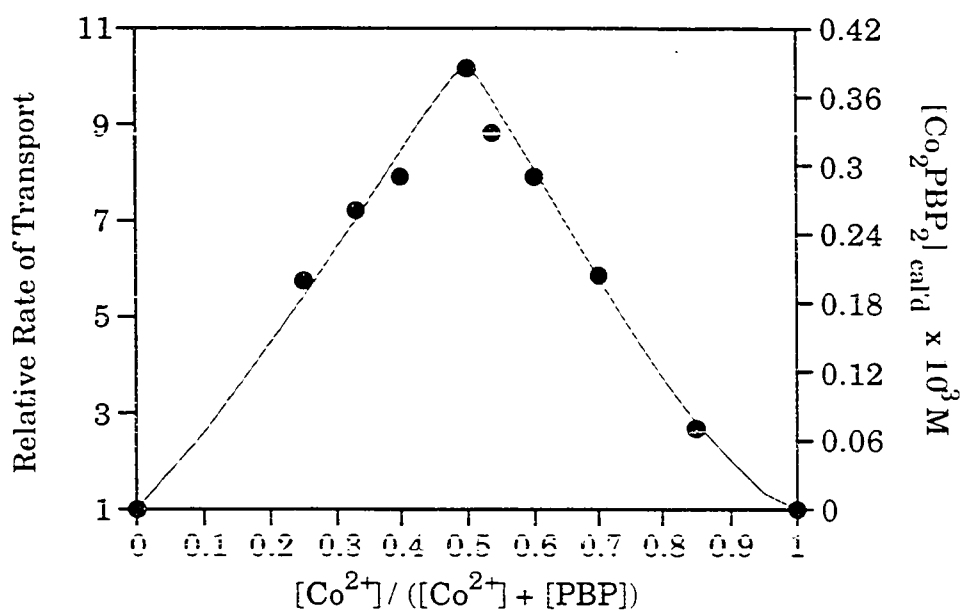


Figure 6. Job's Plot for  $\text{Co}^{2+}$ /PBP complex.  $[\text{PBP}] + [\text{Co}^{2+}] = 1.74 \times 10^{-3} \text{ M}$  at  $\text{pH} = 9.5$ , observed relative transport rate of pyrene ( $\bullet$ ), calculated concentrations of  $\text{Co}_2\text{PBP}_2$  (—) by using the stability constants obtained from the potentiometric titration described below.

The maximum relative transport rate at 1:1 mole ratio in the Job's plot ( $[\text{PBP}^{-1}] + [\text{Co}^{2+}] = 1.74 \times 10^{-3} \text{ M}$ ) confirms that the species responsible for transport has a 1:1 ratio of  $\text{PBP}:\text{Co}^{2+}$ , as expected for a 2:2  $\text{PBP}:\text{Co}^{2+}$  complex. This result is confirmed by theoretical calculation using stability constants which are obtained from potentiometric titration described below. The plot of the  $\text{Co}_2\text{PBP}_2$  concentration vs. the mole ratio between  $\text{Co}^{2+}$  and PBP matches exactly with the result of transport experiments (Figure 6).

The pyrene transport rate is directly proportional to the concentration of  $\text{Co}^{2+}$  where the concentration of PBP is altered to maintain 1:1 ratio between  $\text{Co}^{2+}$  and PBP (Figure 7). This result provides another piece of evidence for the 1:1  $\text{Co}/\text{PBP}$  complex mediated transport of pyrene through the aqueous phase. Extraction experiments show an 8-fold increase in the concentration of pyrene in water at equilibrium with  $1.0 \times 10^{-2} \text{ M}$  pyrene in iso-octane due to the presence of  $9.6 \times 10^{-4} \text{ M}$  each of  $\text{Co}^{2+}$  and  $\text{PBP}^{-1}$ . This nicely matches the 8-fold increase in transport rate of the regression line.

The results of pyrene transport experiments can be summarized as follows: 1) the transport of pyrene is not accelerated in the presence of  $\text{Co}^{2+}$  or  $\text{PBP}$  alone, 2) the  $\text{Co}^{2+}$  complex with tyrosine does not facilitate the transport of pyrene, 3) the facilitated transport rate in the presence of  $\text{Co}^{2+}$  complex with PBP dropped to the background rate upon addition of EDTA, 4) a maximum facilitated transport rate was observed at a 1:1 mole ratio between  $\text{Co}^{2+}$  and PBP, 5) the relative transport rate is directly proportional to the concentration of  $\text{Co}^{2+}$  in the presence of same amount of  $\text{PBP}$ . These experimental results are consistent with the idea that the carrier molecule responsible for the acceleration of pyrene transport is a 1:1 or 2:2  $\text{Co}^{2+}/\text{PBP}$  complex.

$\text{Co}^{2+}$ /PBP complex mediated transport shows the substrate selectivity expected for binding into a discrete receptor, as opposed to a detergent solubilization. A correlation between the transport rate and the binding affinity of substrate to a carrier had been reported.<sup>41</sup>  $\text{Co}^{2+}$ /PBP complex

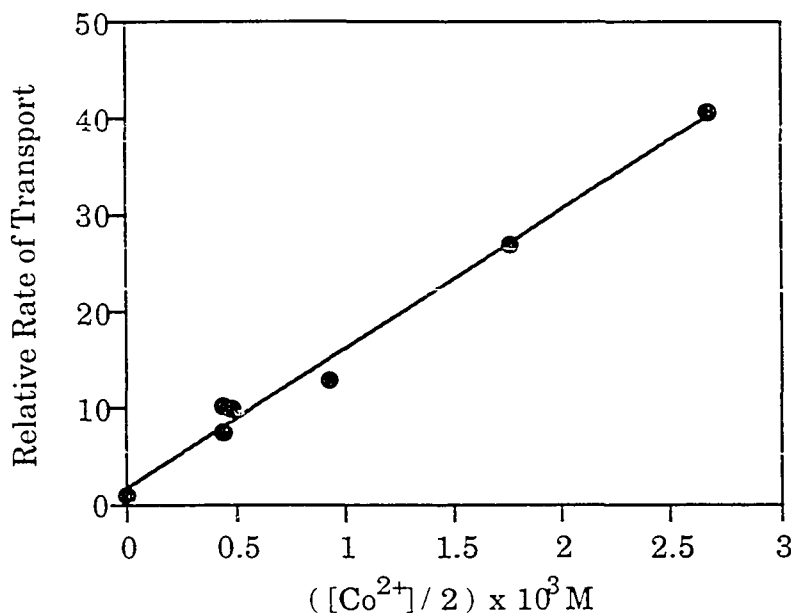


Figure 7. Relative transport rate of pyrene through aqueous phase as a function of  $\text{Co}^{2+}$  (at a 1:1 ratio of  $\text{Co}^{2+}$ : PBP).

transports pyrene with a 10 fold rate acceleration ( $\pm 20\%$ ) relative to background at  $9.6 \times 10^{-4} \text{ M}$ , while it transports 9-bromoanthracene with the rate barely distinguishable from the unfacilitated rate (Figure 8).

A CPK model study shows that the cavity of macrocyclic  $\text{Co}_2\text{PBP}_2$  is about the size required for a naphthalene to fit in an equatorial orientation. Therefore 9-bromoanthracene has a shape incompatible with the cavity and

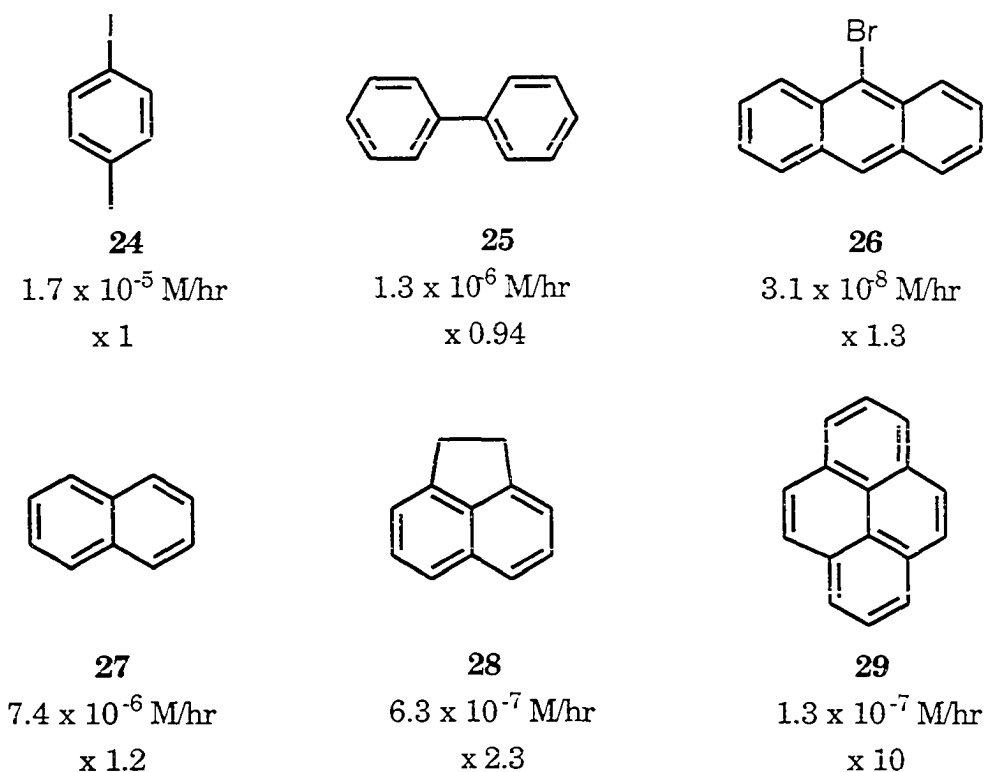


Figure 8. Transport rate of arenes through aqueous phase without  $\text{Co}_2\text{PBP}_2$ . Multiplied numbers are acceleration of the rate due to the presence of  $9.6 \times 10^{-4}$  M  $\text{Co}_2\text{PBP}_2$ .

*p*-iodophenol is too small for the cavity. While acenaphthene transport was increased by 2.3 fold, naphthalene does not show enhanced transport even though both of those are expected to fit into the cavity. This is presumably because the solubility of naphthalene in water is too high. Similar results have been reported by Diederich et al.: the transport rate of pyrene has been accelerated by 430 times but only 3.7 fold acceleration was found for naphthalene transport.<sup>77</sup> The results of  $\text{Co}^{2+}/\text{PBP}$  complex mediated transport experiments can be accounted for by comparing the background rates with the facilitated rates. Facilitated

rates of biphenyl, acenaphthene, and pyrene are the same, within error limits, with a value of  $1.3 \times 10^{-6}$  M/hr. The coincidence of accelerated rates suggests that there is an upper limit in the facilitated transport rate under a given set of conditions. The background transport rate for naphthalene exceeds the maximum facilitated rate, so that even if binding occurs, it may not manifest itself as measurably enhanced transport.

Transport experiments showed that the  $\text{Co}^{2+}$  complex with PBP behaved as we expected: substrate binding selectivity corresponds to that expected for a discrete self-assembled receptor. Also, it suggested that  $\text{Co}_2\text{PBP}_2$  was the  $\text{Co}^{2+}$ /PBP complex responsible for the transport facilitation. However, it did not provide information about the nature of that complex. So, the question remaining at this point was the nature of the complex.

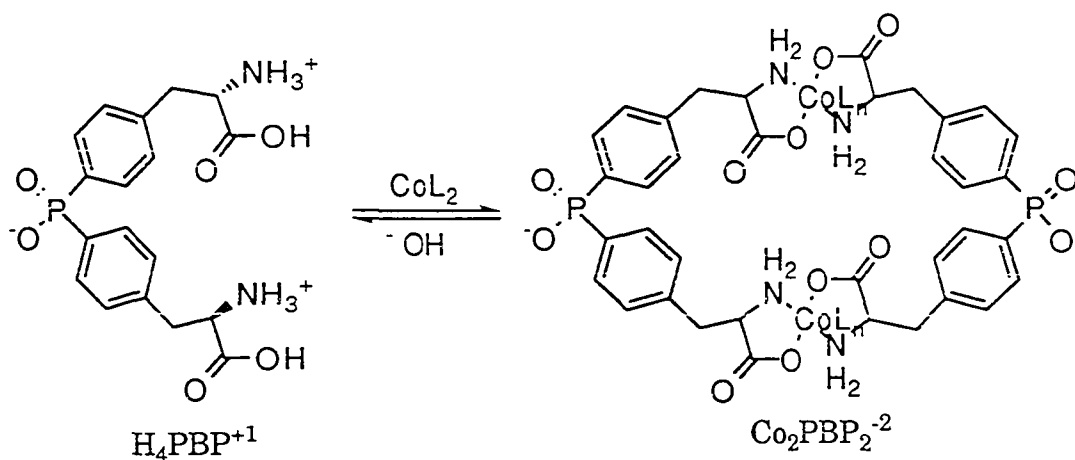
## Structural Studies of Receptor

### Potentiometric titration

It is well known that amino acids can form stable bis or tris complexes with various transition metal ions, where the coordination takes place via the  $\alpha$ -amino and carboxylate groups so as to form 5-membered chelate rings.<sup>95</sup> The macrocycle  $\text{M}_2\text{PBP}_2$  was designed by using these metal-amino acid interactions in the cyclization process. Carrier mediated transport experiments showed that  $\text{Co}^{2+}$  and  $\text{Ni}^{2+}$  complexes with PBP can bind aromatic substrates of naphthalene size and most of the binding studies were performed with the  $\text{Co}^{2+}$  complex. Therefore, further studies were focused on  $\text{Co}_2\text{PBP}_2$ .

$\text{Co}_2\text{PBP}_2$  self-assembles from two PBP molecules in the presence of the

cobalt(II) metal ion in basic aqueous solution as shown in Scheme 5. The stability of the  $\text{Co}_2\text{PBP}_2$  complex depends largely on the stability constants of  $\text{Co}^{2+}$ -amino acid complex. Therefore determination of stability constants for  $\text{Co}^{2+}$  complex with PBP was carried out by potentiometric titration.



Scheme 5. Self-assembly of  $\text{Co}_2\text{PBP}_2$ .

Although stability constants for the  $\text{Co}^{2+}$  complexes with phenylalanines are reported, those values can not be directly applied to the  $\text{Co}_2\text{PBP}_2$  system not only because phenylalanine was modified by a substitution at the para position of the phenyl group, but also, more importantly, because of the cyclic nature of  $\text{Co}_2\text{PBP}_2$ . Stability constants of  $\text{Co}^{2+}$  complexes with PBP were determined by potentiometric titrations as described by Martell.<sup>96</sup> Potentiometric titrations of 1:1.25  $\text{Co}^{2+}$  : PBP with hydroxide from pH 2.5 to 9.5 at  $25.0 \pm 0.1^\circ\text{C}$  were carried out under an argon atmosphere. The ionic strength of the solution was kept constant at 0.1 M with KCl. The stability constants and the protonation constants were then calculated by fitting the titration results using the program 'BEST'.<sup>96</sup> In contrast to the way "PBP" is used to refer to all protonation states

of that molecule in other sections of this thesis, all ionic compounds will be assigned charges here.

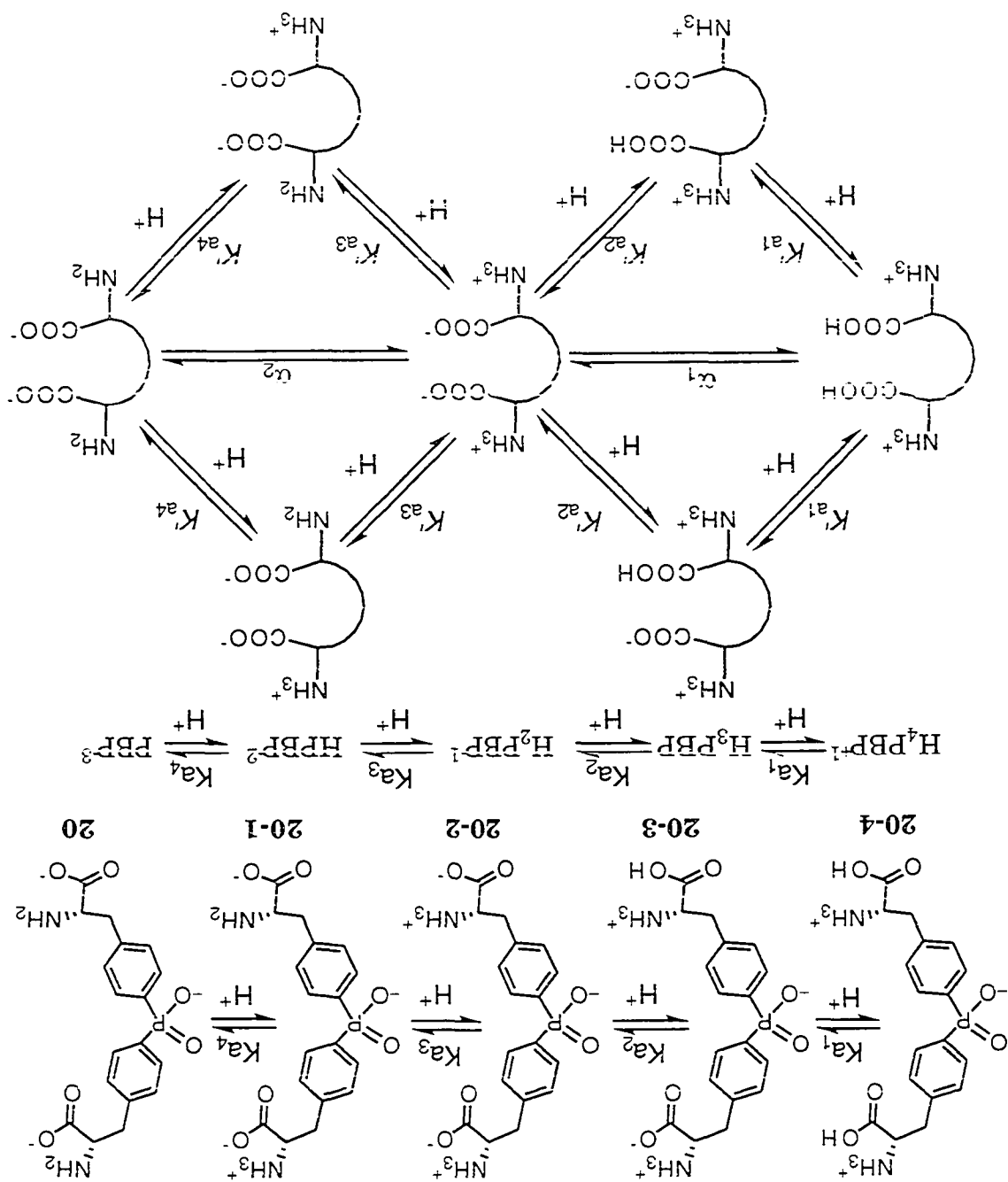
### **Protonation constants of $H_4PBP^+$**

Protonation constants of  $H_4PBP^+$  needed for determination of the stability constants were determined by titration.  $H_4PBP^+$  is composed of two molecules of phenylalanine and one phosphinic acid group which provide  $H_4PBP^+$  with three acidic (one phosphinic and two carboxylic) and two  $\alpha$ -amino groups. All amino acids undergo two reversible proton dissociation steps in fairly well separated ranges:  $pH = 2-3$  for carboxylic and  $pH = 8-9$  for  $\alpha$ -amino groups. Protonation equilibria of  $H_4PBP^+$  are described in Scheme 6. Protonation of the phosphinate is not considered because it is too acidic to be calculated correctly with the pH range used in the potentiometric titration experiments. Therefore,  $H_4PBP^+$  is treated as a tetrabasic acid within the 2.3-10.5 pH range .

Even though two amino acid groups are present at the same molecule, they are separated far enough to be considered independently. However, the observed protonation constants ( $K_a$ ) are macroscopic constants because the actual donor sites where the protons reside are not specified and are not unique. The macroscopic constants are influenced not only by chemical factors but also by statistical factors.<sup>95, 96</sup> The microscopic constants ( $K'_a$ ) are equilibrium constants for the equilibria involving individual species in solution. The microscopic constants can be replaced by the macroscopic constants if the interactions between the functional groups are negligible. With the assumption that the two amino acids of  $PBP^{-3}$  behave independently



Scheme 6. Protonation equilibria of  $H_4PBP^+$  and the protonation constants.



and have equivalent chemical properties, the microscopic constants can be deduced from the macroscopic constant by considering the statistical factors:

$$Ka_1 = K'_{a1} + K'_{a1} \quad (1)$$

$$\alpha_1 = Ka_1 \times Ka_2 = K'_{a1} \times K'_{a2} \quad (2)$$

$$Ka_3 = K'_{a3} + K'_{a3} \quad (3)$$

$$\alpha_2 = Ka_3 \times Ka_4 = K'_{a3} \times K'_{a4} \quad (4)$$

where  $\alpha_i$  : overall constants,  $Ka_i$  : macroscopic constants, and  $K'_{ai}$  : microscopic constants.

The macroscopic constants are obtained from curve fitting of the pH profile and the microscopic constants are calculated by using above equations (1)-(4). The potentiometric titration result is shown at Figure 9. This titration curve is fitted with the program "BEST"<sup>96</sup> by refining four protonation constants of  $H_4PBP^+$ . Protonation constant refinement is the process whereby the computer adjusts several parameters with a programmed algorithm for the purpose of obtaining the best possible least-squares fit of calculated data to the observed data. The goodness of fit is measured by  $\sigma_{fit}$  which is a measure of the weighted sum of squares of the  $p[H]_{cal} - p[H]_{obs}$  differences and the object is to minimize  $\sigma_{fit}$  through refinement of these parameters.<sup>96</sup>

$$\sigma_{fit} = (U/N)^{1/2} \quad (5)$$

where  $U = \sum w (p[H]_{obs} - p[H]_{cal})^2$ ,  $w = 1/(p[H]_{i+1} - p[H]_{i-1})^2$ , and  $N = \sum w$ .

In the beginning of the refinement, protonation constants of  $H_4PBP^+$  are approximated from the literature values of phenylalanine which are shown in Table 2. During the refinement process, all four protonation constants are subjected to change without any constraint. The good agreement between the observed data and the calculated curve (Figure 9) implies that the postulation

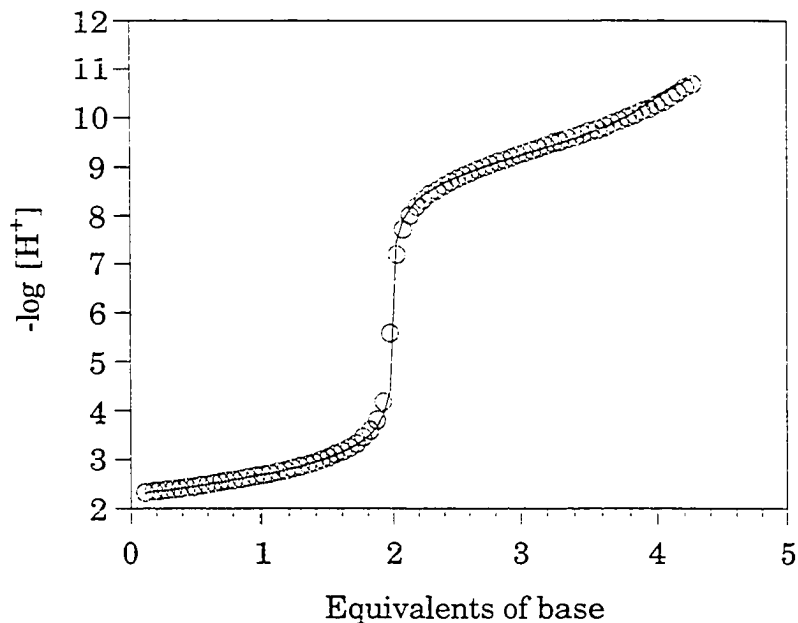


Figure 9. Potentiometric titration curves for  $H_4PBP^+$ . Solution is  $25.0\text{ }^\circ\text{C}$ ,  $\mu = 0.1\text{ M}$  (KCl), continuously flushed with saturated argon gas.  $[PBP^{-3}] = 4.1 \times 10^{-3}\text{ M}$  (O), result of curve fitting (-).

of tetrabasic acid (Scheme 6) is correct and the calculated protonation constants are reliable. Calculated macroscopic and microscopic constants are given in Table 2.

The difference between  $-\log K'_{a1}$  and  $-\log K'_{a2}$  suggests that there are some sort of interactions between the functional groups making two carboxylic groups not chemically identical. However, two amino groups are turned out chemically identical without any interactions ( $-\log K'_{a3} \approx -\log K'_{a4}$ ).

Table 2. The macroscopic and microscopic constants of  $H_4PBP^+$  and the known protonation constants for phenylalanine.<sup>a</sup>

Calculated for $H_4PBP^+$		Reported for Phenylalanine	
$\mu = 0.1 \text{ M KCl}$		$\mu = 0.05 \text{ M}^{97}$	$\mu = 0.1 \text{ M KCl}^{98}$
$-\log K_{a1} = 1.37$	$-\log K'_{a1} = 1.67$		
$-\log K_{a2} = 2.59$	$-\log K'_{a2} = 2.29$	$-\log K_{a1} = 2.18$	$-\log K_{a1} = 1.80$
$-\log K_{a3} = 9.00$	$-\log K'_{a3} = 9.30$		
$-\log K_{a4} = 9.50$	$-\log K'_{a4} = 9.20$	$-\log K_{a2} = 9.11$	$-\log K_{a2} = 9.10$

<sup>a</sup>  $K_{ai}$ : macroscopic constant,  $K'_{ai}$ : microscopic constant.

There are big discrepancies between the macroscopic protonation constants of  $H_4PBP^+$  with those of phenylalanine because  $H_4PBP^+$  has two indistinguishable phenylalanine groups. As a result, microscopic constants of  $H_4PBP^+$  should be compared with macroscopic constants of phenylalanine. The first microscopic protonation constant of carboxylate ( $-\log K'_{a1} = 1.67$ ) is lower than that of phenylalanine ( $-\log K_{a1} = 1.80$ ) while the second protonation constant of carboxylate ( $-\log K'_{a2} = 2.29$ ) is higher. Although the reason for this difference is not established, it seems possible that the effect is due to the protonation of phosphinate group which is not considered in the protonation scheme of  $H_4PBP^+$ . However, these values are not important because they do not contribute to the next calculation of stability constants. The protonation constants of amino groups ( $-\log K'_{a3} = 9.30$  and  $-\log K'_{a4} = 9.20$ ) are reasonably close to those of phenylalanine ( $-\log K_{a2} = 9.10$ ). The species distribution curves based on the calculated protonation constants are shown in Figure 10.

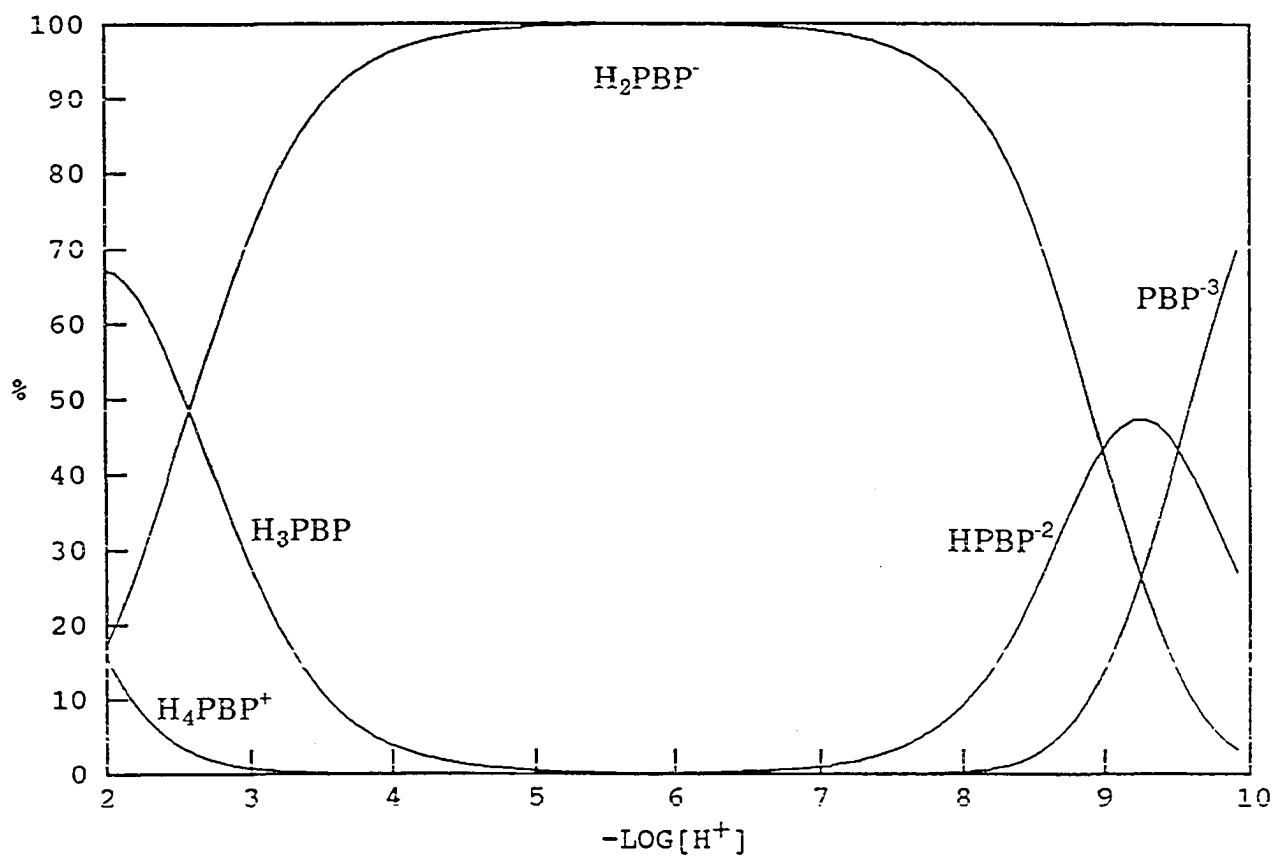


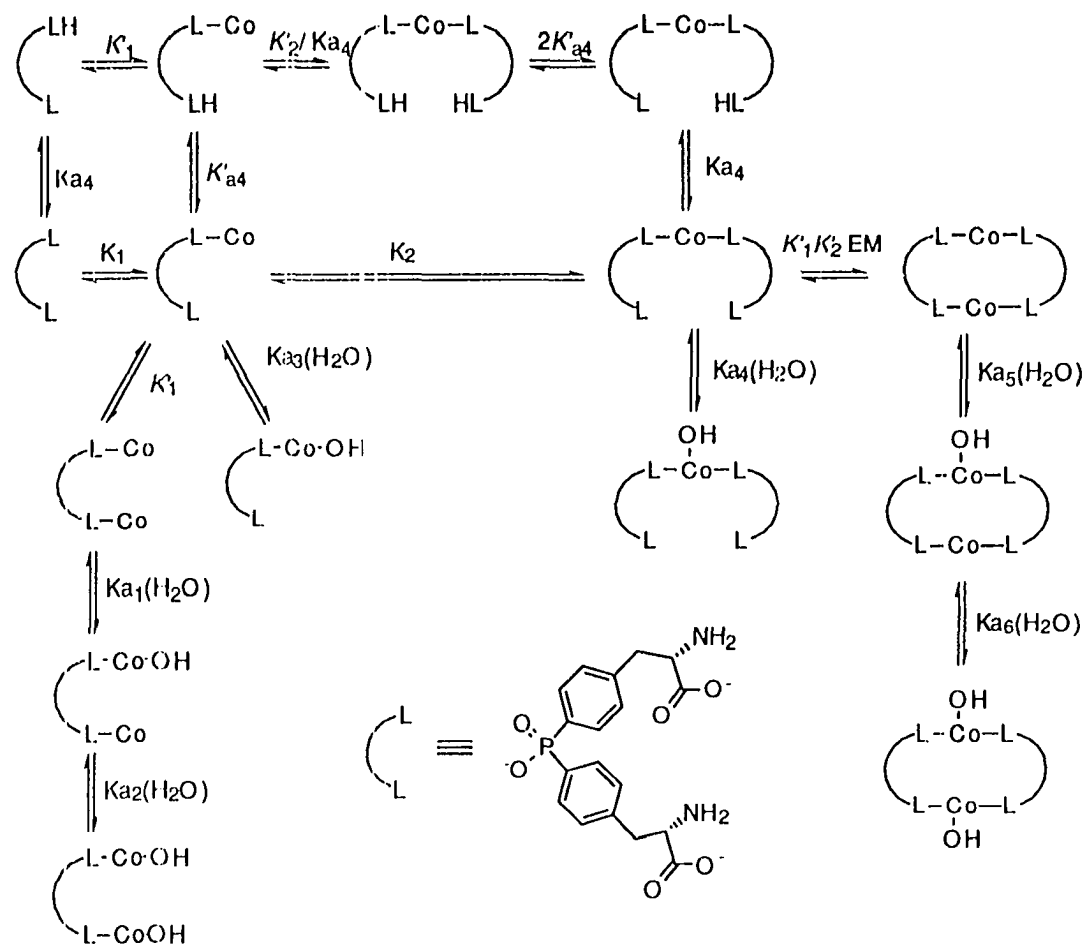
Figure 10. Species distribution as a function of pH.  $[\text{H}_4\text{PBP}^+] = 4.11 \times 10^{-3} \text{ M}$

### Stability constants of $\text{Co}^{2+}$ complexes with $\text{PBP}^{-3}$

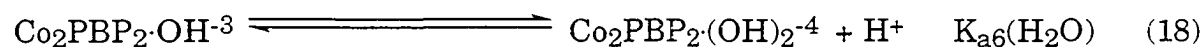
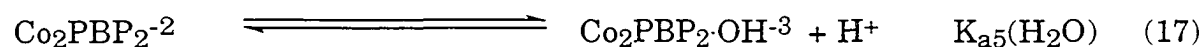
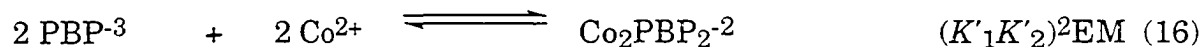
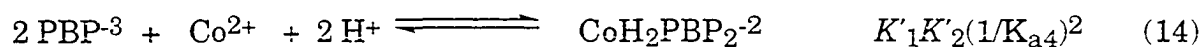
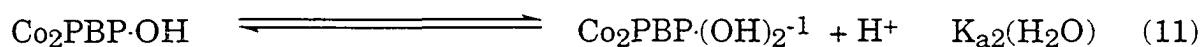
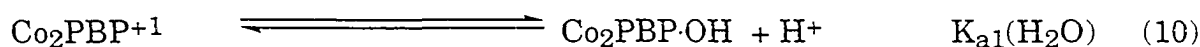
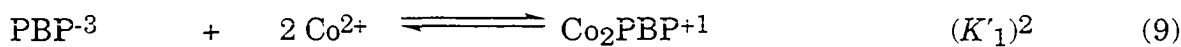
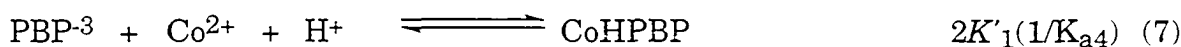
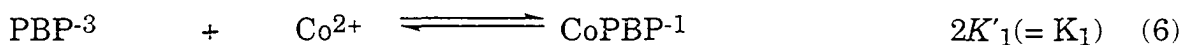
The self-assembly of the  $\text{Co}_2\text{PBP}_2$  is described by several equilibria including dimerization. The macrocyclic  $\text{Co}_2\text{PBP}_2$  is expected to form through dimerization of two monomeric  $\text{CoPBP}^{-1}$ . However, step by step equilibria are considered in calculation. All the equilibria considered in the calculation of stability constants are described in Scheme 7 where some reagents are not included for the purpose of clarity. Stability constants for each equilibrium are described in equations (6)-(18).

The relationships between the microscopic constants ( $K'_i$ ) and macroscopic constants ( $\bar{K}_i$ ) are also applied to stability constants of  $\text{Co}^{2+}$  complexes with  $\text{PBP}^{-3}$  ( $K_1 = 2 \times K'_1$ ,  $K_2 = 2 \times K'_2$ ).  $K_{a_i}(\text{H}_2\text{O})$  values are protonation constants of water bound to cobalt (II) metal ions.  $K'_{ai}$  values are microscopic protonation constants of  $\text{H}_4\text{PBP}^+$  which were obtained in the previous experiment and are not allowed to change during refinement. The stability constants in the dimerization processes can be described in terms of an "effective molarity" (EM) in addition to stability constants  $K_1$  and  $K_2$ .<sup>99, 100</sup>

This set of equations can not be fit unambiguously to our data because the large number of variables would not lead to a single solution. Therefore some constraints were made. First, the protonation constants for the free amines of PBP in  $\text{Co}^{2+}$  complexes with PBP are assumed to be same as those of  $\text{H}_4\text{PBP}^-$  (equation 7, 13, and 14) and kept constant at  $\log \bar{K}_4 = 9.50$ . Second,  $\text{pK}_a$  values for the deprotonation of water coordinated to  $\text{Co}^{2+}$  with a single PBP amino acid ligand (equations 8, 10, 11, and 15) have been approximated from the similar systems and are kept constant.  $\text{pK}_{a1}$ ,  $\text{pK}_{a2}$  and  $\text{pK}_{a3}$  are estimated as 9.58 from the stability constants of  $\text{Co}(\text{OH})_2$  ( $\log \beta_1 = 4.2$  and  $\log \beta_2 = 8.5$ )<sup>97</sup>



Scheme 7. The considered Equilibria of  $\text{Co}^{2+}$  with PBP-3.  $K_{ai}$ ,  $K'_{ai}$ : macroscopic and microscopic protonation constant of  $\text{H}_4\text{PBP}^+$ ,  $K_i$ ,  $K'_i$ : macroscopic and microscopic stability constant of  $\text{Co}^{2+}$  complex with PBP-3,  $K_{ai}(\text{H}_2\text{O})$ : macroscopic protonation constant of water molecule coordinated to  $\text{Co}^{2+}$ .



while  $\text{p}K_{a4}$  is assumed to be same with that of CoEDDA (EDDA:

ethylenediamine-N,N'-diacetate,  $\text{p}K_a = 10.6$ ).<sup>97</sup> This constraint can be rationalized by the facts that the amount of those species are less than 1 % of total concentration of  $\text{H}_4\text{PBP}^{-1}$  in the whole pH range studied and changing these constants does not affect the  $\sigma_{\text{fit}}$ . As a result, our model can be described with fewer parameters:  $K_1$ ,  $K_2$ , EM,  $\text{p}K_{a5}(\text{H}_2\text{O})$ , and  $\text{p}K_{a6}(\text{H}_2\text{O})$ .

Inspection of the species distribution curve shows that  $\text{Co}_1\text{PBP}_2$ , in its variously protonated forms, constitutes at most 6 % of the total  $\text{Co}^{2+}$ , and that in a pH region containing variously protonated forms of  $\text{Co}_1\text{PBP}_2$  at greater concentration, several of whose concentration are varying rapidly with pH in this region. These are the only species that allow determination of  $K_2$  not in combination with EM. Not surprisingly,  $K_2$  and EM are highly correlated.



For our stability constant refinement, the estimated value 3.63 was used for  $K_2$ . Details of the estimation of  $K_2$  are described in the EXPERIMENTAL SECTION. The potentiometric titration results with the calculated curve are shown in Figure 11.

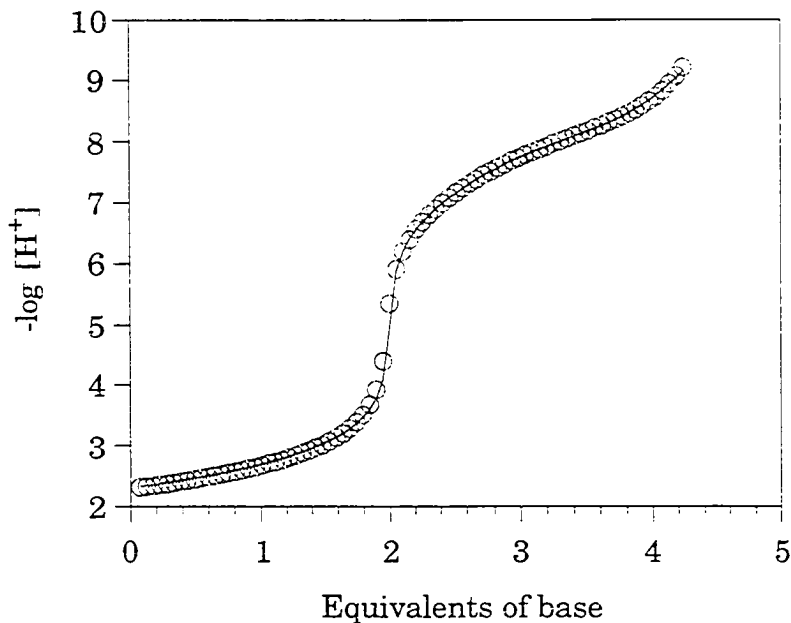


Figure 11. Potentiometric titration curves for 1:1.25 solutions for  $\text{Co}^{2+}$  and PBP. Solution is 25.0 °C,  $\mu = 0.1 \text{ M}$  (KCl), and water saturated argon gas was being flushed.  $[\text{PBP}^{-3}] = 4.0 \times 10^{-3} \text{ M}$  (○), calculated curve for formation of  $\text{Co}^{2+}$  complexes with PBP (—).

The potentiometric titration can not proceed above pH 9.5 because of formation of water insoluble  $[\text{Co}(\text{OH})_2]^{2+}$ . The formation  $[\text{Co}(\text{OH})_2]^{2+}$  with its high solubility product ( $K_{\text{sp}} = 2.5 \times 10^{-15}$ ) caused an unstable pH reading and its water insolubility interferes the reliable curve fitting. The basic algorithm of the program "BEST" is based on the mass balance relationships, therefore for

systems which form an insoluble phase the mass balance relationships employed with homogeneous solutions for  $[\text{H}_4\text{PBP}^-]_{\text{tot}}$ ,  $[\text{Co}^{2+}]_{\text{tot}}$ , and  $[\text{H}^+]_{\text{tot}}$  do not hold. The calculated stability constants and protonation constants are listed in Table 3.

Table 3. The calculated macroscopic and microscopic constants and the reported stability constants for phenylalanine.

Calculated for $\text{Co}_2\text{PBP}_2$		Literature values for $\text{Co}(\text{Phe})_2$ <sup>97</sup>	
$\mu = 0.1 \text{ M KCl}$		$\mu = 0.05 \text{ M KCl}$	$\mu = 3.0 \text{ M NaClO}_4$
$\log K_1 = 4.79$	$\log K'_1 = 4.49$	$\log K_1 = 4.05$	$\log K_1 = 4.45$
$\log K_2 = 3.93$	$\log K'_2 = 3.63^a$	$\log K_2 = 3.50$	$\log K_2 = 3.99$
$\log \text{EM} = -1.21$			
$\text{pKa}_5(\text{H}_2\text{O}) = 8.27$	$\text{pK}'_{a5}(\text{H}_2\text{O}) = 8.57$		
$\text{pKa}_6(\text{H}_2\text{O}) = 9.31$			

<sup>a</sup> estimated  $K_2$  value of  $\text{Co}(\text{Phe})_2$

Stability constants of equations (6, 7, 9) and (16, 17, 18) are relatively consistent.  $\log K_1$  is always refined to the value between 4.5 and 4.8 while  $\log \{(K'_1 K'_2)^2 \text{EM}\}$  is refined between 14.0 and 15.0 regardless of other constants. This result implies that the calculated value of  $K_1$  and  $(K'_1 K'_2)^2 \text{EM}$  are reliable. The  $\log \text{EM}$  value can be calculated by using estimated  $\log K'_2$  value and considered with  $\pm 0.2$  error. The calculated effective molarity is  $(6.2 \pm 1.6) \times 10^{-2} \text{ M}$ . This means that the complex between  $\text{Co}^{2+}$  and  $\text{PBP}^{-3}$  prefers to be a macrocyclic form

in basic solution when PBP-3 (or  $\text{Co}^{2+}$ ) concentration is below  $(6.2 \pm 1.6) \times 10^{-2}$  M.

The pKa values for the deprotonation of water coordinated to the  $\text{Co}^{2+}$ /PBP-3 complexes are lower by several log units than the aqueous value 13.75.<sup>97</sup> Billo compared pKa values of water bound to  $\text{Co}^{2+}$  coordinated with several ligands and suggested that the coordination geometry as well as hydrophobic interactions affects the acidity of the metal coordinated water molecule.<sup>101</sup> A water molecule coordinated to a  $\text{Co}^{2+}$  octahedral complex with ethylenediamine-*N,N'*-diacetate (EDDA) has a pKa value of 10.6 while pKa of water molecule coordinated to  $\text{Co}^{2+}$  square pyramidal complex with 1,5-diazacyclooctane-*N,N'*-diacetic acid (DACODA) is 9.27. As the coordination number decreases, the Lewis acidity of the metal may increase and deprotonation of the metal coordinated water molecule is facilitated. The pKa value of a water molecule coordinated to  $\text{Co}^{2+}$ -Me<sub>6</sub>tren is 8.80 which is significantly lower than for the analogous  $\text{Co}^{2+}$ -tren (10.22) even though both complexes have same trigonal bipyramidal coordination geometry. The increased acidity was considered to be a result of the local hydrophobic environment provided by the methyl group. Extremely low pKa values have been proposed for inner-sphere-coordinated water molecule in metal-enzyme complexes such as horse liver alcohol dehydrogenase (HLADH).<sup>102</sup> The pKa values for  $\text{Co}^{2+}$ -HLADH( $\text{H}_2\text{O}$ ) and  $\text{Co}^{2+}$ -HLADH( $\text{NAD}^+$ ,  $\text{H}_2\text{O}$ ) complexes are 9 and 7, respectively. The hydrophobic properties of the active site cavity are thought to be the reason for a further lowering of the water pKa. While the origin of the observed extraordinary pKa values in  $\text{Co}^{2+}$  complexes with PBP-3 has not been established, it seems possible that the effect is due either to a 5 coordinated geometry of  $\text{Co}^{2+}$  complex (trigonal bipyramidal or square pyramidal) or to the hydrophobic environment which is provided by aryl groups in the  $\text{Co}^{2+}$  complex

with PBP<sup>-3</sup>. The species distribution curves based on the calculated stability constants are shown in Figure 12 as a function of solution pH. Around neutral pH, acyclic complexes CoHPBP and Co<sub>2</sub>PBP<sup>+</sup> are the predominant complexes. As the solution pH increases, acyclic complexes begin to dimerize to macrocyclic Co<sub>2</sub>PBP<sub>2</sub> complexes. Above pH 9, where all binding studies were carried out, essentially all Co<sup>2+</sup> ions in the solution make the macrocycle which is responsible for the substrate binding. The exceptionally low pK<sub>a</sub> of bound water makes deprotonated form Co<sub>2</sub>PBP<sub>2</sub>·OH<sup>-3</sup> a major component in the pH range 8.5-9.5. The EM value of  $(6.2 \pm 1.6) \times 10^{-2}$  M gives the preference for a cyclic structure. Above this concentration, some higher oligomers may form. Below this concentration, doubly amino acid ligand cobalt is confidently assigned to the Co<sub>2</sub>PBP<sub>2</sub> complexes.

### **Paramagnetic susceptibility**

The formation of macrocyclic Co<sub>2</sub>PBP<sub>2</sub> is supported by the potentiometric titrations, and its binding ability is observed. Even though the coordination number of Co<sup>2+</sup> in Co<sub>2</sub>PBP<sub>2</sub> was suggested with the potentiometric titration results, more direct evidences are needed to determine the geometry of Co<sup>2+</sup> in Co<sub>2</sub>PBP<sub>2</sub>. To determine the geometry, the paramagnetic susceptibility of Co<sub>2</sub>PBP<sub>2</sub> was measured.

The measurement of the magnetic moment of a coordination complex containing unpaired electron spins is useful in establishment of the valency of the metal atom, and in many cases also helps to determine the geometrical structure of the complex. The fact that the chemical shift of a molecule in the <sup>1</sup>H NMR spectrum depends on the bulk susceptibility of the medium where the molecule is situated enables one to measure the magnetic susceptibility of the molecule by <sup>1</sup>H NMR. The <sup>1</sup>H NMR method for measurement of magnetic susceptibilities has

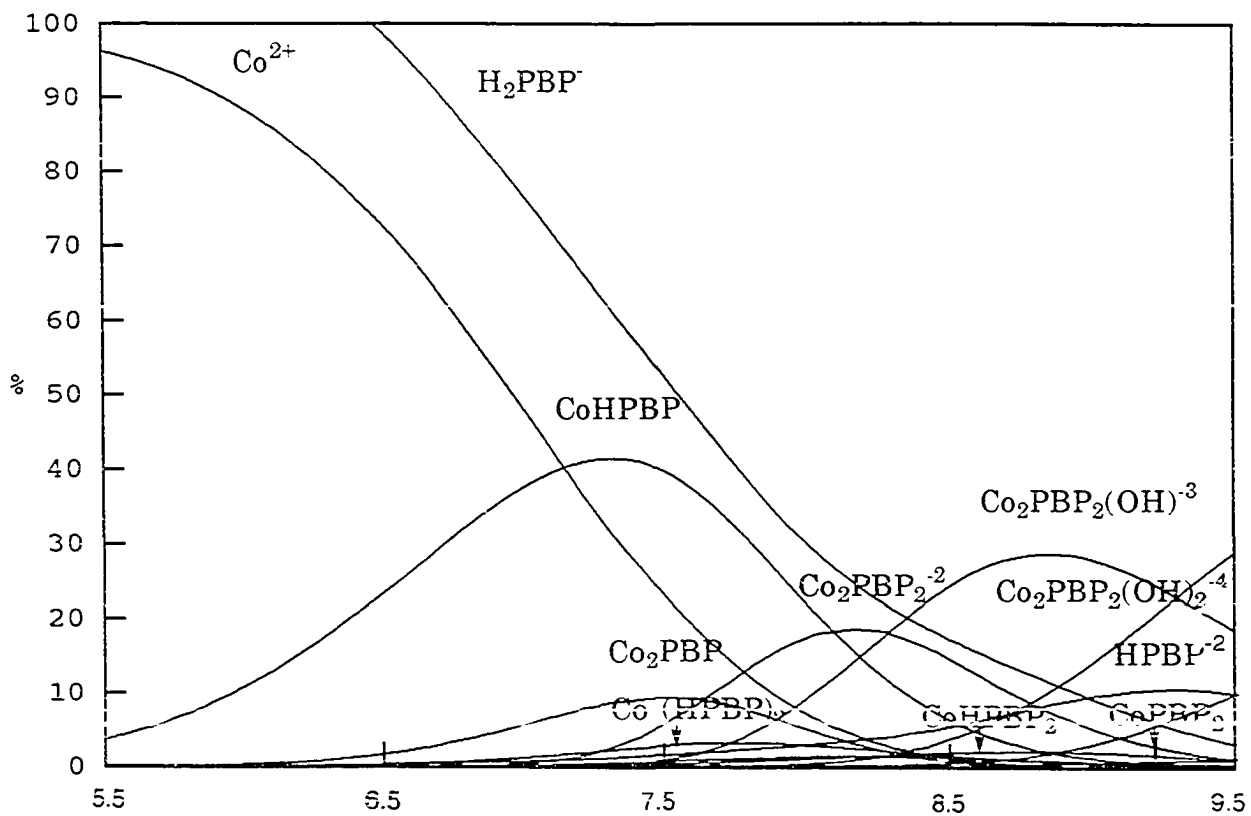


Figure 12. Species distribution as a function of solution pH.

$[\text{PBP}^{3-}] = 4.03 \times 10^{-3} \text{ M}$ ,  $[\text{Co}^{2+}] = 3.22 \times 10^{-3} \text{ M}$ ,  $\mu = 0.1 \text{ M (KCl)}$ .

been developed by Evans<sup>103</sup> and improved by other researchers.<sup>104, 105</sup>

The paramagnetic susceptibility of  $\text{Co}_2\text{PBP}_2$  was measured by  $^1\text{H}$  NMR using the Evans method.<sup>103-105</sup> Chemical shifts of an inert "indicator" in different media are measured by using a set of coaxial NMR tubes. *t*-BuOH is used for the indicator. The difference in chemical shifts is used to calculate the magnetic susceptibility and the effective magnetic moment of  $\text{Co}_2\text{PBP}_2$  according to equation (20)-(22).

$$\chi = \frac{3 \cdot \Delta\nu}{4 \cdot \pi \cdot \nu \cdot m} + \chi_0 \quad (20)$$

$$\chi_m = \chi \times \text{M.W.} \quad (21)$$

$$\mu_M = \sqrt{2.344 \times 10^3 \cdot \chi_m} \quad (22)$$

$\chi$  : mass susceptibility,  $\chi_0$  : paramagnetic susceptibility of the solvent ( $-0.72 \times 10^{-6}$  for dilute *t*-butyl alcohol solution),  $\chi_m$  : molar susceptibility,  $\mu_M$ : effective magnetic moment in Bohr magnetons (B.M.),  $\nu$  : frequency at which the proton resonance is studied in cycles/sec,  $\Delta\nu$  : frequency separation between the two lines in cycles/sec.  $m$  : mass of substance contained in 1 ml of solution.

The observed effective magnetic moment of  $\text{Co}_2\text{PBP}_2$  is  $6.6 \pm 0.6$  B.M. at 19 °C. Using the equation (23), the effective magnetic moment for the individual  $\text{Co}^{2+}$  was calculated as 4.7 B.M. The magnetic moment is higher than the "spin-only" value of 3.87 for 3 unpaired electrons (equation (24)) because the  $\text{Co}^{2+}$  complex exhibits spin-orbital coupling.

$$(\mu_M)^2 = (\mu_1)^2 + (\mu_2)^2 \quad (23)$$

$$\mu_M = \{ n(n+2) \}^{1/2} \quad (24)$$

where  $\mu_1, \mu_2$  are the magnetic moment of each  $\text{Co}^{2+}$  and  $n$  is the number of unpaired electrons.

Table 4. Typical values of the room temperature effective magnetic moments of  $\text{Co}^{2+}$  complexes in various coordination environments.

	$\mu_M$ (B.M.)			
	Octahedral	Square pyramidal	Trigonal bipyramidal	Tetrahedral
Typical values <sup>106</sup>	4.77 - 5.40	4.28 - 5.07	4.26 - 5.03	3.98 - 4.82
$\text{Co}(\text{H}_2\text{O})_6$ <sup>110</sup>	5.12			
$\text{Co}(\text{Me}_6\text{tren})_2$ <sup>108</sup>			4.51	
$\text{Co}(\text{DACODA})_2$ <sup>109</sup>		4.81		
$\text{Co}(\text{His})_2$ <sup>110</sup>	5.16			4.48
$\text{Co}(\text{Phe})_2$ <sup>92</sup>				4.20
$\text{Co}(\text{Gly})_2$			$5.0 \pm 0.4$	
$\text{Co}_2(\text{PBP})_2$			$4.7 \pm 0.4$	

According to Table 4, the observed magnetic moment of 4.7 B.M. corresponds to the lower range of the typical value of high-spin octahedral  $\text{Co}^{2+}$  complexes and to the higher range of tetrahedral complexes. The magnetic moment of the tetrahedral  $\text{Co}(\text{Phe})_2$  complex has been reported as 4.20 B.M.<sup>107</sup>

Five-coordinate  $\text{Co}^{2+}$  complexes have similar magnetic moments to that of  $\text{Co}_2\text{PBP}_2$ . For example, trigonal bipyramidal complex  $\text{Co}(\text{Me}_6\text{tren})$  has 4.51 B.M.<sup>108</sup> and square pyramidal complex  $\text{Co}(\text{DACODA})$  has 4.81 B.M.<sup>109</sup> In addition to the potentiometric titration results which provide the evidence of water coordination to  $\text{Co}^{2+}$ , the magnetic moment value provides the clue in assuming the complex geometry. The similarity of magnetic moment between  $\text{Co}_2\text{PBP}_2$  and 5-coordinate complex suggests that  $\text{Co}^{2+}$  in  $\text{Co}_2\text{PBP}_2$  may be 5-coordinated. The unusually low pKa values of the water coordinated to  $\text{Co}_2\text{PBP}_2$  also support a 5-coordinate structure.

One of the interesting characteristics of  $\text{Co}_2\text{PBP}_2$  is its stability to oxidation. Unlike typical octahedral or tetrahedral  $\text{Co}^{2+}$  amino acid complexes,  $\text{Co}^{2+}$  of  $\text{Co}_2\text{PBP}_2$  did not oxidize to  $\text{Co}^{3+}$  with hydrogen peroxide in the presence of air. Averill et al. reported that square pyramidal complex  $\text{Co}(\text{DACODA})(\text{H}_2\text{O})$  was stable to the oxidation.<sup>109</sup> Neither air nor hydrogen peroxide in the presence or absence of charcoal produced a  $\text{Co}^{3+}$  complex. They explained that the ligand DACODA might kinetically inhibit the oxidation. The stability of  $\text{Co}_2\text{PBP}_2$  to oxidation suggest as well a 5-coordinate structure.

### **Electrospray mass spectroscopy**

The macrocycle  $\text{Co}_2\text{PBP}_2$  exists in equilibrium with its components  $\text{Co}^{2+}$  and PBP. The nature of the substitutionally labile  $\text{Co}^{2+}$  complex requires very



mild ionization conditions to be detected in mass spectroscopy. While no peak was detected in FAB mass, the ionic character of the  $\text{Co}_2\text{PBP}_2$  complex makes the negative ion electrospray method the best option. Negative ion electrospray mass spectroscopy was performed on a Hewlett Packard MS engine model B. The skimmer and voltage have been kept at minimum to minimize in source fragmentation. The sample was prepared by adding 0.9 equivalent  $\text{Co}^{2+}$  to the aqueous  $1.85 \times 10^{-3}$  M PBP solution which had been prepared by dissolving PBP Li salt and converting it to a trianion with 2 equivalents of LiOH. Nanopure water was used which had been degassed by boiling for an hour and argon gas flushing to prevent the possible oxidation of  $\text{Co}^{2+}$  to  $\text{Co}^{3+}$ .

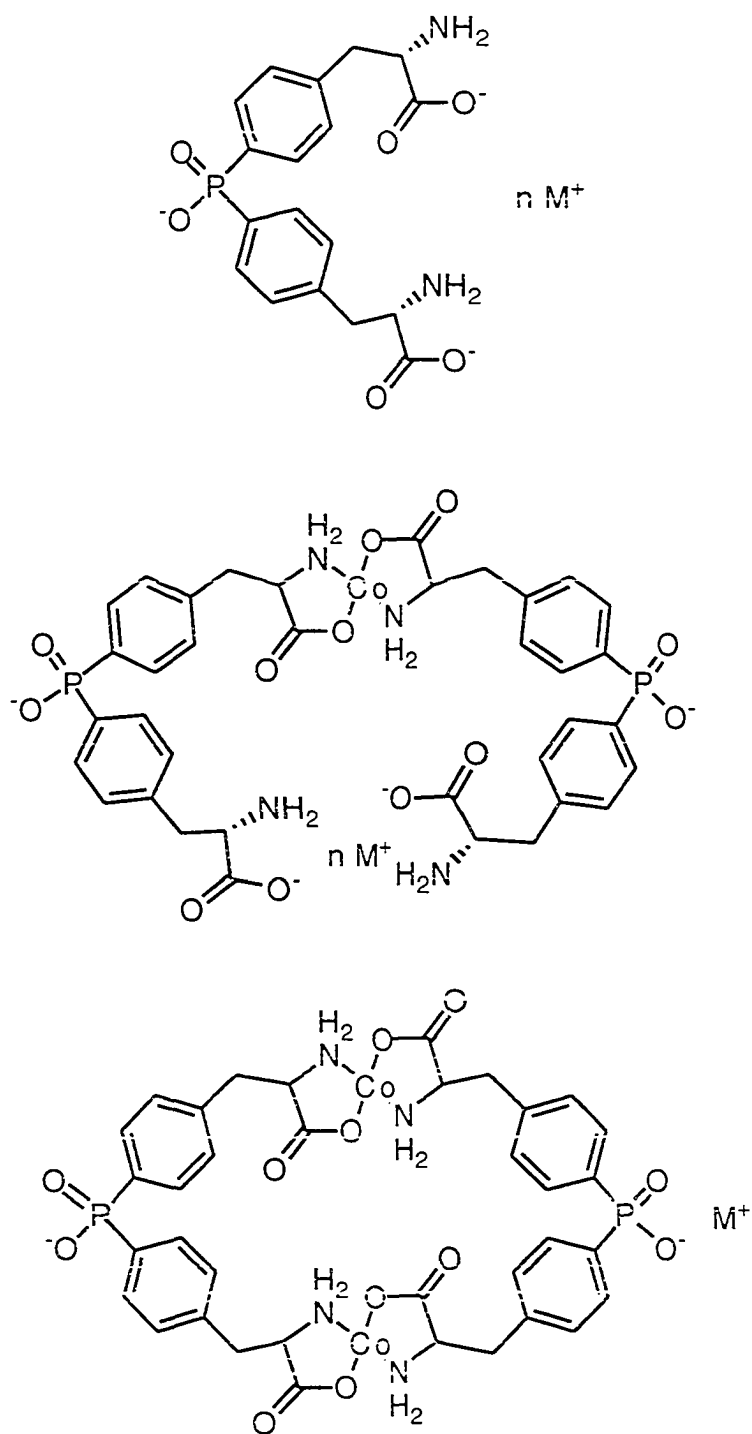
The mass spectral data show the presence of three main species of the  $\text{Co}^{2+}$ /PBP complex: free PBP, one  $\text{Co}^{2+}$  ligated by two PBP, and the macrocyclic dimer  $\text{Co}_2\text{PBP}_2$ . The results are shown in Figure 13, 14, 15 and Table 5. The base peak at  $M/z = 448.3$  corresponds to the dianionic form of  $\text{Co}_2\text{PBP}_2$  **23**. The next most intense peak at  $M/z = 391.3$  corresponds to free PBP **20**. Less intense peaks at high  $M/z$  values result from the monoanionic form of  $\text{Co}(\text{PBP})_2$  **23**, **23 (a, b, c, d)** and  $\text{Co}_2\text{PBP}_2$  **21 (a, b)** complexes. The peak at  $M/z = 1981$  can not be explained with any possible combination of the components including higher oligomers. The fact that this peak is not accompanied by isotope peaks suggest that it may be an artifact.

The interesting point is that there are no peaks corresponding to  $\text{Co}^{2+}$ -PBP complex with ligated water, while potentiometric titration and magnetic moment results suggest the water ligation to the  $\text{Co}^{2+}$ . Even though the reason for this result has not been established, it seems that  $\text{Co}^{2+}$  of  $\text{Co}_2\text{PBP}_2$  may

Table 5. Assignments of M/z of mass spectrum with the possible compounds.\*

	Abbreviation	Charge	Formula	M/z
20	PBP	-1	C <sub>18</sub> H <sub>20</sub> N <sub>2</sub> P O <sub>6</sub>	391.3
20(a)	PBP Li	-1	C <sub>18</sub> H <sub>19</sub> N <sub>2</sub> P O <sub>6</sub> Li	397.3
23	Co(PBP) <sub>2</sub>	-1	C <sub>36</sub> H <sub>39</sub> N <sub>4</sub> P <sub>2</sub> O <sub>12</sub> Co	840.6
23(a)	Co(PBP) <sub>2</sub> Li	-1	C <sub>36</sub> H <sub>38</sub> N <sub>4</sub> P <sub>2</sub> O <sub>12</sub> Co Li	846.5
23(b)	Co(PBP) <sub>2</sub> Li <sub>2</sub>	-1	C <sub>36</sub> H <sub>37</sub> N <sub>4</sub> P <sub>2</sub> O <sub>12</sub> Co Li <sub>2</sub>	852.5
23(c)	Co(PBP) <sub>2</sub> Li <sub>3</sub>	-1	C <sub>36</sub> H <sub>36</sub> N <sub>4</sub> P <sub>2</sub> O <sub>12</sub> Co Li <sub>3</sub>	858.4
23(d)	Co(PBP) <sub>2</sub> Li <sub>2</sub> Na	-1	C <sub>36</sub> H <sub>36</sub> N <sub>4</sub> P <sub>2</sub> O <sub>12</sub> Co Li <sub>2</sub> Na	874.5
21	Co <sub>2</sub> (PBP) <sub>2</sub>	-2	C <sub>36</sub> H <sub>36</sub> N <sub>4</sub> P <sub>2</sub> O <sub>12</sub> Co <sub>2</sub>	448.3
21(a)	Co(PBP) <sub>2</sub> H	-1	C <sub>36</sub> H <sub>37</sub> N <sub>4</sub> P <sub>2</sub> O <sub>12</sub> Co <sub>2</sub>	897.5
21(a)	Co(PBP) <sub>2</sub> Li	-1	C <sub>36</sub> H <sub>36</sub> N <sub>4</sub> P <sub>2</sub> O <sub>12</sub> Co <sub>2</sub> Li	903.5

\* Structures are shown in Figure 16.



	$n \text{ M}^+$
20	$\text{H}^+, \text{H}^+$
20(a)	$\text{H}^+, \text{Li}^+$

	$n \text{ M}^+$
23	$\text{H}^+, \text{H}^+, \text{H}^+$
23(a)	$\text{H}^+, \text{H}^+, \text{Li}^+$
23(b)	$\text{H}^+, \text{Li}^+, \text{Li}^+$
23(c)	$\text{Li}^+, \text{Li}^+, \text{Li}^+$
23(d)	$\text{Li}^+, \text{Li}^+, \text{Na}^+$

	$\text{M}^+$
21	--
21(a)	$\text{H}^+$
21(b)	$\text{Li}^+$

Figure 13. Structures of  $\text{Co}^{2+}$  complexes with PBP.

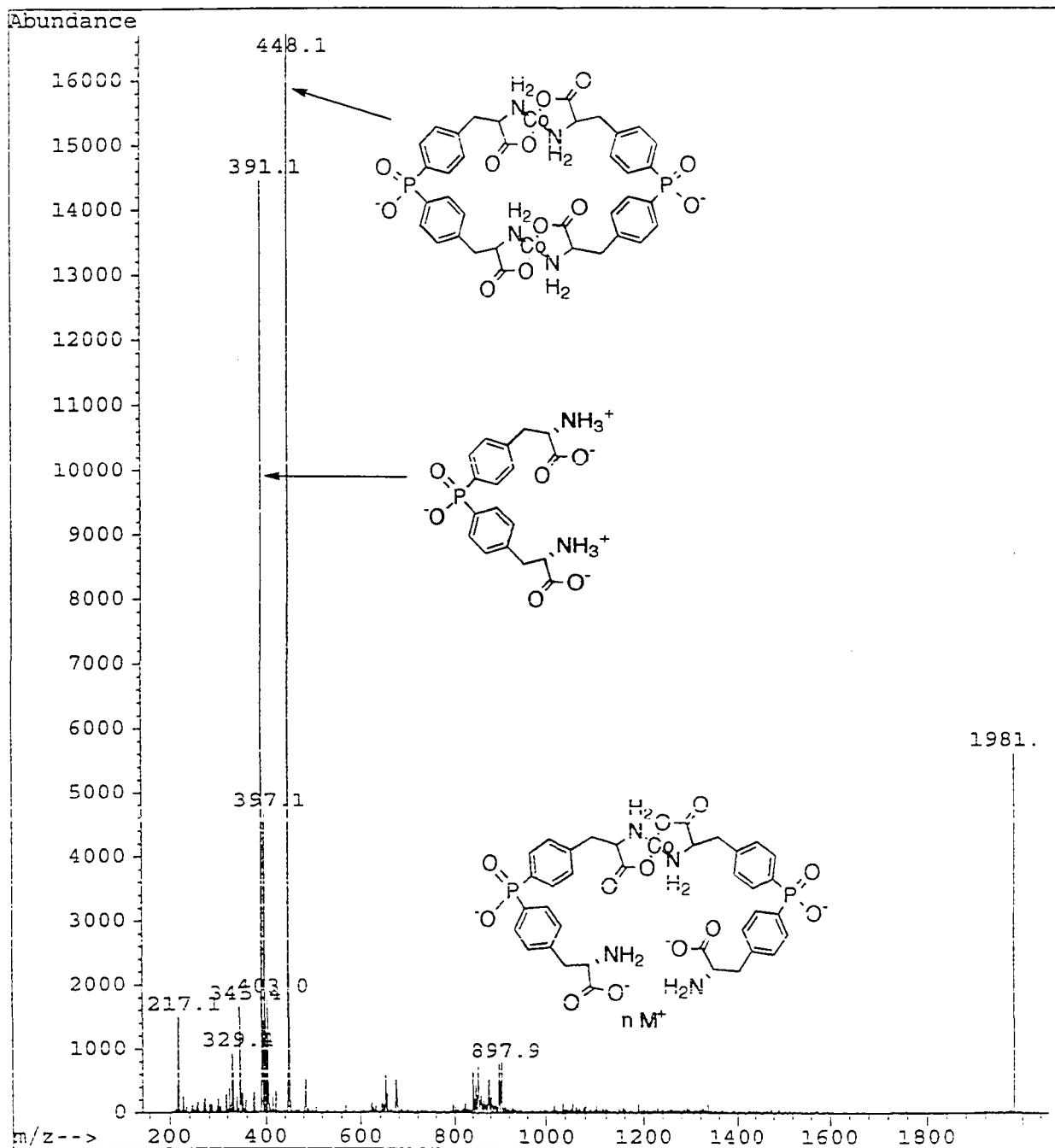


Figure 14. Negative ion electrospray mass spectrum of  $\text{Co}_2\text{PBP}_2$ .

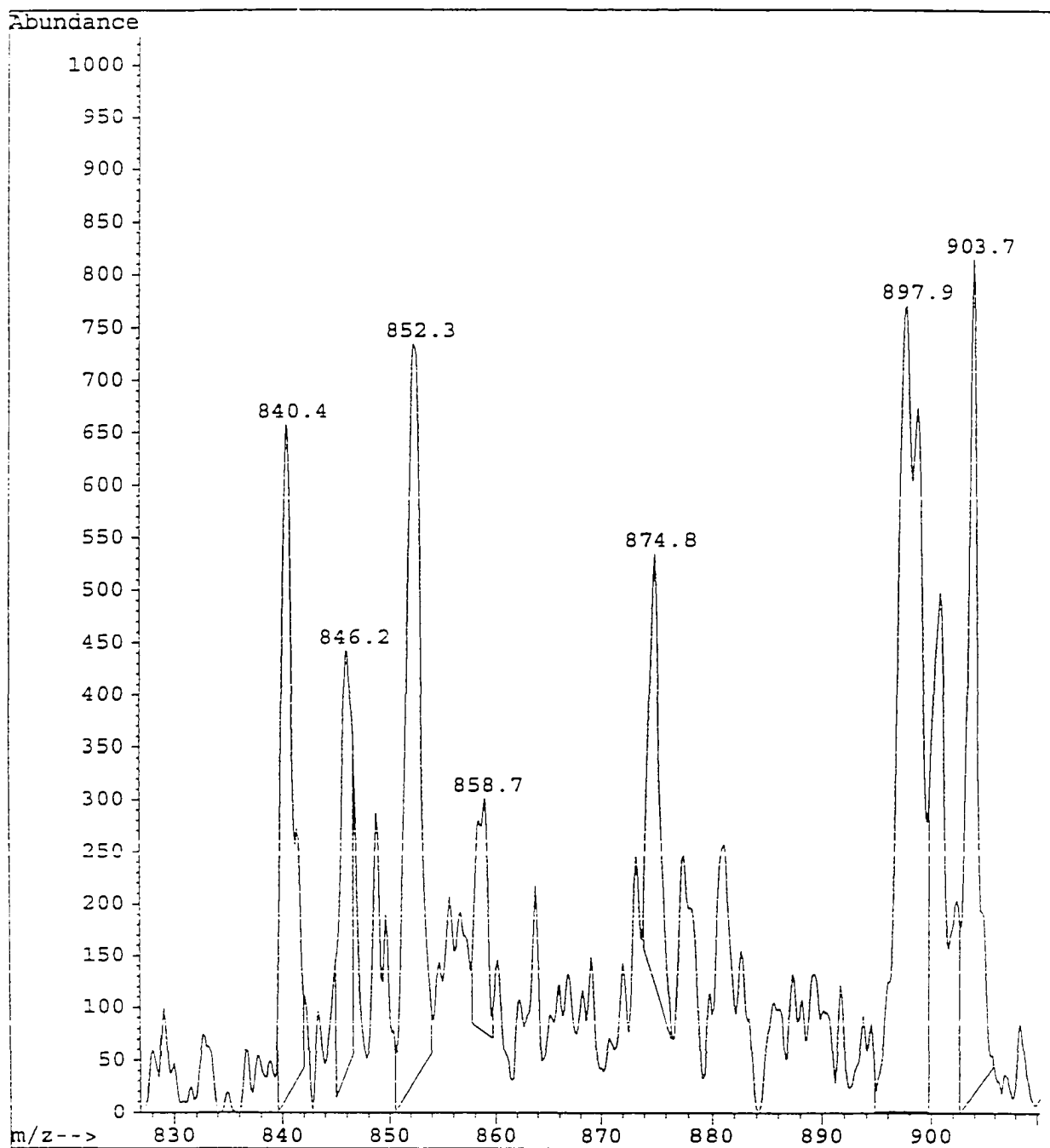


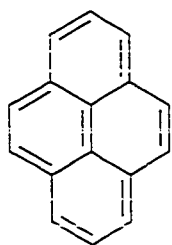
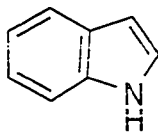
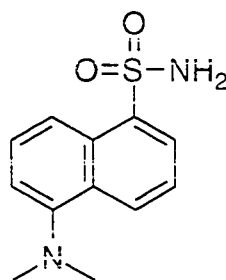
Figure 15. Negative ion electrospray mass spectrum of  $\text{Co}_2\text{PBP}_2$ . Expansion of Figure 14 from  $M/z = 830$  to  $M/z = 910$ .

exist in a 4 coordinated structure in the gas phase. These MS data show that PBP is present mostly as either dimeric  $\text{Co}_2\text{PBP}_2$  or free PBP in basic aqueous solution. This result coincides very well with other evidence such as the potentiometric titration and  $^1\text{H}$  NMR spectra of  $\text{Co}_2\text{PBP}_2$  discussed below.

### Fluorescence spectra

We observed binding ability of  $\text{Co}_2\text{PBP}_2$  qualitatively by carrier mediated transport experiments. Fluorescence spectroscopy is one of the most frequently applied methods for detection of host-guest complexation. Quantitative binding studies using fluorescence spectroscopy were planned.

Fluorescence indicators exhibit either notable changes in fluorescence intensities or emission wavelength shifts when they are in hydrophobic organic solvents or complexed in lipophilic host cavity in aqueous solution. Most applications of fluorimetry to binding are fluorescence intensity measurements. Pyrene **29**, indole **30**, and dansyl amide **58** have been used for fluorescence indicators in binding studies of receptor  $\text{Co}_2\text{PBP}_2$ .

**29** $\lambda_{\text{ex}}$  268 nm $\lambda_{\text{em}}$  342 nm**30** $\lambda_{\text{ex}}$  334 nm $\lambda_{\text{em}}$  371 nm**58** $\lambda_{\text{ex}}$  328 nm $\lambda_{\text{em}}$  576 nm

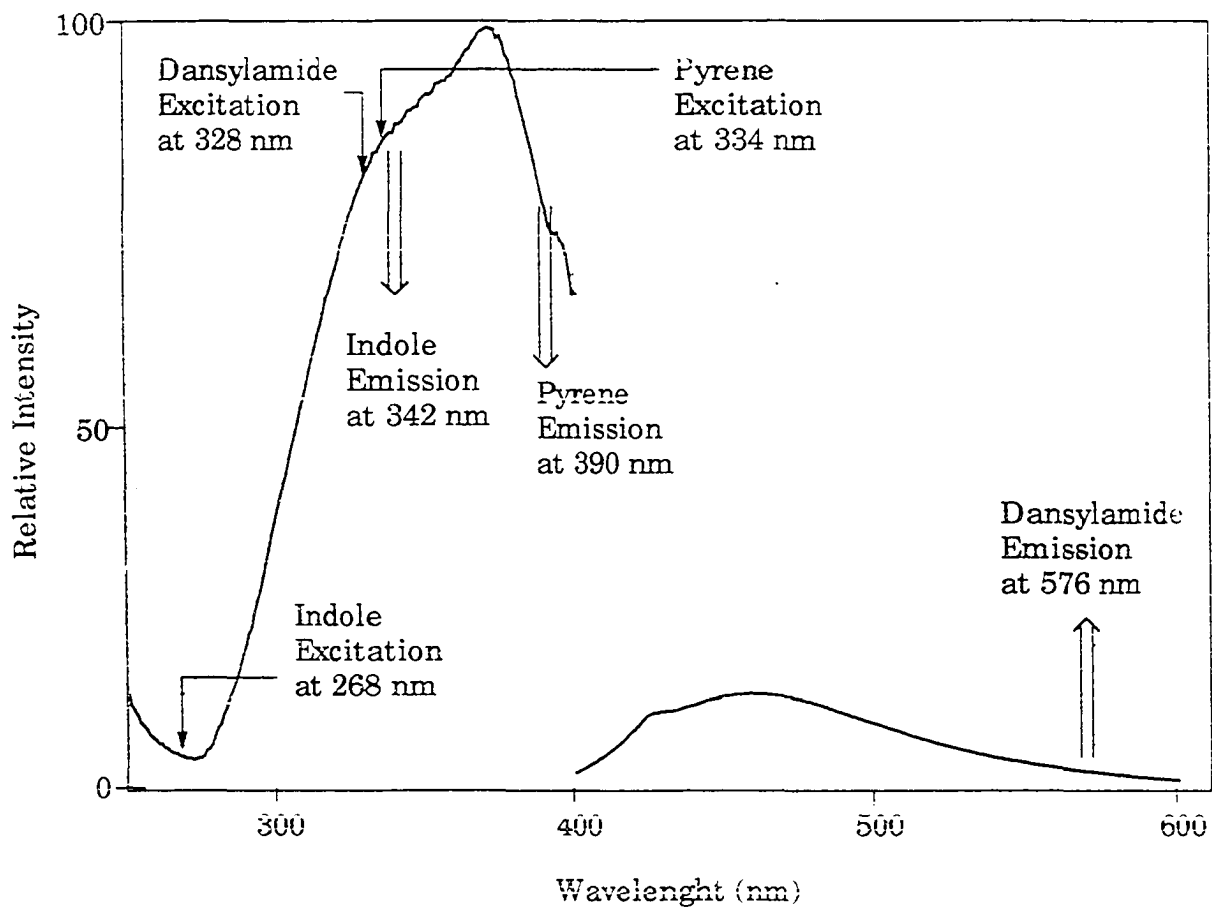


Figure 16. Fluorescence spectrum of  $\text{Co}_2\text{PBP}_2$  in 0.1 M borate buffer.

The receptor  $\text{Co}_2\text{PBP}_2$  itself shows fluorescence at 457 nm when excited at 372 nm in aqueous 0.1 M borate buffer (Figure 16). The  $\text{Co}_2\text{PBP}_2$  absorption interferes with excitation, emission (or both) wavelength for all the substrates tried, preventing accurate binding measurement.

### Quantitative Binding Studies with $^1\text{H}$ NMR

NMR has been widely applied for the evaluation of host-guest phenomena. NMR methods have advantages over UV and fluorescence methods because NMR is not subject to misinterpretations caused by minor impurities. NMR can also reveal valuable information about complexes in solution, primarily from chemical shift measurements of the complexed species.<sup>111, 112</sup> Quantitative binding studies of receptor  $\text{Co}_2\text{PBP}_2$  were carried out by the NMR method.

The presence of a paramagnetic transition metal ion in a coordination compound produces large isotropic shifts in the NMR spectra that result from contact interactions and dipolar interactions.<sup>110, 113</sup>  $\text{Co}^{2+}$  introduces paramagnetic anisotropy in  $^1\text{H}$  NMR of macrocycle  $\text{Co}_2\text{PBP}_2$ . Extraordinary high downfield chemical shifts of all protons of PBP upon the formation of macrocycle  $\text{Co}_2\text{PBP}_2$  are shown in Figure 17. The  $\alpha$ -proton resonance is shifted from 3.6 ppm to 121 ppm and  $\beta$ -protons are shifted from 3.0 and 2.8 ppm to 16 ppm (the doubled AB quartet has coalesced to a single unresolved resonance), and aromatic proton signals are shifted from 7.4 and 7.1 ppm to 8.1 and 9.1 ppm, respectively. Isotropic shifts of  $\text{Co}^{2+}$  complexes with glycine and alanine are reported in the same chemical shift range.<sup>110</sup>



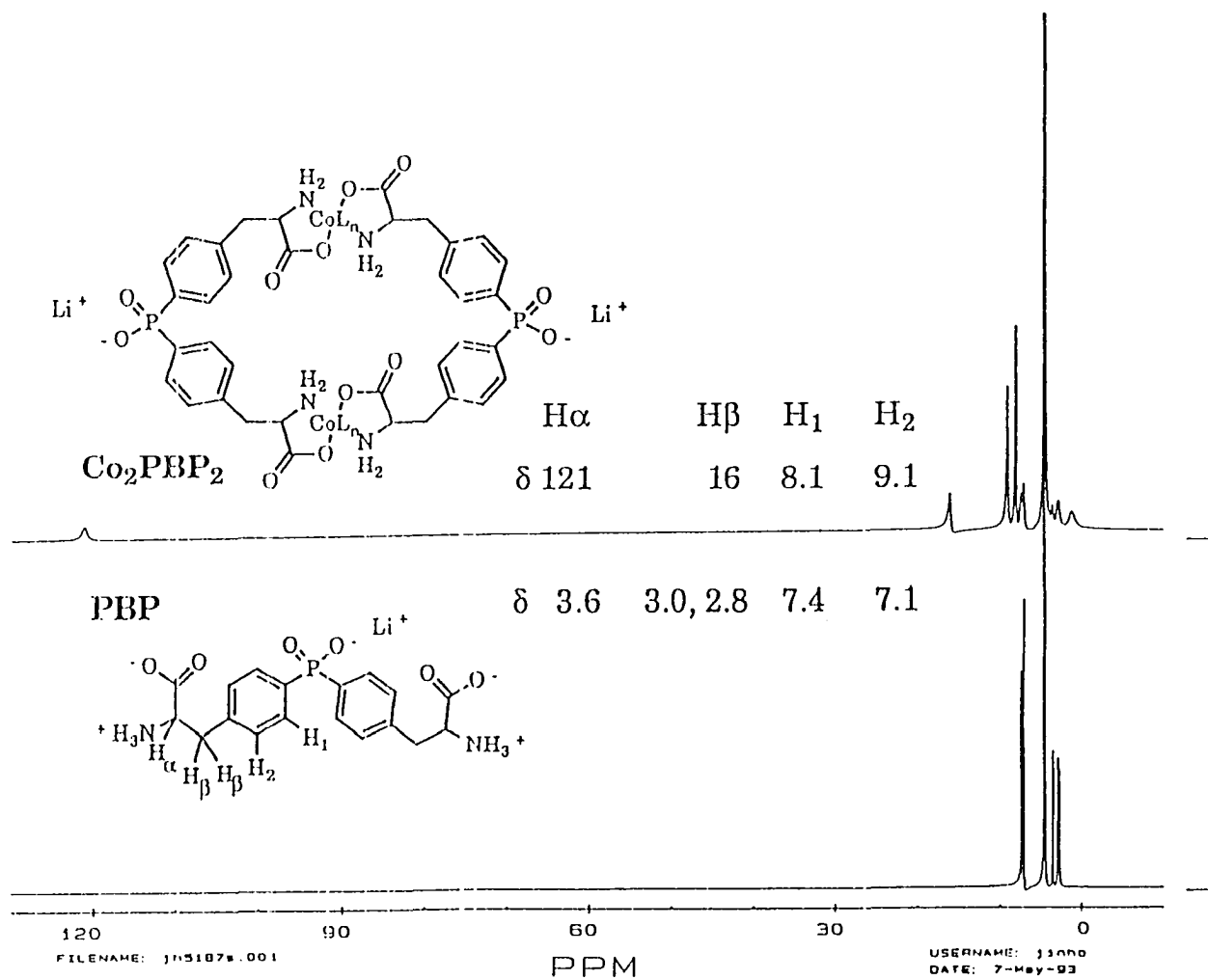


Figure 17.  $^1\text{H}$  NMR spectra of PBP and  $\text{Co}_2\text{PBP}_2$  at 0.2 M pD 9 borate buffer.

$$[\text{PBP}] = 7.2 \times 10^{-3} \text{ M}, [\text{Co}_2\text{PBP}_2] = 1.3 \times 10^{-3} \text{ M}$$

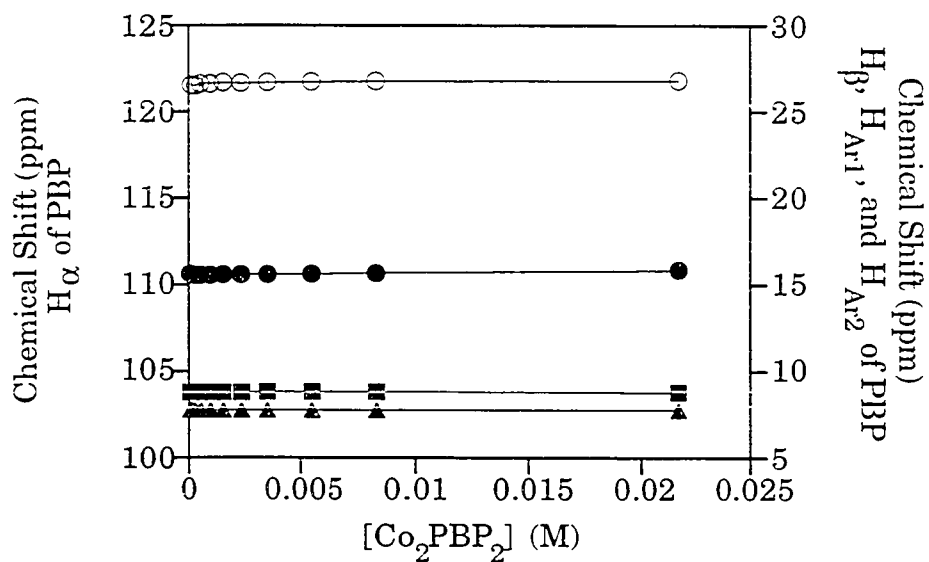


Figure 18. <sup>1</sup>H NMR chemical shifts of Co<sub>2</sub>PBP<sub>2</sub> as a function of [Co<sub>2</sub>PBP<sub>2</sub>]: α proton (○), β proton (●), aromatic proton 1 (■), aromatic proton 2 (▲).

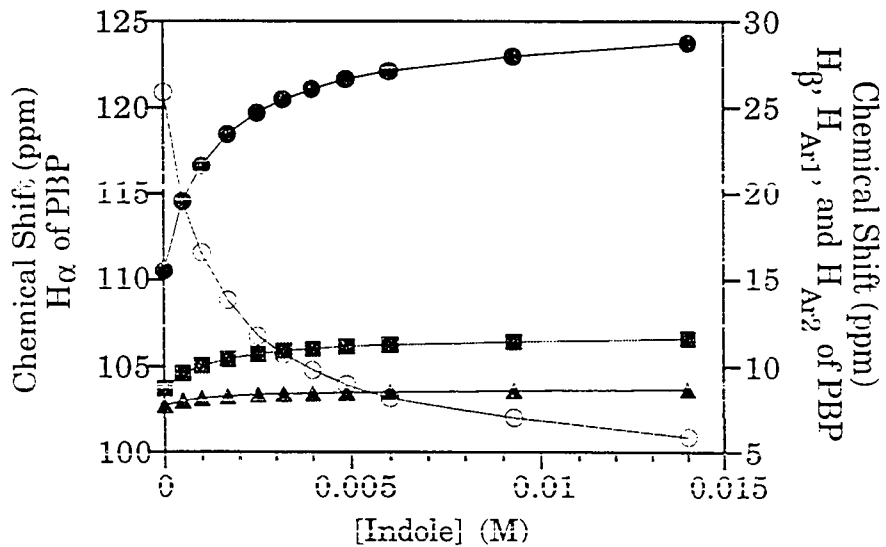


Figure 19. <sup>1</sup>H NMR of Co<sub>2</sub>PBP<sub>2</sub>: Effect of Indole: [Co<sub>2</sub>PBP<sub>2</sub>] = 4.0 × 10<sup>-4</sup> M, α proton (○), β proton (●), aromatic proton 1 (■), aromatic proton 2 (▲).

The positions of these chemical shifts are not affected by the concentration change of  $\text{Co}_2\text{PBP}_2$  from  $6.3 \times 10^{-5}$  M up to  $2.2 \times 10^{-2}$  M (Figure 18), which implies that any critical aggregation concentration (CAC) of  $\text{Co}_2\text{PBP}_2$  is higher than  $2.2 \times 10^{-2}$  M. Chemical shifts of protons of PBP unbound to  $\text{Co}^{2+}$  remain in their original positions regardless of concentration changes, and are observable since they do not exchange rapidly with  $\text{Co}_2\text{PBP}_2$ . Note that, at concentrations of  $\text{Co}_2\text{PBP}_2$  below  $2 \times 10^{-4}$  M where the  $\text{Co}_2\text{PBP}_2$  begins to dissociate and the *integrals* decrease (discussed in Circular Dichroism section), the chemical shifts of  $\text{Co}^{2+}$  bound material remain constant.

Chemical shifts of  $\text{Co}_2\text{PBP}_2$  protons are changed by the addition of arenes to the aqueous solution of the macrocycle. Chemical shifts of  $\text{Co}_2\text{PBP}_2$  protons are plotted as a function of the concentration of added indole in Figure 19. While the chemical shift of the  $\alpha$ -proton shows an upfield shift, the  $\beta$ -protons and aromatic protons show a downfield shift. Changes of chemical shifts increase with the concentration of the arene and show saturation at high arene concentration. These chemical shift changes, caused by inclusion complexation, are used for calculation of binding affinity. Dissociation constants were obtained by non-linear least squares fitting of the chemical shift change with  $K_D$  and  $\Delta\delta_{\text{max}}$  as the only variable parameters to Wilcox's equation:<sup>96</sup>

$$\delta_{\text{obs}} = \delta_o + \frac{\Delta\delta_{\text{max}}}{2H_o} \left( S - \sqrt{S^2 - 4H_oG_o} \right) \quad (25)$$

where  $S = H_o + G_o + K_D$ ,  $K_D$  is the dissociation constant,  $H_o$  is the total host concentration added to the sample,  $G_o$  is the corresponding guest concentration,  $\delta_{\text{obs}}$  is the observed chemical shift of the host,  $\delta_o$  is the shift of the free host, and  $\Delta\delta_{\text{max}}$  is the extrapolated shift of fully complexed host.

These chemical shift changes fit nicely to 1:1 binding isotherm providing

evidence of 1:1 complexation between indole guest and  $\text{Co}_2\text{PBP}_2$  host. The same dissociation constant  $K_D$  ( $1.18 \pm 0.11$ )  $\times 10^{-3}$  M was obtained by fitting the shifts of each protons.  $\Delta\delta_{\text{max}}$  values are listed in Table 6 and 7.

In a separate, reverse titration, the changes in indole shifts on binding also fit the 1:1 binding equation (with lower precision) to yield the same dissociation constant ( $7.1 \pm 5.3$ )  $\times 10^{-4}$  M, supporting the stoichiometry of the receptor composition and its complex with indole. However, in contrast to the downfield shifts of the PBP protons on exposure to  $\text{Co}^{2+}$ , all indole protons are shifted upfield on binding (Figure 20). This may represent a structurally significant difference in the orientation of the guest and the host hydrogens to the partially filled metal orbitals. Similar  $\Delta\delta_{\text{max}}$  values between  $\text{H}_3$  and  $\text{H}_5$ ,  $\text{H}_2$  and  $\text{H}_6$ ,  $\text{H}_4$  and  $\text{H}_7$  suggest that indole binds inside of the  $\text{Co}_2\text{PBP}_2$  cavity in an equatorial orientation, consistent with our expectation based on CPK model study.

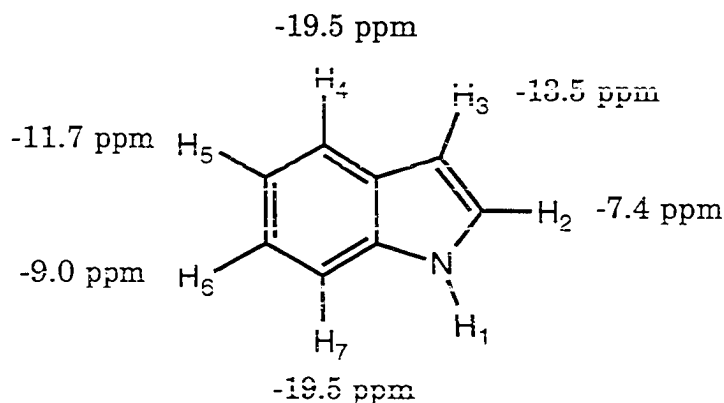
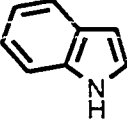
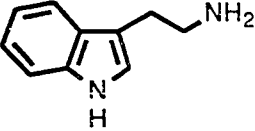
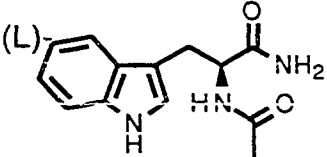
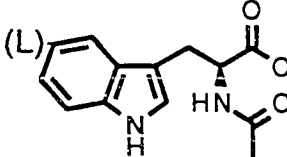
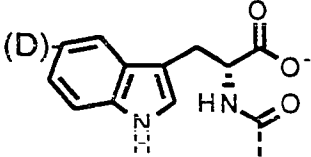
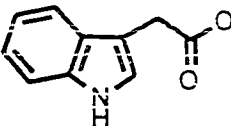
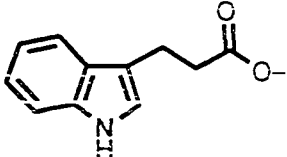
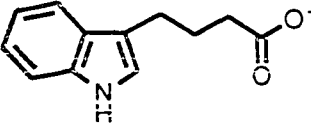


Figure 20.  $\Delta\delta_{\text{max}}$  values of Indole in the presence of  $\text{Co}_2\text{PBP}_2$

The affinities of Co<sub>2</sub>PBP<sub>2</sub> receptor for a series of indole guests **30-37** and naphthalene guests **38-45** were measured by NMR and are given in Table 6 and 7. A substituent at the 3 position of the indole (3-indoleethylamine **31**, N-acetyl tryptophan amide **32**) causes more than an order of magnitude drop in the binding affinity compared to that of indole **30**. This suggests that the substituent at the 3 position of the indole causes a steric interference with the optimal indole binding geometry to Co<sub>2</sub>PBP<sub>2</sub> receptor. N-Acetyl tryptophans (**33**, **34**), with anionic sidechains, bind with another order of magnitude lower affinity. This is consistent with ionic repulsion between the anionic sidechain of guests and the anionic host (Co<sub>2</sub>PBP<sub>2</sub><sup>-2</sup> or Co<sub>2</sub>PBP<sub>2</sub>(OH)<sup>-3</sup>). Removal of the acetamide substituent from **33** or **34** gives indole propionic acid **36**, which, despite the presence of the C3 substituent and the anionic sidechain, binds 37 times more strongly than **33** or **34**, almost as well as indole **30** itself. Indole acetic acid **37** and indole butyric acid **35** bind still more tightly. The fact that anionic substrates are bound tightly to an anionic receptor can rule out ion-pairing as a driving force for the enhanced binding. Addition of carboxylate, tethered through a three carbon link in **37**, provides 10-14 fold stronger binding, depending on which neutral 3-substituted indole (**31** or **32**) is taken as the standard.

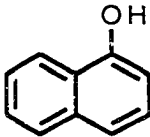
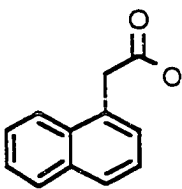
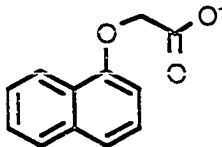
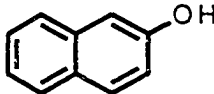
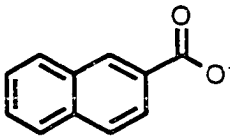
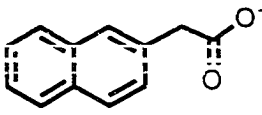
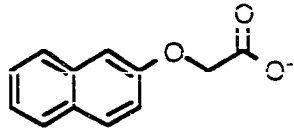
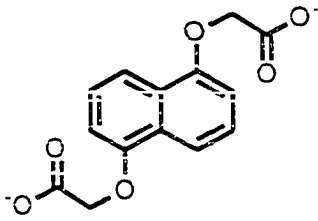
1-Naphthylacetic acid **39**, with an anionic sidechain, binds 2.5 times less tightly than the neutral 1-naphthol **38**. However, the decrease of binding affinity is only 2.5 fold, rather than the 10 fold decrease for **33** and **34** compared to **31** or **32**. With the optimal sidechain for naphthalene, 1-naphthoxyacetic acid **40** binds 2.5 times more strongly than does the neutral 1-naphthol **38**. 2-Naphthoxyacetic acid **43** binds as tightly as neutral 2-naphthol **41** while other

Table 6. Binding of guests to Co<sub>2</sub>PBP<sub>2</sub> in 0.2 M borate buffer in D<sub>2</sub>O

	Guests	$\Delta\delta_{\max}$ (ppm)				$K_D$ (M)
		$\bar{H}_\alpha$	$\bar{H}_\beta$	$\bar{H}_{Ar1}$	$\bar{H}_{Ar2}$	
30		-21	14	3.1	1.0	$(1.18 \pm 0.11) \times 10^{-3}$
31		-26	16	3.2	1.1	$(1.60 \pm 0.14) \times 10^{-2}$
32	(L) 	-25	14	2.0	0.8	$(2.18 \pm 1.20) \times 10^{-2}$
33	(L) 	-33	16	2.1	0.9	$(1.57 \pm 0.23) \times 10^{-1}$
34	(D) 	-28	14	2.2	0.8	$(1.55 \pm 0.19) \times 10^{-1}$
35		a	a	2.2	0.7	$(1.94 \pm 0.51) \times 10^{-3}$
36		a	a	2.5	0.9	$(4.21 \pm 0.77) \times 10^{-3}$
37		a	a	2.8	1.1	$(1.55 \pm 0.45) \times 10^{-3}$

a: Broadened to unobservability

Table 7. Binding of guests to Co<sub>2</sub>PBP<sub>2</sub> in 0.2 M borate buffer in D<sub>2</sub>O

	Guests	$\Delta\delta_{\max}$ (ppm)				$K_D$ (M)
		$\bar{H}_\alpha$	$\bar{H}_\beta$	$\bar{H}_{Ar1}$	$\bar{H}_{Ar2}$	
38		-22	15	3.3	1.0	$(4.15 \pm 0.27) \times 10^{-4}$
39		a	a	2.4	0.8	$(1.02 \pm 0.13) \times 10^{-3}$
40		a	a	2.7	0.7	$(1.65 \pm 0.52) \times 10^{-4}$
41		-22	15	3.1	1.1	$(2.97 \pm 0.06) \times 10^{-3}$
42		-28	14	2.5	c	$(4.17 \pm 0.57) \times 10^{-2}$
43		a	15 <sup>b</sup>	2.5	0.7	$(2.85 \pm 0.70) \times 10^{-3}$
44		-27	16	3.0	0.9	$(1.11 \pm 0.20) \times 10^{-2}$
45		a	a	a	1.7	$(4.62 \pm \quad) \times 10^{-5}$

b: Extrapolated from the first few points before disappearance, assuming the  $K_D$  determined from other resonances.

c: Obscured by guest signals.

naphthalene derivatives, with an anionic sidechain at 2 position (**42**, **44**), bind far less tightly.

These data suggest that the host-guest complexation occurs with ditopic binding: ligation of the cobalt ion by carboxylate in those complexes where the carboxyl group is appropriately positioned upon binding of the aromatic portion of guest to the Co<sub>2</sub>PBP<sub>2</sub>. In support of this notion, in all cases where there is an anomalously high affinity for an anionic ligand, the NMR resonances for the  $\alpha$  and  $\beta$  protons of the PBP are broadened to the point of undetectability upon addition of substrate.

The geometric requirement of ditopic binding moderates the preference for 1- over 2- substitution of naphthalene: **40** is preferred over the isomeric **44** by 67 fold, while the related **39** is preferred over its isomer **43** by only 2.8 fold. The binding affinity difference between **39** and **43** is even smaller than that of **38:41** (ratio of 7.2). The higher binding affinity of 1-naphthol **38** over 2-naphthol **41** suggests that substituents at 2-position of naphthalene is not suitable for the optimal binding geometry. The ligation of carboxylate substituent of 2-naphthyl acetate **43** compensates for the steric repulsion. The lower binding affinity of 1-naphthyl acetate **39** compared to 1-naphthoxy acetate **40** suggests that the carboxylate group of **39** is not oriented at the optimum position for ligation. These two factors cause only 2.8 fold difference in binding affinity between **39** and **43**. Compared to **40**, 2-naphthoxy acetate **44** has an anionic substituent at 2-position which is not able to ligate to Co<sup>2+</sup>. Both steric and ionic repulsion cause **44** bind 67 times less tightly than **40**.

A ditopic receptor should prefer binding to substrates that allow both binding interactions. The extent to which the two interactions cooperate to

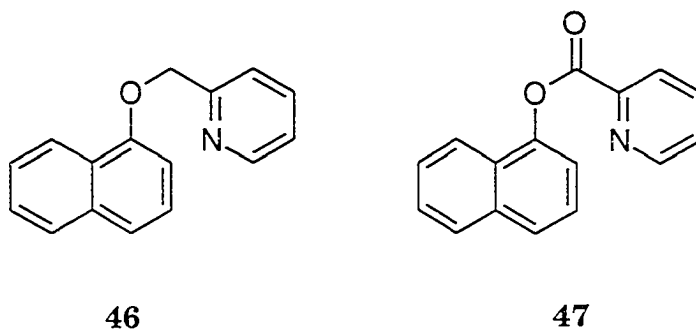


achieve such selectivity can be described in terms of an effective molarity (EM) for the carboxylate groups of bound substrate in the presence of the metal. Estimating the binding constant of a carboxylate ion to the charge-neutral  $\text{Co}^{2+}$  center as  $K_D \sim 1.2 \text{ M}$  (the  $K_3$  of acetate for  $\text{Co}^{2+}$ ),<sup>82</sup> the EM for binding of the indole and carboxylate moieties of indole butyric acid **37** is  $\text{EM} = 12 \text{ M}$ . This value, though well below the  $10^8 \text{ M}$  estimated limit, is quite large compared to most synthetic receptors,<sup>115, 116</sup> Nonetheless, it is an underestimate of EM because it does not take into account the repulsion by the anionic receptor: correction (by  $K_{(32)}/K_{(33)} = 7.3$ ) gives an EM of 88 M. If this analysis is correct, then the modest  $\sim 10$  fold selectivity for **37** over **31** or **32** is due to nice geometric placement of an intrinsically extremely weak attraction. A metal-ligand interaction comparable in strength to the hydrophobic affinity would yield selectivity for bifunctional substrate binding proportionally larger.

The binding study of 1,5-dinaphthoxy diacetate **45** to  $\text{Co}_2\text{PBP}_2$  provides information on stereochemistry at the metal center. If the naphthalene binds so as to position itself symmetrically in the middle of a symmetrical host cavity, a second carboxylate could bind to the second cobalt, adding at least as much to the binding affinity as the first carboxylate did. (More, because of the probable lesser entropy to be frozen out by the second binding event.) The 1,5-disubstitution precludes binding of both carboxylates from the same face of the macrocycle, as a probable  $\text{C}_2$  symmetry conformation would require. In fact, each carboxylate enhances binding: **45** binds 4 times more strongly than **40**, which binds 2.5 times more strongly than **38**. If the second carboxylate did not assist the binding, the charge repulsion would cause lower affinity for **45** than **40**. This suggests that ligation by both carboxylates is possible, but the fact that  $\Delta\delta_{\text{max}}$  for  $\text{H}_{\text{Ar}2}$  is 5

standard deviations greater for **45** than for the other substrates suggests that a different geometry is enforced in this case.

The carboxylate side chain of naphthalene and indole enhanced the binding affinity by providing ditopic binding through ligation to  $\text{Co}^{2+}$ . Compounds **46** and **47** were prepared to see whether the neutral pyridine ligand would also encourage ditopic binding. However, these arenes with pyridyl side chain were not soluble enough in water to perform a proper  $^1\text{H}$  NMR titration. Therefore, the binding affinity was determined using the extraction method.<sup>92</sup> Two naphthalene derivatives (1-naphthyl 2-picolinyl ether **46** and 1-naphthyl 2-picolinate **47**) were added to  $\text{Co}_2\text{PBP}_2$  ( $5.8 \times 10^{-4}$  M) in 0.2 M borate buffer in  $\text{D}_2\text{O}$  and the mixtures stirred for 9 days



$^1\text{H}$  NMR spectrum of the solution stirred with **46** shows small chemical shift change of  $\text{Co}_2\text{PBP}_2$  protons. The shifting patterns resemble those of guests which bind and ligate: the peaks of  $\alpha$  and  $\beta$  protons are broadened. These results provide evidence that the compound **46** binds to the  $\text{Co}_2\text{PBP}_2$  ditopically. The dissociation constant was approximated to  $6.2 \times 10^{-3}\text{M}$  (more than 50% error range) by assuming  $\Delta\delta_{\text{max}}$  is same as for the other naphthalene derivatives, and estimating the concentration of **46** by NMR integration. The solution which was

stirred with compound **47** gave a  $^1\text{H}$  NMR spectrum with no anisotropic down field shifted  $\alpha$  and  $\beta$  protons of  $\text{Co}_2\text{PBP}_2$  while the other protons remained at the unshifted chemical shift. This implies that the compound **47** was hydrolyzed and the hydrolyzed product 1-picolinate disassembles the  $\text{Co}_2\text{PBP}_2$  complex by sequestering  $\text{Co}^{2+}$ . This is confirmed by hydrolysis experiments: more than 95 % of the ester was hydrolyzed within 1 hour at pH 8.2 irrespective of the presence or absence of  $\text{Co}_2\text{PBP}_2$ .

The species distribution (Figure 12) showing that various protonation states  $\text{Co}_2\text{PBP}_2(\text{OH})^{-3}$  and  $\text{Co}_2\text{PBP}_2(\text{OH})_2^{-4}$  of a single macrocyclic complex predominate in solution above pH 9 is supported by the fact that each PBP proton of  $\text{Co}_2\text{PBP}_2$  gives a corresponding single peak in the  $^1\text{H}$  NMR spectrum when the concentration of PBP is about  $1 \times 10^{-3}$  M at pD = 9. However, if the concentrations of PBP and  $\text{Co}^{2+}$  are raised above the EM, higher oligomers are expected to form. The formation of higher oligomers was monitored by  $^1\text{H}$  NMR by changing the concentration of PBP. As the concentration of PBP increases over  $8 \times 10^{-3}$  M, several peaks are observed in 100-30 ppm range. The evidence of the formation of higher oligomer is provided by the peak integration. The concentration of PBP which is calculated from integration of  $^1\text{H}$  NMR peaks starts to deviate from the added amount as the concentration increases (Figure 21). Taking into account the fact that the integration of largely broadened peaks is not accurate, there is a fairly good correlation up to  $8 \times 10^{-3}$  M of PBP. According to the calculated effective molarity, the formation of desired macrocycle is preferred below  $(6.2 \pm 2.5) \times 10^{-2}$  M. These results suggest that macrocyclic  $\text{Co}_2\text{PBP}_2$  can be prepared without making other equilibrium species by controlling pH of the solution and concentrations of PBP and  $\text{Co}^{2+}$ .

The macrocycle  $\text{Co}_2\text{PBP}_2$  may dissociate when its concentration becomes too low because it is in equilibrium with  $\text{Co}^{2+}$  and PBP. Dilution studies in  $^1\text{H}$  NMR show dissociation of  $\text{Co}_2\text{PBP}_2$  below  $1.0 \times 10^{-3}$  M. However, the inaccuracy in integration of largely broadened peaks, especially in low concentration, makes only semi-quantitative analysis. A more quantitative treatment can be found in the section on CD data.

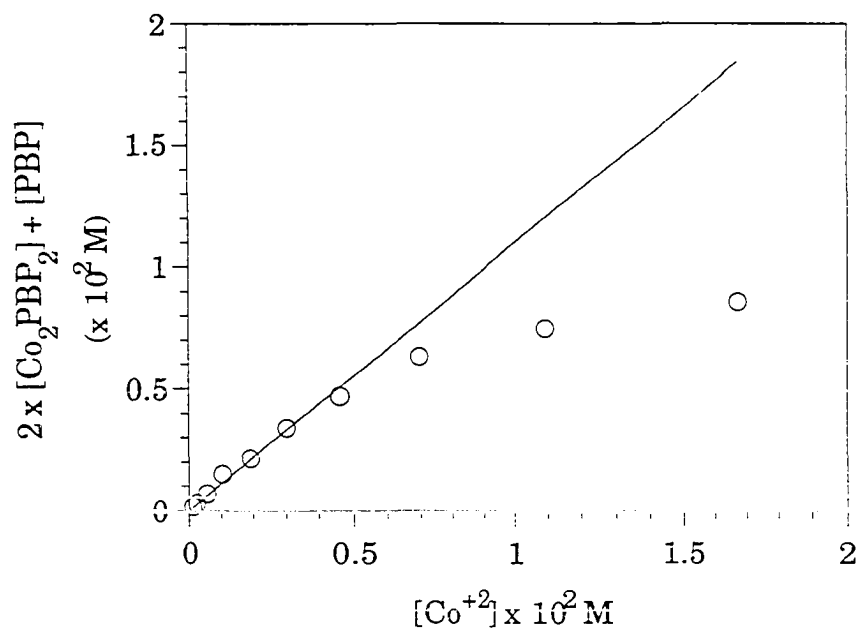


Figure 21. Relationship between added  $[\text{PBP}]_{\text{tot}}$  and calculated  $[\text{PBP}]_{\text{tot}}$ . Added  $[\text{PBP}]_{\text{tot}} = 1.1 \times [\text{Co}^{2+}]_{\text{tot}}$  (-), calculated  $[\text{PBP}]_{\text{tot}}$  from NMR integration ( $\circ$ ).

## Other Properties of Receptor

### Enantioselectivity in host-guest complexation

Host molecules which utilize hydrogen bonding often exhibit strong binding as well as a high degree of enantioselection.<sup>8</sup> This is due to both the strength and the high degree of directionality of hydrogen bonds. This directionality enables host molecules to be designed to bind guests strongly only in a particular conformation. Minor deviations in the structure of the guests can greatly weaken binding by changing the conformation of the complex and distorting the geometry of the hydrogen bonds. Since hydrogen bonding interactions are less effective in aqueous media,  $\pi$ -stacking and hydrophobic interactions are often used to bind a substrate in water. The relatively non-directed nature of these forces makes the design of enantioselective hosts more challenging since small changes in binding conformation will not necessarily result in large changes in binding strength. These hosts usually tightly encapsulate their guests, making intimate contact over a large surface rather than at discrete points.

The ditopic binding between  $\text{Co}_2\text{PBP}_2$  and naphthalene derivatives with an anionic side chain could provide enantioselectivity in substrate binding. A methyl substituent at C2 position of 1-naphthoxyacetic acid is expected to affect the orientation of the carboxylate group. CPK model studies of  $\text{Co}_2\text{PBP}_2$  and 2-(1-naphthoxy) propionate complex suggested that the methyl group of R-isomer would interfere with proper orientation of the carboxylate group for ligation when it was bound inside the cavity of  $\text{Co}_2\text{PBP}_2$  as shown in Figure 22. As a result, the ditopic binding provides the directionality in guest binding geometry which in turn provides enantioselection.

The binding affinity of (S)-isomer (**49**) is 9 fold higher than that of (R)-isomer (**48**) ( $K_D = (2.73 \pm 1.12) \times 10^{-4}$  M and  $(2.57 \pm 1.01) \times 10^{-3}$  M, respectively at  $[\text{Co}_2\text{PBP}_2] = 5.8 \times 10^{-4}$  M). This result is interesting because the enantioselection is relatively high considering that it is obtained in aqueous solution. As mentioned previously, the enantioselection by synthetic receptors in aqueous solution is usually low. One of the largest enantioselections observed by binding neutral substrates in aqueous solution is 4.6 fold, reported by Dougherty et al.<sup>44</sup>

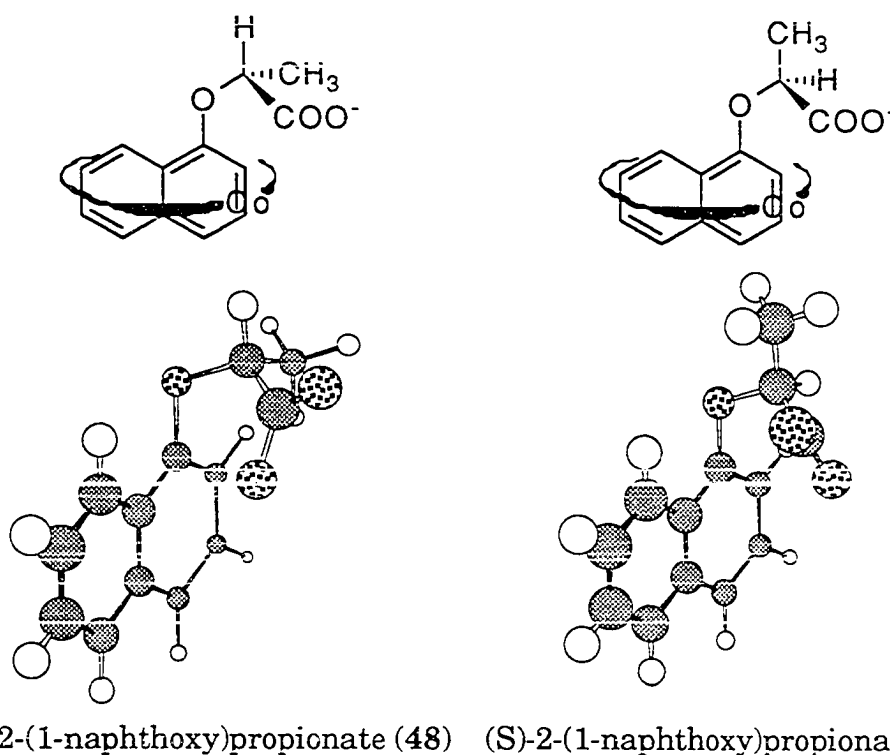


Figure 22. The proposed three dimensional structures of both enantiomers of 2-(1-naphthoxy)propionate, held into a conformation which allows ligation of carboxylate to metal of  $\text{Co}_2\text{PBP}_2$ .

## Circular Dichroism spectra

$\text{Co}_2\text{PBP}_2$  is expected to be optically active because it has 6 stereogenic centers: 4 chiral  $\alpha$ -carbons of phenylalanine and 2 metals. Dougherty used CD to determine binding constants of host-guest complexes.<sup>45</sup> The CD method operates in a lower concentration range than other methods for determining binding constants, which is especially useful when binding constants are large or when the host or guest is not very water soluble.

The CD method seemed very promising to obtain the information of coordination geometry of  $\text{Co}_2\text{PBP}_2$  and determine the binding constant. However, I could not run the CD experiments because Iowa State University did not have spectropolarimeter. Dr. Schwabacher took the  $\text{Co}_2\text{PBP}_2$  and obtained good CD spectra from Princeton University

The CD spectrum of PBP at pH 9.1 shows big change on addition of equivalent amount of  $\text{Co}^{2+}$  (Figure 23). This result implies that the change is caused by the formation of  $\text{Co}^{2+}$  complex with PBP.

The Job's plot was tried with CD (Figure 24). It shows maximum ellipticity between 0.3 and 0.4 mole ratio of  $\text{Co}^{2+}$ . The previous Job's plot provided the evidence that the complex responsible of pyrene transport was 2:2  $\text{Co}^{2+}/\text{PBP}$  complex and that was confirmed by calculation using stability constants. These results suggest that various protonation states of  $\text{Co}_1\text{PBP}_2$  contributes to CD but not to transport while those of  $\text{Co}_2\text{PBP}_2$  contribute to both.

At a constant 1.25:1 ratio of  $\text{PBP}:\text{Co}^{2+}$  (where the major complex should be  $\text{Co}_2\text{PBP}_2$ ), the ellipticity is directly proportional to the concentration of  $\text{Co}^{2+}$

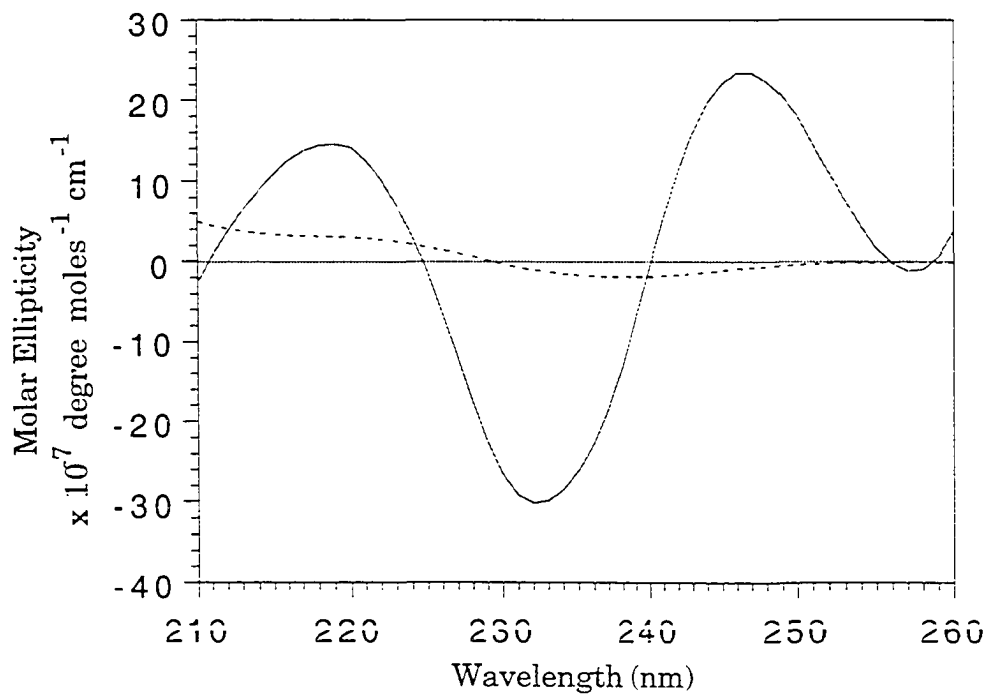


Figure 23. CD spectra of PBP and Co<sup>2+</sup> complex with PBP in 0.1 M borate buffer. [PBP] = 2.0 x 10<sup>-4</sup> M (---), addition of 2.0 x 10<sup>-4</sup>M of Co<sup>2+</sup> (-).



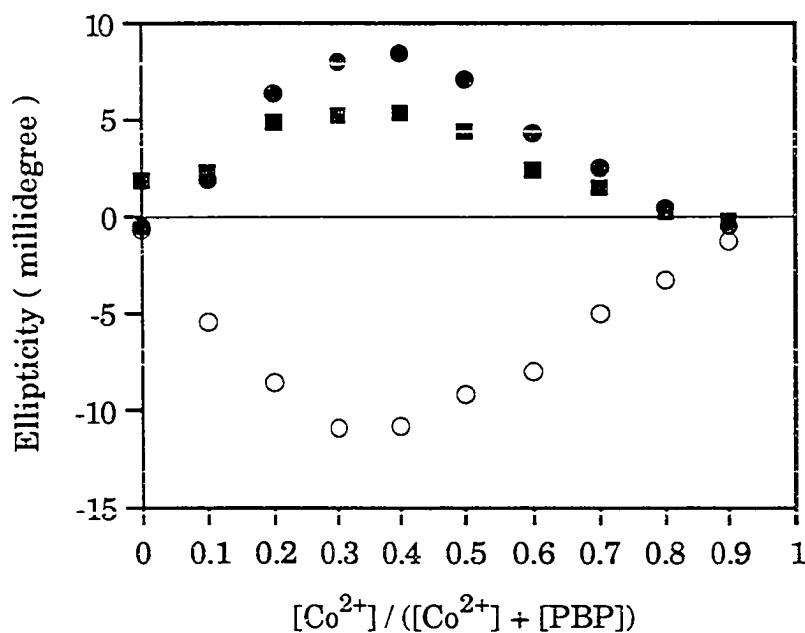


Figure 24. Job's plot using CD of  $\text{Co}^{2+}$  complex with PBP at 0.1 M borate buffer.  $[\text{Co}^{2+}] = [\text{PBP}] = 4.0 \times 10^{-4}$  M. 219 nm (■), 232 nm (○), 247 nm (●).

between  $3.0 \times 10^{-4}$  M and  $1.5 \times 10^{-3}$  M (Figure 25, Figure 26). However, the ellipticity is not proportional to the concentration when it decreases below  $3.0 \times 10^{-4}$  M indicating dissociation of the  $\text{Co}_2\text{PBP}_2$ . This concentration dependence is very similar to that of the calculated  $\text{Co}_2\text{PBP}_2$  concentration (Figure 27), corroborating the potentiometric titration derived constants. As the concentration of total PBP decreases below  $2 \times 10^{-4}$  M, the desired macrocycle starts to dissociate.

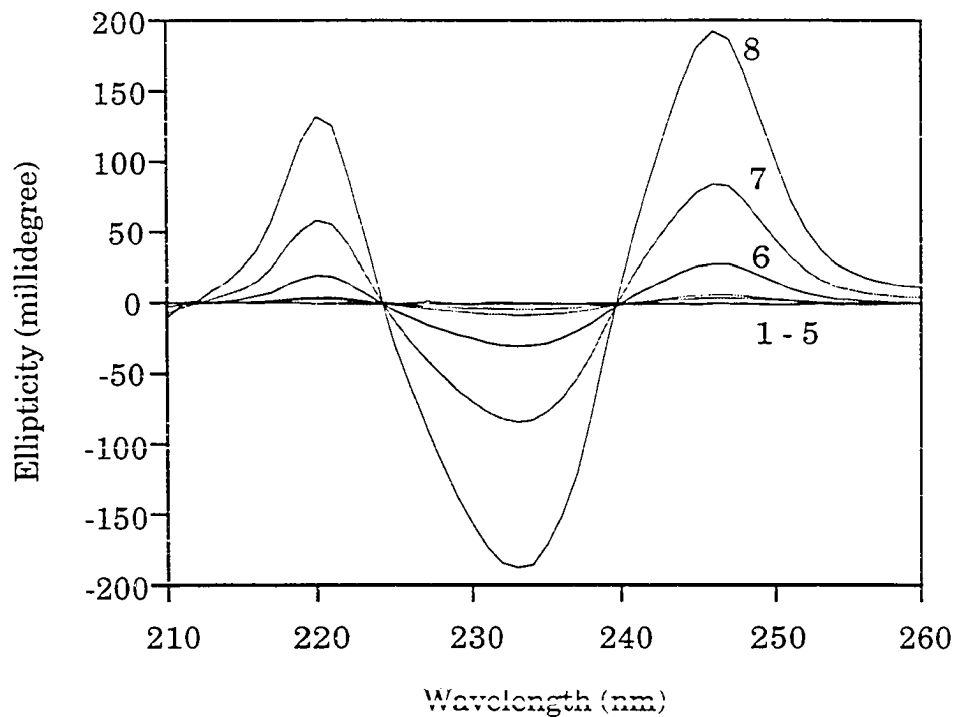


Figure 25. Circular dichroism of  $\text{Co}^{2+}$  complex with PBP as a function of  $\text{Co}^{2+}$  concentration in 0.1 M borate buffer. Concentration of PBP maintained in 1.25:1 ratio with that of  $\text{Co}^{2+}$ .  $\text{Co}^{2+}$  concentration; 1,  $0.2 \times 10^{-4}$  M; 2,  $0.4 \times 10^{-4}$  M; 3,  $0.8 \times 10^{-4}$  M; 4,  $1.2 \times 10^{-4}$  M; 5,  $1.5 \times 10^{-4}$  M; 6,  $3.0 \times 10^{-4}$  M; 7,  $7.5 \times 10^{-4}$  M; 8,  $15.0 \times 10^{-4}$  M.

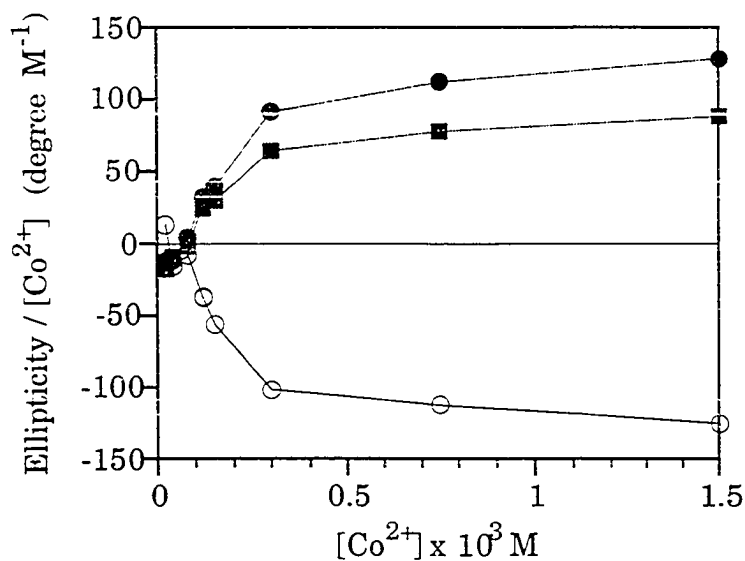


Figure 26. Concentration dependence of the ellipticity of Co<sup>2+</sup> complex with PBP at 0.1 M borate buffer. Concentration of PBP maintained in 1.25:1 ratio with that of Co<sup>2+</sup>. 220 nm (■), 233 nm (○), 246 nm (●).

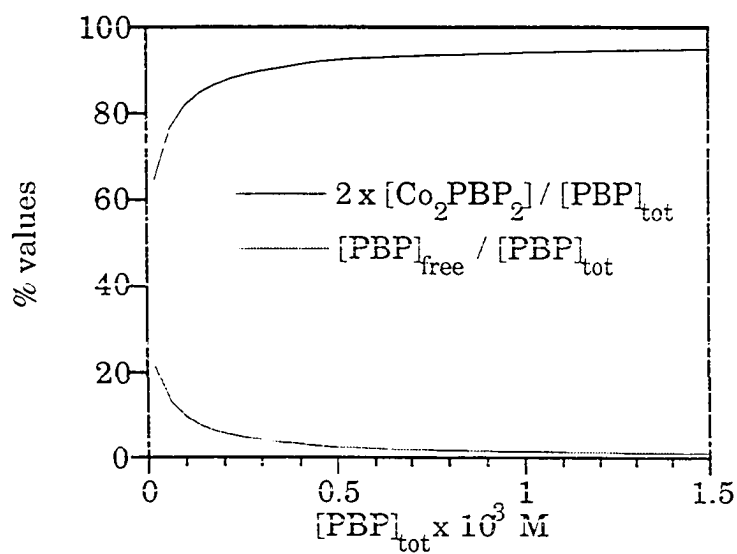
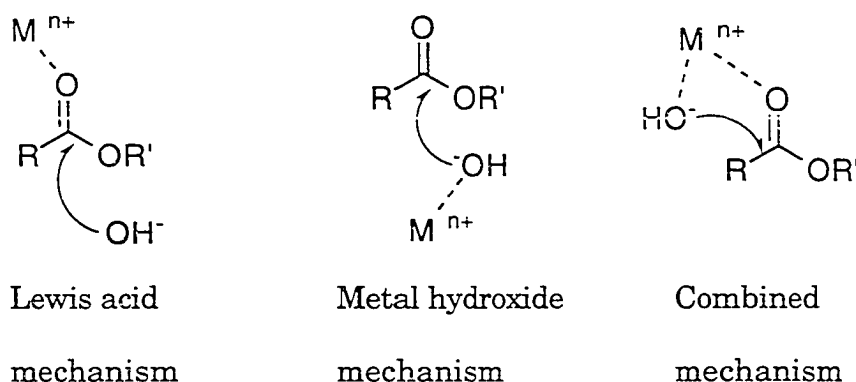


Figure 27. % values of free PBP and Co<sub>2</sub>PBP<sub>2</sub>, calculated from stability constants, as a function of total concentration of PBP.

### Catalytic effect of $\text{Co}_2\text{PBP}_2$ on the hydrolysis of esters

Transition metal ions are known to catalyze the hydrolysis of esters and amides.<sup>117-119</sup> Two possible mechanisms, the Lewis acid mechanism and the metal hydroxide mechanism, have been discussed extensively (Scheme 8). Chin et al. reported a superior combined third mechanism, in which the Lewis acid and metal hydroxide work simultaneously.<sup>118</sup>



Scheme 8. Proposed mechanisms for transition metal catalyzed hydrolysis of ester.

1-Naphthoxy acetate **40** binds very tightly to the  $\text{Co}_2\text{PBP}_2$  through ditopic binding. The facts that the carboxyl group of the 1-naphthoxy acetate ligates to the cobalt(II) metal in  $\text{Co}_2\text{PBP}_2$  and one of the waters ligated to the cobalt metal has been deprotonated above pH 9 suggest the possibility of catalytic hydrolysis of the corresponding ester.

Hydrolysis of ethyl 1-(5-hydroxy)naphthoxy acetate **50** in the presence of  $\text{Co}_2\text{PBP}_2$  was followed by HPLC. The pseudo-first order rate constant for hydrolysis at pH 8.2 of **50** in the presence of  $\text{Co}_2\text{PBP}_2$  is the same as that with

Co(Gly)<sub>2</sub> (Table 8). However, the hydrolysis rate of **50** was slowed by a factor of 4 in the presence of Co<sub>2</sub>PBP<sub>2</sub> compared to that with Co(Gly)<sub>2</sub> at pH 9.5. The pseudo-first order rate constants are  $(4.5 \pm 0.1) \times 10^{-2} \text{ h}^{-1}$  and  $(20 \pm 2) \times 10^{-2} \text{ h}^{-1}$  for Co<sub>2</sub>PBP<sub>2</sub> and Co(Gly)<sub>2</sub>, respectively.

Table 8. Pseudo-first order hydrolysis rates of ethyl 1-(5-hydroxy)naphthoxy acetate (**50**) at 25°C. [Ethyl 1-(5-hydroxy)naphthoxy acetate] =  $7.8 \times 10^{-5} \text{ M}$

	Borate buffer	Co(Gly) <sub>2</sub>	Co <sub>2</sub> PBP <sub>2</sub>
	0.1 M	$7.8 \times 10^{-4} \text{ M}$	$3.9 \times 10^{-4} \text{ M}$
pH = 8.2		$(1.3 \pm 0.3) \times 10^{-2} \text{ h}^{-1}$	$(1.2 \pm 0.3) \times 10^{-2} \text{ h}^{-1}$
pH = 9.5	$(20 \pm 2) \times 10^{-2} \text{ h}^{-1}$	$(20 \pm 2) \times 10^{-2} \text{ h}^{-1}$	$(4.5 \pm 0.1) \times 10^{-2} \text{ h}^{-1}$

If the dissociation constant of **50** is assumed to be  $4 \times 10^{-4} \text{ M}$ , the same as that of 1-naphthol **38**, the amount of **50** as the complex with Co<sub>2</sub>PBP<sub>2</sub> is only 46% of added **50** which can not explain the observed four fold rate decrease in the presence of Co<sub>2</sub>PBP<sub>2</sub>. For these results to make sense, **50** must bind about 2 times stronger than 1-naphthol and the hydrolysis rate of the ester bound to Co<sub>2</sub>PBP<sub>2</sub> must be less than a quarter of that of the unbound ester. Product formation as a function of time in the presence of Co<sup>2+</sup> complexes are shown in Figure 28.

Rate retardation by host-guest complexation requires stronger binding than rate acceleration would. The active site of substrate should be shielded from the attacking reactant by complexation and the complex formation should be strong

enough to compete with the reaction outside of the binding cavity. Schneider et al. has reported that a macrocyclic polyphenolate causes the retardation of hydrolysis of choline acetate by a factor of ten through charge repulsive destabilization.<sup>102</sup>

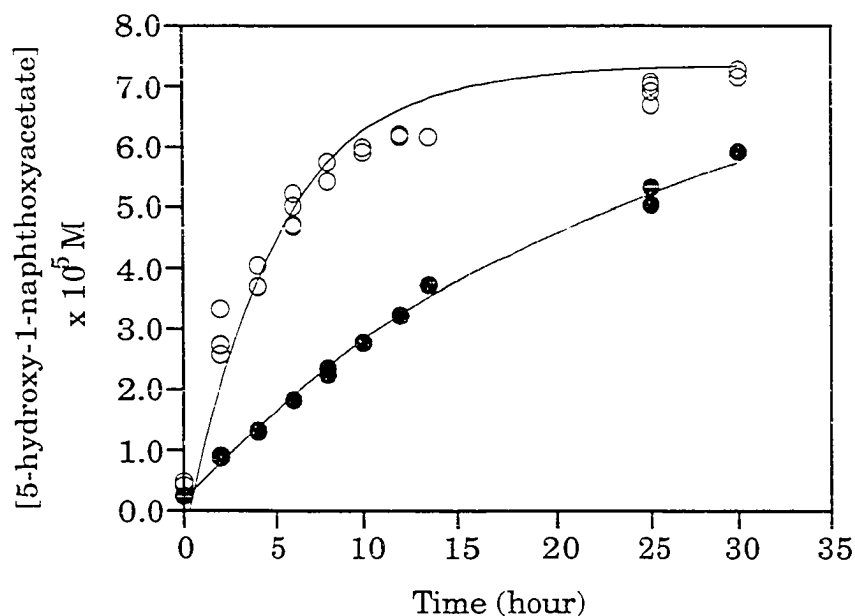
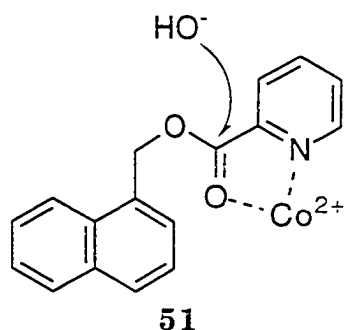


Figure 28. Hydrolysis of Ethyl 1-(5-hydroxy)naphthoxy acetate: [Ethyl 1-(5-hydroxy)naphthoxy acetate] =  $7.8 \times 10^{-5}$  M, in 0.1 M pH 9.5 borate buffer, (○) [Co(Gly)<sub>2</sub>] =  $7.8 \times 10^{-4}$  M or buffer only, (●) [Co<sub>2</sub>PBP<sub>2</sub>] =  $3.9 \times 10^{-4}$  M.

The result, the hydrolysis rate of **50** in Co(Gly)<sub>2</sub> solution is same with the rate in buffer solution, shows that the hydrolysis of **50** at pH 9.5 is not a Co<sup>2+</sup> catalyzed reaction. While the origin of the observed rate retardation in the presence of Co<sub>2</sub>PBP<sub>2</sub> has not been established, it seems possible that the effect is due to the shielding of the ester from the hydroxide attack. The anionic character

of the  $\text{Co}_2\text{PBP}_2$  may interfere with the approach of free hydroxide by ionic repulsion and cause the rate retardation. Note that the less anionic host formed at pH 8.2 does not inhibit hydrolysis.

To increase the ligating ability of the side chain in naphthalene derivatives, esters were prepared by using picolinate. (1-Naphthyl)methyl picolinate **51** can ligate  $\text{Co}^{2+}$  as a bidentate ligand. We were hoping that the coordination of the carbonyl oxygen of ester to the  $\text{Co}^{2+}$  may cause the catalytic hydrolysis through the Lewis acid mechanism (Scheme 9).



Scheme 9. Proposed Lewis acid mechanism for the hydrolysis picolinate.

As expected, the rate of hydrolysis of (1-naphthyl)methyl picolinate was accelerated 36 times in the presence of  $3.93 \times 10^{-4}$  M  $\text{Co}_2\text{PBP}_2$  compared to the buffer solution at pH = 8.2. However, the same hydrolysis rate was observed in the presence of  $\text{Co}(\text{Gly})_2$  (Table 9). With both  $\text{Co}^{2+}$  complexes, the observed pseudo-first order rate constant of hydrolysis is  $6.4 \times 10^{-1} \text{h}^{-1}$ , while  $2.5 \times 10^{-2} \text{h}^{-1}$  without complexes at pH = 8.2. Even at pH = 9.5 where **50** has been hydrolyzed without any catalytic effect of  $\text{Co}^{2+}$ , all **51** has been hydrolyzed within 3 hours in the presence of  $\text{Co}^{2+}$  complexes while only half of **51** has been hydrolyzed in buffer solution.

Table 9. Pseudo-first order hydrolysis rates of (1-naphthyl)methyl picolinate (**51**) at 25 °C. [(1-Naphthyl)methyl picolinate] =  $6.18 \times 10^{-5}$  M

	Borate buffer	Co(Gly) <sub>2</sub>	Co <sub>2</sub> PBP <sub>2</sub>
	0.1 M	$7.87 \times 10^{-4}$ M	$3.93 \times 10^{-4}$ M
pH = 8.2	$(2.5 \pm 0.5) \times 10^{-2} \text{ h}^{-1}$	$(6.5 \pm 0.3) \times 10^{-1} \text{ h}^{-1}$	$(6.4 \pm 0.1) \times 10^{-1} \text{ h}^{-1}$

These results suggest that the hydrolysis of **51** is catalyzed by Co<sup>2+</sup>. However, the strong ligation ability of picolinate group of **51** to Co<sup>2+</sup> seems override the proximity effect caused by binding to Co<sub>2</sub>PBP<sub>2</sub> and there is no rate difference between the hydrolysis catalyzed by Co<sub>2</sub>PBP<sub>2</sub> or Co(Gly)<sub>2</sub>.



## CONCLUSION

A new type of water soluble macrocycle exhibiting molecular recognition was developed. This macrocycle displays interesting structural and functional features: self assembly in macrocyclization and cooperativity in substrate binding. The evidence of the formation of macrocycle  $\text{Co}_2\text{PBP}_2$  which is able to bind aromatic substrates was demonstrated by the carrier mediated transport experiments, potentiometric titration,  $^1\text{H}$  NMR titration experiments, and CD experiments.

The macrocycle  $\text{Co}_2\text{PBP}_2$  was constructed by self assembly through the complexation between  $\text{Co}^{2+}$  and amino acid groups of PBP while PBP was constructed by connecting two phenyl groups of two phenylalanine by phosphorus atom. Evidences that the self assembled  $\text{Co}^{2+}$  complex with PBP is 2:2 ratio and  $\text{Co}_2\text{PBP}_2$  complex is the major component in equilibria above solution pH 9 are provided in several experimental results: maximum carrier mediated transport rate at 1:1 ratio of  $\text{Co}^{2+}$  to PBP in Job's plot, species distribution curve from potentiometric titration, and the base peak in electrospray MS corresponds to the  $m/z$  of  $\text{Co}_2\text{PBP}_2^{-2}$ . Even though  $\text{Co}^{2+}/\text{PBP}$  complexes could exist as many structural isomers, most of them can be excluded because of the cyclic nature of the  $\text{Co}_2\text{PBP}_2$ . This is supported by the simple spectrum pattern in  $^1\text{H}$  NMR when concentration of  $\text{Co}_2\text{PBP}_2$  lower than  $4 \times 10^{-3}$  M. The geometry of  $\text{Co}^{2+}$  in  $\text{Co}_2\text{PBP}_2$  is suggested as 5 coordinated structure from experimental results that the magnetic moment value of  $\text{Co}_2\text{PBP}_2$  is close to that of 5 coordinated  $\text{Co}^{2+}$  complexes and the unusually low  $\text{pK}_a$  values for hydrolysis of ligated water in  $\text{Co}_2\text{PBP}_2$ .

In addition to the substrate selectivity, positive cooperativity was observed in binding of lipophilic guests into the host Co<sub>2</sub>PBP<sub>2</sub>. Naphthalene and indole derivatives with suitable anionic side chain bind to Co<sub>2</sub>PBP<sub>2</sub> with high binding affinities although it is an anionic host. Also the position of side chain in naphthalene affects the binding affinity: 1-naphthoxy acetate binds 67 times more strongly than does 2-naphthoxy acetate. These data suggest that the host-guest complexation occurs through ditopic binding: ligation of the cobalt(II) ion by carboxylate in those complexes where the carboxyl group is appropriately positioned upon binding of the aromatic portion of guest to the Co<sub>2</sub>PBP<sub>2</sub>. Two different types of interactions, hydrophobic and coordination, work cooperatively in binding aromatic substrates and increase the binding affinity.

Co<sub>2</sub>PBP<sub>2</sub> shows high enantioselectivity in substrate binding through ditopic binding. The binding affinity of (S)-2-(1-naphthoxy)propionate is 9 fold higher than that of (R)-isomer ( $K_D = (2.73 \pm 1.12) \times 10^{-4}$  M and  $(2.57 \pm 1.01) \times 10^{-3}$  M, respectively at  $[Co_2PBP_2] = 5.8 \times 10^{-4}$  M). This enantioselection is twice that of Dougherty et al.<sup>19(a)</sup> which had been known as one of the largest enantioselection for neutral substrates in aqueous solution.

Co<sub>2</sub>PBP<sub>2</sub> shows negative catalytic effect on the hydrolysis of naphthalene derived ester. The hydrolysis rate of ethyl 1-(5-hydroxy)naphthoxy acetate was slowed 4 times in the presence of Co<sub>2</sub>PBP<sub>2</sub> compare to that of Co(Gly)<sub>2</sub> at pH 9.5: pseudo-first order rate constants were  $(4.1 \pm 0.1) \times 10^{-2}$  h<sup>-1</sup> and  $(20.0 \pm 2.0) \times 10^{-2}$  h<sup>-1</sup> for Co<sub>2</sub>PBP<sub>2</sub> and Co(Gly)<sub>2</sub>, respectively.

As a conclusion, the macrocycle Co<sub>2</sub>PBP<sub>2</sub> demonstrates several interesting features:

1. Formation of binding site through self assembly.

2. Metal complex geometry determines shape and cavity size of macrocycle.
3. Composed with naturally occurring L-phenylalanine.
4. Formation of inclusion complex with substrate selectivity.
5. Cooperativity of two types of interaction in binding substrates.
6. Enantioselectivity in binding.
7. Negative catalytic effects on hydrolysis of ester.

These structural and functional features implies that the  $\text{Co}_2\text{PBP}_2$  is an excellent mimic of metalloenzymes because the active site of metalloenzymes are formed by self assembly of peptides where transition metals play structural and functional role.

## EXPERIMENTAL SECTION

### General Procedure

$^1\text{H}$  NMR spectra were obtained at 300 MHz on a Nicolet NT-300 or Varian VXR-300 and  $^{13}\text{C}$  NMR spectra at 75.43 MHz on the same instruments; chemical shifts of  $^1\text{H}$  NMR spectra are reported relative to TMS in organic solvents and DSS in aqueous solutions; coupling constants (J) are in Hz.  $^{13}\text{C}$  NMR spectra are  $^1\text{H}$  decoupled; the coupling constants reported are for doublets due to  $^{31}\text{P}$ .  $^{31}\text{P}$  NMR spectra were obtained at 121.42 MHz on a Varian VXR-300, chemical shifts are reported relative to external standard  $\text{H}_3\text{PO}_4$ . Mass spectra were obtained on a Kratos MS-50. Electrospray mass spectrum was obtained on a Hewlett Packard MS engine model B. Circular Dichroism spectra were obtained with Aviv 60 D6 Circular Dichroic spectrophotometer. Fluorescence spectra were obtained with Spex Fluoromax. UV-Vis spectra were obtained with Hewlett Packard 8452A Diode Array Spectrophotometer. pH was measured with Fisher Scientific Accument pH meter 925 equipped with combined pH electrode. Melting points were determined on a Fisher-Johns melting point apparatus and were not corrected. Thin-layer chromatography (TLC) was performed on commercially prepared E. Merck silica gel 60F glass plated (0.25 mm) and flash chromatography was carried out as described by Still et al.<sup>120</sup> with the use of E. Merck silica gel Kieselgel 60 (230-400 mesh). Elemental analyses were performed by Galbraith Laboratory.

All the chemicals were used as obtained from commercial suppliers unless otherwise noted. S-(-)-1-phenylethylamine was purified by vacuum distillation at 32-34 °C and the optical purity was checked with polarimetry. Measured;

$[\alpha]_D^{24} = -39.95^\circ$  (neat), Aldrich;  $[\alpha]_D^{20} = -39^\circ$  (neat). Pyrene was purified by sublimation after recrystallization from n-hexane. Indole was purified by sublimation. 1-Hydroxynaphthalene was purified by recrystallization after activated charcoal treatment followed by sublimation. 1,5-Dihydroxynaphthalene was purified by recrystallization from nitromethane. Indole acetic acid, indole propionic acid, indole butyric acid, tryptamine, indole-3-acetamide, N-acetyl-L-tryptophanamide, 1-naphthyl acetic acid, 2-naphthyl acetic acid, 1-naphthyl acetamide, and 2-naphthoic acid were used as obtained after purity check by TLC. Acetonitrile used for reactions was freshly distilled from  $P_4O_{10}$ . Methylene chloride, pyridine, tetrahydrofuran, and diisopropylethylamine used for reactions were freshly distilled from  $CaH_2$ . DMF was dried over activated 4A<sup>o</sup> molecular sieves. Glassware was pre-dried at  $>80^\circ C$ .

#### **4-Iodo-L-phenylalanine (16)**

L-Phenylalanine (40.14 g,  $2.43 \times 10^{-1}$  mole) was dissolved in 220 ml in HOAc and 29 ml of sulfuric acid. The solution was poured into a flask containing iodine (24.64 g,  $9.71 \times 10^{-2}$  mole) and potassium iodate (13.0 g,  $6.07 \times 10^{-3}$  mole). The mixture was heated slowly to  $80^\circ C$  and stirred at that temperature for 27 hours. TLC (MEK:HOAc:H<sub>2</sub>O 16:3:2.5, product R<sub>f</sub> = 0.54, phenylalanine R<sub>f</sub> = 0.46) showed the reaction was complete. HOAc was removed by rotary evaporation. The dark oily residue was dissolved in 400 ml of H<sub>2</sub>O. The aqueous layer was washed with 4 x 50 ml Et<sub>2</sub>O and decolorized by boiling with 5 g of Norit and filtered through Celite. Neutralization of the filtrate with conc. aqueous NH<sub>3</sub> to pH 7 caused precipitation. The precipitate was collected by vacuum filtration, and washed with cold water and EtOH. Purification was achieved by

recrystallization from AcOH (300 ml) to yield 4-iodo-L-phenylalanine (32.3 g, 45%) mp 254-255 °C literature: 251°C (Aldrich). <sup>1</sup>H NMR (D<sub>2</sub>O/DCl) δ (ppm) 7.82 (d, J = 8.1, 2H), 7.15 (d, J = 8.1, 2H), 4.43 (t, J = 6.2, 1H), 3.36(dd, J = 5.8, 14.7, 1H), 3.25 (dd, J = 7.5, 14.4, 1H).

#### **4-Iodo-L-phenylalanine methyl ester hydrochloride (17)**

Thionyl chloride (12 ml, 0.164 mole) was added slowly with stirring to 10 ml of MeOH at <0 °C . This mixture was added to the 40 ml of MeOH solution of p-iodophenylalanine (9.52 g, 0.033 mole) at 0 °C and the resulting mixture was stirred for 22 hours at room temperature. TLC (2-butanone: acetic acid: water 12:3:2.5, product R<sub>f</sub> = 0.79, starting material R<sub>f</sub> = 0.62) showed the reaction to be complete. After all liquids were evaporated, 70 ml of hot EtOH was added. By cooling to 0 °C, white solid crystallized out and it was collected. More product was collected from the filtrate by crystallization from EtOH and ether mixture (25 ml: 50 ml). The purified yield was 9.42 g (84%). mp 190-191 °C; <sup>1</sup>H NMR (CD<sub>3</sub>OD) δ (ppm) 7.72 (d, J = 8.2, 2H), 7.05 (d, J = 8.2, 2H), 4.31 (t, J = 6.8, 1H), 3.81 (s, 3H), 3.22 (dd, J = 14.4, 6.3, 1H), 3.13 (dd, J = 11.4, 7.2, 1H), Anal. Cal'd for C<sub>10</sub>H<sub>13</sub>ClINO<sub>2</sub>: C, 35.16; H, 3.84; N, 4.10. Found: C, 35.17; H, 3.88; N, 4.15.

#### **N-t-Boc-4-iodo-L-phenylalanine methyl ester (18)**

To 4-iodo-L-phenylalanine methyl ester hydrochloride (20.0 g, 5.86 x 10<sup>-2</sup> mole) and NaHCO<sub>3</sub> (1.76 x 10<sup>-1</sup> mole) in 100 ml of MeOH was added di-t-butylidicarbonate (17.0 g, 7.79 x 10<sup>-2</sup> mole). The mixture was stirred at room temperature for 5 hours. The white precipitate formed during stirring was filtered out and MeOH was removed by rotary evaporator. The residue was dissolved in

150 ml of EtOAc and washed with 2 x 50 ml of H<sub>2</sub>O , 2 x 30 ml 0.5 M citric acid, and 2 x 50 ml sat'd NaCl solution. The EtOAc layer was dried over Na<sub>2</sub>SO<sub>4</sub>, and EtOAc was removed by reduced pressure. The crude product was purified by recrystallization (CH<sub>2</sub>Cl<sub>2</sub>: n-hexane 10 ml : 100 ml). Product was obtained as white crystal (20.06 g, 82%). mp 74-76 °C; <sup>1</sup>H NMR ( CDCl<sub>3</sub>) δ (ppm) 7.61 (d, J = 8.2, 2H), 6.87 (d, J = 8.2, 2H), 5.04-4.95 (m, 1H), 4.61-4.52 (m, 1H), 3.72 (s, 3H), 3.08 (q, J = 5.7, 13.8, 1H), 2.98 (q, J = 5.7, 14.1, 1H), 1.42 (s, 9H).

**4,4'-(Methoxyphosphinylidene)bis{[N-(1,1-dimethylethoxy) carbonyl]-L-phenylalanine methyl ester} (19)**

Anhydrous crystalline phosphinic acid (1.0268 g,  $1.55 \times 10^{-2}$  mole), prepared by rotary evaporation of 50% aqueous phosphinic acid and drying under vacuum, was weighed carefully and mixed with trimethyl orthoformate (8.3 g,  $7.9 \times 10^{-2}$  mole) in a flask under N<sub>2</sub>. The mixture was stirred at room temperature under N<sub>2</sub> for one hour whereupon the formation of methyl phosphinate was complete. (S)-N-t-Boc-4-iodophenylalanine methyl ester (2.3257 g,  $5.5 \times 10^{-3}$  mole), bis(triphenyl phosphine)palladium chloride (0.3486 g,  $2.85 \times 10^{-4}$  mole) and propylene oxide (2.0 ml,  $2.9 \times 10^{-2}$  mole) were placed in a flask and were dissolved in 20 ml freshly distilled CH<sub>3</sub>CN. Methyl phosphinate solution was added by syringe. The reaction mixture was heated to reflux in a ~75 °C oil bath for 2 hours. CH<sub>3</sub>CN was removed by rotary evaporation. The residue was diluted with 50 ml of EtOAc and washed with sat. NaHCO<sub>3</sub> and H<sub>2</sub>O. The EtOAc layer was dried over Na<sub>2</sub>SO<sub>4</sub> and the solvent was removed under reduced pressure. The dark brown residue was redissolved into 20 ml of CH<sub>3</sub>CN and (S)-N-t-Boc-p-iodophenylalanine methyl ester (2.4536 g,  $5.8 \times 10^{-3}$  mole), bis(triphenyl phosphine)palladium chloride

(0.3350 g,  $2.73 \times 10^{-4}$  mole) and propylene oxide (2.4 ml,  $3.4 \times 10^{-2}$  mole) were added. The reaction mixture was refluxed for 5 hours and  $\text{CH}_3\text{CN}$  was removed by rotary evaporator. The crude product was purified by silica gel flash chromatography (1st flash with EtOAc, product  $R_f = 0.52$ , after 1st flash, the EtOAc layer was decolorized by boiling with norit and the filtrate was used for 2nd flash; 2nd flash with  $\text{CH}_2\text{Cl}_2/\text{CH}_3\text{CN}$ , 2:1, product  $R_f = 0.26$ ). The major impurity 22 has very close  $R_f$  values with both eluting solvents. It could be distinguished by  $^1\text{H}$  NMR of  $\text{CH}_3\text{O-P}$  protons: doublet at 3.75 ppm ( $J = 11$  Hz) and  $^{31}\text{P}$  NMR: 21.91 ppm. The purified product was obtained in 60% yield (2.09g) as a white solid. mp 74-76 °C;  $^1\text{H}$  NMR ( $\text{CDCl}_3$ )  $\delta$  (ppm) 7.72 (dd,  $J = 8.1, 12.0$ , 4H), 7.23 (dd,  $J = 2.7, 8.1$ , 4H), 4.99-4.97 (m, 2H), 4.61-4.59 (m, 2H), 3.74 (d,  $J = 11.1$ , 3H), 3.71 (s, 6H), 3.18-3.02 (m, 4H), 1.40 (s, 18H);  $^{31}\text{P}$  NMR ( $\text{CDCl}_3$ )  $\delta$  (ppm) 33.51.

#### **4,4'-(Hydroxyphosphinylidene) bis-L-phenylalanine (PBP) (20)**

Hydrobromic acid (15 ml) was added to the 4,4'-(methoxy phosphinylidene)bis([N-(1,1-dimethylethoxy)carbonyl]-L-phenylalanine methyl ester) (2.1 g,  $3.3 \times 10^{-3}$  mole) and the resulting solution was refluxed for 3 hours. 80 ml of water was added to the reaction mixture and the aqueous layer was washed with chloroform (3 x 30 ml). All liquids were removed by rotary evaporator and the residue was redissolved in 5 ml of water. After the solution was neutralized with 1 M LiOH, the product was purified by fractional precipitation using water:acetone (7:4.5) mixture. Addition of acetone (4.5 ml) to 7 ml of aqueous solution of the product caused the precipitation of white solid. The white precipitate was separated by centrifuge and was subjected to repeated dissolution in  $\text{H}_2\text{O}$  and precipitation with acetone. This procedure was repeated until only one



peak could be seen in  $^{31}\text{P}$  NMR spectrum ( $\delta$  of pure PBP = 23.82 ppm,  $\delta$  of impurity = 13.73 ppm in  $\text{D}_2\text{O}$ ). At least 5 successive precipitations were needed to obtain analytically pure PBP. mp : decomp.>300 °C.  $^1\text{H}$  NMR ( $\text{D}_2\text{O}$ )  $\delta$  (ppm) 7.50 (q,  $J = 8.4, 3.3, 8.4, 4\text{H}$ ), 7.20 (q,  $J = 2.4, 5.7, 2.7, 4\text{H}$ ), 3.82 (q,  $J = 5.4, 3.3, 5.1, 2\text{H}$ ), 3.05 (dq,  $J = 4.8, 9.9, 4.8, 8.1, 6.3, 8.4, 4\text{H}$ );  $^{13}\text{C}$  NMR ( $\text{D}_2\text{O}$ )  $\delta$  (ppm) 170.08, 134.36 (d,  $J = 10.8$ ), 132.63 (d,  $J = 528$ ), 127.68 (d,  $J = 40.5$ ), 125.58 (d,  $J = 49.2$ ), 52.17, 32.59;  $^{31}\text{P}$  NMR ( $\text{D}_2\text{O}$ )  $\delta$  (ppm) 23.82; Anal. Calc'd for  $\text{C}_{18}\text{H}_{28}\text{N}_2\text{P}_1\text{O}_{10}\text{Li}$  (PBP·Li·4 $\text{H}_2\text{O}$ ): C, 46.17; H, 5.79; N, 5.96. Found: C, 45.96, H, 6.07; N, 5.95.

**Bis-[(4,4'-(Hydroxyphosphinylidene) bis-L-phenylalanine)  
cobalt (II)] (Co<sub>2</sub>PBP<sub>2</sub>)**

Macrocycle Co<sub>2</sub>PBP<sub>2</sub> was produced by adding an equivalent or 10-20 % smaller amount of Co<sup>2+</sup> to the PBP solution in pH 9.1 borate buffer. Potentiometric titration results show that most of the added Co<sup>2+</sup> and PBP are present as a [Co<sub>2</sub>PBP<sub>2</sub>(OH)]<sup>-3</sup> form at solution pH 9.1 (Figure 13). Co<sub>2</sub>PBP<sub>2</sub> was made in situ and used for binding studies without isolation.  $^1\text{H}$  NMR (1.0 x 10<sup>-2</sup> M Na<sub>2</sub>B<sub>4</sub>O<sub>7</sub> in  $\text{D}_2\text{O}$ , Figure 20)  $\delta$  (ppm) 121 (s, 4H), 16 (s, 8H), 9.1 (s, 8H), 8.1 (s, 8H);  $\mu_{\text{eff}} = 6.6 \pm 0.57$  B.M.; Fluorescence (1.0 x 10<sup>-1</sup> M pH 9.1 borate buffer, Figure 17)  $\lambda_{\text{em}} = 457$  nm at  $\lambda_{\text{ex}} = 372$  nm.; mass (negative ion electrospray) m/z 448.3 ({Co<sub>2</sub>PBP<sub>2</sub>}<sup>-2</sup>).

**Transport Measurements.**

All measurements were conducted at  $25 \pm 1$  °C using an H-shaped tube (Figure 1) originally designed by Murakami et al.<sup>79</sup> H-shaped tubes were held

in equivalent positions relative to a magnetic stirring motor in all measurements.

One sidearm of the tube was filled with  $1.0 \times 10^{-2} \text{M}$  solution of a guest in 3.0 mL of iso-octane as a source phase (phase I). The other sidearm of the tube was filled with 3.0 mL of pure iso-octane as a receiving phase (phase III). The amount of transported guest was monitored by measuring the concentration of guest in the receiving phase by electronic absorption spectroscopy. The two organic phases were separated by a 5.0 mL aqueous phase containing PBP or metal salt at the bottom of the tube (phase II).

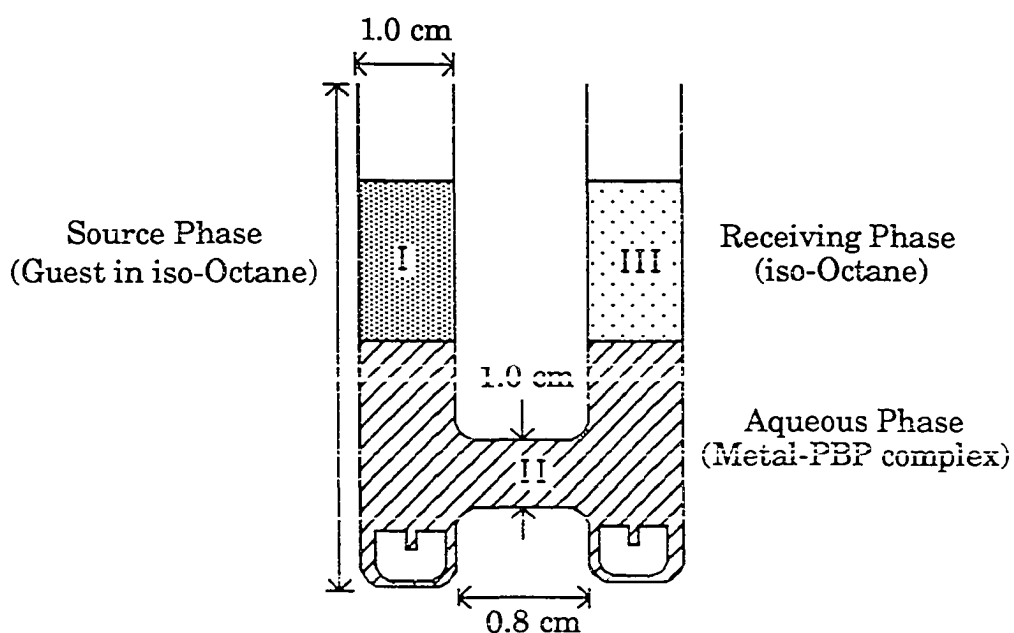


Figure 1. H-Shaped tube used for transport experiments.

After the background transport rate was measured, metal salt or PBP was added to the aqueous phase, containing PBP or metal salt, to provide the facilitated transport rate. The aqueous phase was agitated with cylindrical magnetic stirring bars which have a cross-groove at one face, at a stirring rate which retains clear separation of the two organic phases. Aqueous phase was either nanopure water or pH 9.1 borate buffer at 0.1 M. PBP solution was prepared by dissolving PBP Li salt and converting it to a trianion with 2 equivalents of LiOH.

Points in Job's plot was obtained from 3 sets of transport experiments where each set had 4 different compositions. Each of these sets of experiments included one run at a 1:1 mole ratio. Because experimental variables such as stirring rate were constant within a set, but not between sets, the data were adjusted by multiplying the rates determined by a constant to give these replicate runs the same value.

### **Potentiometric titrations**

Potentiometric titrations were carried out following Martell's experimental procedure.<sup>81</sup> The reaction solution was made up and studied in a cell equipped with a magnetic stirrer and electrode. The temperature was controlled to  $25.0 \pm 0.1$  °C by circulation of thermostatted water through the jacket which was enclosing the cell. The solution was completely sealed from the atmosphere and O<sub>2</sub> and CO<sub>2</sub> had been removed by flushing the inert gas (Ar) which was humidified by bubbling through a 0.1M KCl solution. The standard base was added by syringe while keeping the tip of the needle beneath the surface of the solution. pH measurements were carried out with the pH meter equipped with

combination glass electrode. pH meter readings were corrected to p[H] by a calibration curve ( plot of p[H] vs pH meter reading ) which was obtained from titration of standard acid in 0.1 M KCl solution with 0.104 M KOH solution. All solutions were made with nanopure water which was made carbonate-free by boiling 2 hours followed by N<sub>2</sub> bubbling for more than 4 hours. The measured carbonate content by Gran's plot was less than 2.4 % which was closed to the recommended upper limit (~ 2 %).<sup>95</sup> The ionic strength of the solution was adjusted to 0.1 M with 1.0 M KCl solution while considering the contribution of the metal salt and the ligands to the ionic strength through the use of the ionic strength formula  $\mu = 1/2 \sum m_i z_i^2$  (  $m_i$  = concentration of ionic species,  $z_i$  = charge of ionic species).

Titration were carried out by adding standard base to the gently stirred acidic solution of ligand or ligand metal mixture. The increment of added base was sufficiently small to provide more than 50 experimental points for each run. The resulting p[H] profiles were used for the computer calculation of protonation constants and stability constants. The computer calculations were performed with program "BEST" whose basic algorithm could be stated in term of equation (10).<sup>96</sup>

$$T_i = \sum_{j=i}^{NS} e_{ij} \beta_j \prod_{k=i}^i [C_k]^{c_{kj}} \quad (10)$$

where  $T_i$ : total concentration of components, NS: all species present,  $e_{ij}$ : stoichiometric coefficient,  $\beta_j$ : overall stability constant,  $[C_k]$ : individual component concentration.

$K'_2$  value for calculation of stability constants was approximated from the reported stability constant of Co(Phe)<sub>2</sub> complex.  $K_2$  value of Co(Phe)<sub>2</sub> complex at  $\mu = 0.1$  M is calculated by using equation (19) because only available data are at

0.05 and 3.0 M ionic strength.<sup>122</sup> Activity coefficient value of 3.0 M NaClO<sub>4</sub> solution is estimated by averaging the values from the extrapolation of those of KCl and NaClO<sub>4</sub> solution.<sup>123</sup>

$$K_{\mu} = \frac{K_0}{\gamma_{\pm}^2} \quad (19)$$

where  $K_0$  = stability constant at 1.0 activity coefficient, and  $\gamma_{\pm}$  = activity coefficient.

Protonation constants of H<sub>4</sub>PBP<sup>-1</sup> were determined first and those values were used for calculation of stability constants of Co<sub>2</sub>PBP<sub>2</sub>. The p[H] profile for the calculation of stability constants were obtained by titrating the mixture of Co<sup>2+</sup> and H<sub>4</sub>PBP<sup>-1</sup> ( 1 : 1.25 ) with 0.104M KOH solution. Concentrations of H<sub>4</sub>PBP<sup>-1</sup> were kept below 5 x 10<sup>-3</sup> M to rule out the formation of undesired complex at higher concentration.

The estimated log K<sub>2</sub> value was 3.63 ± 0.20. This value was used for log K'<sub>2</sub> and it is forced to be constant throughout the refinement. The refinement was performed in following steps: i) use two constraints which were described above, ii) refined EM with equations (16, 17, 18), iii) refined K<sub>1</sub> with equations (6, 7, 9, 12, 13, 14) while K<sub>2</sub> value was kept constant, iv) refined K<sub>1</sub> and EM together with equations (6, 7, 9, 12, 13, 14, 16, 17, 18) while K<sub>2</sub> value was kept constant.

### **<sup>1</sup>H NMR titrations**

<sup>1</sup>H NMR titrations were performed on a VXR 300 MHz at temperature of 20.0 ± 0.5 °C. 0.2 M borated buffer in D<sub>2</sub>O was prepared using anhydrous Na<sub>2</sub>B<sub>4</sub>O<sub>7</sub>. All volumes were measured by microsyringes. In each titration, the host concentration was kept constant by adding host and guest mixture to the same concentration of host solution in NMR tube except one reverse titration

where the guest concentration was kept constant and the concentration of host was changed. After addition of the appropriate amount, the mixture was mixed thoroughly by inverting 10 times followed by mixing with Vortex-genie. Concentrations of host  $\text{Co}_2\text{PBP}_2$  were between  $3 \times 10^{-3}$  M and  $3 \times 10^{-4}$  M to maintain the probability of binding to the optimal range ( $0.2 < p < 0.8$ ).<sup>96</sup> For the titration of naphthyl-1,5-dioxy diacetate **45**, the high binding affinity requires less than  $10^{-4}$  M concentration. However, the fact that the macrocycle  $\text{Co}_2\text{PBP}_2$  starts to dissociate below  $2 \times 10^{-4}$  M prevents the use of  $\text{Co}_2\text{PBP}_2$  concentration less than that. Therefore, the dissociation constant of **45** was calculated by averaging the results of 3 repeated titration with  $\text{Co}_2\text{PBP}_2$  concentrations slightly above the low limit to reduce the possible error which might occur from the fact that the dissociation constant calculated from the titration result with high probability of binding values can cause error. The dissociation constants were determined using a computer-assisted non-linear least-squares curve-fitting procedure described in RESULTS AND DISCUSSION section.

#### **1-Naphthyl 2-picoyl ether (46)**

1-Naphthol (0.1895 g,  $1.314 \times 10^{-3}$  mole) and 2-picoyl chloride (HCl salt, 0.2822 g,  $1.720 \times 10^{-3}$  mole) were mixed with excess  $\text{K}_2\text{CO}_3$  (0.8126 g,  $5.88 \times 10^{-3}$  mole) in 3 ml of DMF. The mixture was stirred at room temperature for 10 hours. After DMF was removed in vacuo, 50 ml of EtOAc was added and EtOAc layer was washed with sat.  $\text{NaHCO}_3$  solution (10 ml), 0.05 M  $\text{H}_3\text{PO}_4$  solution (3 x 10 ml), and sat.  $\text{NaHCO}_3$  solution (3 x 10 ml). Product was purified by flash chromatography ( $\text{CH}_2\text{Cl}_2$  : EtOAc 20:1,  $R_f = 0.31$ ). Purified yield was 0.101 g (33 %). mp = 43-44 °C;  $^1\text{H}$  NMR ( $\text{CDCl}_3$ )  $\delta$  (ppm) 8.55 (d, J = 4.8, 1H), 8.38 (t, J = 4.8,

1H), 7.75 (t,  $J = 4.5$ , 1H), 7.65-7.35 (m, 5H), 7.28 (t,  $J = 8.0$ , 1H), 7.10 (m, 1H), 6.8 (d,  $J = 7.4$ , 1H), 5.34 (s, 2H).

### **1-Naphthyl 2-picolinate (47)**

1-Naphthol (0.2114 g,  $1.47 \times 10^{-3}$  mole), 2-picolinic acid (0.2741 g,  $2.23 \times 10^{-3}$  mole), and N-hydroxybenzotriazole (0.3158 g,  $2.34 \times 10^{-3}$  mole) were mixed with THF (15 ml). To the mixture was added N,N-dimethylaminopropyl ethyl carbodiimide (0.4397 g,  $2.29 \times 10^{-3}$  mole) at 0 °C. After 1 hour stirring at 0 °C, it was stirred an additional 12 hours at room temperature under N<sub>2</sub> atmosphere. Et<sub>2</sub>O (20 ml) was added after all THF had been removed. Et<sub>2</sub>O layer was washed with water (10 ml), sat. NaHCO<sub>3</sub> solution (10 ml), and sat. NaCl solution (10 ml) followed by drying over anhydrous Na<sub>2</sub>SO<sub>4</sub>. Flash chromatography purification using Et<sub>2</sub>O ( $R_f = 0.66$ ) gave 0.0719 g of purified product (20 %). mp = 99-101°C; <sup>1</sup>H NMR (CDCl<sub>3</sub>)  $\delta$  (ppm) 8.85 (d,  $J = 4.4$ , 1H), 8.31 (d,  $J = 4.2$ , 1H), 7.97 (t,  $J = 4.8$ , 1H), 7.9-7.8 (m, 2H), 7.76 (d,  $J = 8.1$ , 1H), 7.55-7.35 (m, 5H).

### **(R)-2-(1-Naphthoxy) propionic acid (48)**

Prepared according to the general procedure of Heumann et al.<sup>124</sup> To the THF (15 ml) solution of (S)-ethyl lactate (1.1898 g,  $1.01 \times 10^{-2}$  mole), 1-naphthol (1.4435 g,  $1.00 \times 10^{-2}$  mole), and triphenylphosphine (2.6310 g,  $1.00 \times 10^{-2}$  mole) was added diethyl azodicarboxylate (DEAD, 1.7615 g,  $1.01 \times 10^{-2}$  mole) in THF (7 ml). The mixture was stirred for 21 hours at room temperature under N<sub>2</sub> atmosphere. Hydrolysis of the ester was performed without purification. 2 M NaOH solution (10 ml) was added to the MeOH solution (40 ml) of crude product and stirring for 4 hours. After MeOH was evaporated, water (10 ml) was added

and the aqueous solution was washed with diethyl ether (3 x 10 ml).

Neutralization of the aqueous solution with conc. HCl at 0 °C was followed by the product extraction with diethyl ether (3 x 10 ml). The product was purified by recrystallization from n-Hexane (100 ml). Purified yield was 0.3875 g (18 %) with >96 % ee. mp = 152-154 °C; TLC; organic layer of n-BuOH: H<sub>2</sub>O: AcOH (5:4:1), product R<sub>f</sub> = 0.84. <sup>1</sup>H NMR (CDCl<sub>3</sub>) δ (ppm) 9.597 (b, 1H), 8.315 (m 1H), 7.783 (m, 1H), 7.475 (m, 4H), 7.285 (t, J = 7.8, 8.1, 1H), 6.702 (d, J = 7.5, 1H), 4.950 (q, J = 6.9, 6.6, 6.9, 1H), 1.725 (d, J = 6.9, 3H).

#### **(S)-2-(1-Naphthoxy) propionic acid (49)**

Synthesized from (R)-ethyl lactate (0.6147 g, 5.20 x 10<sup>-3</sup> mole) using same procedure with the synthesis of (R)-isomer (48). Purified yield was 0.3682 g (34 %) with >98 % ee.

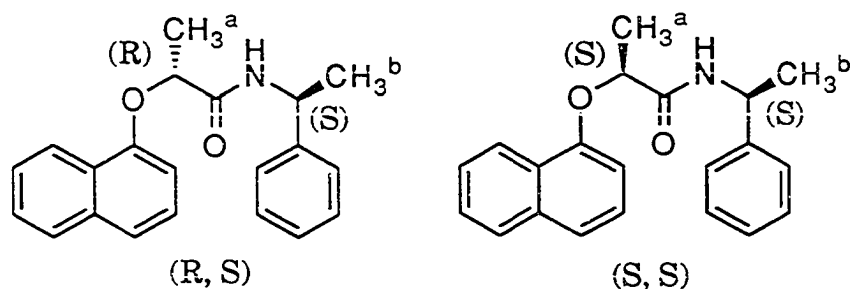
#### **Determination of optical purity**

Optical purity of the (R) or (S) 2-(1-naphthoxy) propionic acid was determined by integration of methyl protons in <sup>1</sup>H NMR and GC after the derivatization to diastereomers by amidation with S-(-)-1-phenylethylamine.

**Synthesis of amide** (S)-1-Phenylethylamine (0.0081 g, 6.7 x 10<sup>-5</sup> mole), 2-(1-naphthoxy) propionic acid (0.0050 g, 2.3 x 10<sup>-5</sup> mole), and N-hydroxybenzotriazole (0.0115 g, 8.5 x 10<sup>-5</sup> mole) were mixed with THF (2 ml). To the mixture was added N,N-dimethylaminopropyl ethyl carbodiimide (0.0160 g, 8.3 x 10<sup>-5</sup> mole) at 0 °C. After 1 hour stirring at 0 °C, it was stirred an additional 12 hours at room temperature (even though TLC check showed that most of the



coupling was done within 2 hours, the reaction mixture was stirred 10 hours more to make sure all the 2-(1-naphthoxy) propionic acid had reacted. TLC: EtOAc only, product  $R_f = 0.96$ , 2-(1-naphthoxy) propionic acid  $R_f = 0.36$ . EtOAc (20 ml) was added after all THF had been removed. EtOAc layer was washed with sat.  $\text{NaHCO}_3$  solution (2 x 10 ml), 0.15 M citric acid solution (2 x 10 ml), and sat.  $\text{NaHCO}_3$  solution (10 ml) followed by drying over anhydrous  $\text{Na}_2\text{SO}_4$ . Diastereomeric ratio was determined after EtOAc had been removed in vacuo.



N-(S)-1-phenylethyl (R or S)-2-(1-naphthoxy)propionyl amide

$^1\text{H NMR}$  ( $\text{CDCl}_3$ )  $\delta$  (ppm): (R, S) isomer  $\text{H}^a$ : 1.69 (d,  $J = 6.6$ ),  $\text{H}^b$ : 1.33 (d,  $J = 6.9$ )  
 (S, S) isomer  $\text{H}^a$ : 1.74 (d,  $J = 6.6$ ),  $\text{H}^b$ : 1.47 (d,  $J = 6.9$ )

### Ethyl 1-(5-hydroxy)naphthoxy acetate (50)

1,5-Dihydroxynaphthalene (0.8082 g,  $5.05 \times 10^{-3}$  mole) and ethyl bromoacetate (0.908 g,  $5.44 \times 10^{-3}$  mole) were mixed with  $\text{K}_2\text{CO}_3$  (0.7551 g,  $5.46 \times 10^{-3}$  mole) in 5 ml of DMF. The mixture was stirred at room temperature for 6 days. After DMF was removed in vacuo, 60 ml of EtOAc was added and EtOAc layer was washed with acidic water (pH = 2 with HCl, 3 x 10 ml). Product was purified by recrystallization from  $\text{CH}_3\text{CN}$  after treated with activated charcoal.

Purified yield was 0.082 g (7 %). mp = 182-184 °C;  $^1\text{H}$  NMR ( $\text{CDCl}_3 / \text{CD}_3\text{OD}$ )  $\delta$  (ppm) 7.85 (t,  $J = 7.7$ , 2H), 7.31 (t,  $J = 7.3$ , 2H), 6.89 (d,  $J = 7.4$ , 1H), 6.74 (d,  $J = 7.7$ , 1H), 4.82 (s, 2H), 4.31 (q,  $J = 7.2$ , 14.1, 2H), 1.33 (t,  $J = 7.2$ , 3H).

#### **(1-Naphthyl)methyl picolinate hydrochloride salt (51)**

1-Naphthylmethanol (0.3479 g,  $2.20 \times 10^{-3}$  mole), 2-picolinic acid (0.4833 g,  $3.93 \times 10^{-3}$  mole), and N-hydroxybenzotriazole (0.5129 g,  $3.80 \times 10^{-3}$  mole) were mixed with THF (15 ml). To the mixture was added N,N-dimethylaminopropyl ethyl carbodiimide (0.7459 g,  $3.89 \times 10^{-3}$  mole) at 0 °C. After 1 hour stirring at 0 °C, it was stirred additional 24 hours at room temperature under  $\text{N}_2$  atmosphere. EtOAc (20 ml) was added after all THF had been removed. EtOAc layer was washed with water (10 ml), sat.  $\text{NaHCO}_3$  solution (10 ml), and sat.  $\text{NaCl}$  solution (10 ml) followed by drying over anhydrous  $\text{Na}_2\text{SO}_4$ . Flash chromatography purification using  $\text{Et}_2\text{O}$  ( $R_f = 0.35$ ) gave 0.1289 g of purified product (20 %). mp = 182-184 °C;  $^1\text{H}$  NMR ( $\text{CDCl}_3$ )  $\delta$  (ppm) 8.70 (d,  $J = 4.4$ , 1H), 8.10 (d,  $J = 8.2$ , 1H), 8.02 (d,  $J = 7.8$ , 1H), 7.83 (t,  $J = 7.3$ , 2H), 7.73-7.60 (m, 2H), 7.57-7.28 (m, 4H), 5.89 (s, 2H).

#### **Dansyl amide (58)**

Dansyl amide was synthesized following reported procedure of amidation of dansyl chloride<sup>104</sup> and used after identification by  $^1\text{H}$  NMR and mp (220-221 °C, literature; 215 °C).  $^1\text{H}$  NMR ( $\text{CDCl}_3/\text{CD}_3\text{CN}$ )  $\delta$  (ppm) 8.53 (d,  $J = 8.3$ , 1H), 8.24 (m, 2H), 7.57 (m, 2H), 7.21 (d,  $J = 8.2$ , 1H), 5.43 (s, 2H), 2.89 (s, 6H).

## REFERENCES

1. Cram, D. J. *Angew. Chem. Int. Ed. Engl.* **1986**, *25*, 1039.
2. Lehn, J. -M. *Angew. Chem., Int. Ed. Engl.* **1988**, *27*, 89-112.
3. *Topics in Current Chemistry*, Springer Verlag, Heidelberg, **1981**, *98*; **1982**, *101*; **1984**, *121*; **1985**, *128*; **1986**, *132*, **1987**, *140*; **1988**, *149*, **1993**, *165*.
4. Dugas, H. *Bioorganic Chemistry*, Heidelberg, Springer Verlag, **1989**.
5. Diederich, F. *Cyclophanes*, The Royal Society of Chemistry, Cambridge, **1991**.
6. Schneider, H., -J.; Durr, H. Eds. *Frontiers in Supramolecular Organic Chemistry and Photochemistry*, VCH, Weinheim, **1991**.
7. Roberts, S. M. Eds. *Molecular recognition: chemical and biochemical problems II*, Royal society of chemistry, Cambridge, **1992**.
8. Webb, T, H.; Wilcox, C. S. *Chemical Society Reviews*, **1993**, 383-395.
9. Cramer, F., *Einschlussverbindungen*, Springer-Verlag, Berlin, **1954**.
10. Bender, M., L.; Komiyama, M., *Cyclodextrin Chemistry*, Springer-Verlag, Berlin, **1978**.
11. D'Souza, V. T.; Bender, M. L. *Acc. Chem. Res.* **1987**, *20*, 146.
12. Breslow, R.; Overman, L. E. *J. Amer. Chem. Soc.* **1970**, *92*, 1075-1077.
13. Breslow, R.; Doherty, J. B.; Guillot, G.; Lipsey, C. *J. Amer. Chem. Soc.* **1978**, *100*, 3227-3229.
14. Breslow, R. *Acc. Chem. Res.* **1991**, *24*, 317-323.
15. Zhang, B.; Breslow, R. *J. Amer. Chem. Soc.* **1993**, *115*, 9353-9354.
16. Tabushi, I.; Shimokawa, K.; Fujita, K. *Tetrahedron Lett.* **1977**, 1527-1530.

17. Tabushi, I.; Kuroda, Y.; Mochizuki, A. *J. Amer. Chem. Soc.* **1980**, *102*, 1152-1153.
18. Tabushi, I. *Acc. Chem. Res.* **1982**, *15*, 66.
19. Bender, M. L.; Komiyama, M. *Cyclodextrin Chemistry*, Springer, New York, **1978**.
20. Saenger, W. in Atwood, J. L.; Davies, E. D.; Macnicol, D. (Eds.) *Inclusion Compounds*, Vol. 2., Academic press, London, **1984**, p. 231.
21. Bergeron, R. J. in Atwood, J. L.; Davies, E. D.; Macnicol, D. (Eds.) *Inclusion Compounds*, Vol. 3., Academic press, London, **1984**, p. 391.
22. Lipkowitz, K. B.; Raghothama, S.; Yang, J. -A. *J. Amer. Chem. Soc.* **1992**, *114*, 1554-1562.
23. Pedersen, C. J. *J. Amer. Chem. Soc.* **1967**, *89*, 2495, 7017.
24. Pedersen, C. J.; Frensdorff, H. K. *Angew. Chem., Int. Ed. Engl.* **1972**, *16*, 16.
25. Lehn, J. -M. *Acc. Chem. Res.* **1978**, *11*, 49.
26. Hamilton, A.; Lehn, J. -M.; Seesler, J. L. *J. Amer. Chem. Soc.* **1986**, *108*, 5158.
27. Hosseini, M. W.; Lehn, J. -M.; Maggiora, L.; Mertes, K. B.; Mertes, M. P. *J. Amer. Chem. Soc.* **1987**, *109*, 537.
28. Lehn, J. -M. *Angew. Chem., Int. Ed. Engl.* **1988**, *27*, 89.
29. Fages, F.; Desvergne, J. -P.; Kampke, K.; Bousa-Laurent, H.; Lehn, J. -M.; Meyer, M.; Albrecht-Gary, A. -M. *J. Amer. Chem. Soc.* **1993**, *115*, 3658-3664.
30. Cram, D. J.; Cram, J. M. *Science* (Washington DC) **1974**, *183*, 803.
31. Cram, D. J.; Cram, J. M. *Acc. Chem. Res.* **1978**, *11*, 8.
32. Cram, D. J.; Trueblood, K. N. *Top. Curr. Chem.* **1981**, *98*, 43.
33. Cram, D. J.; Lam, P. Y.; Ho, S. P. *J. Amer. Chem. Soc.* **1986**, *108*, 839.

34. Cram, D. J. *Angew. Chem., Int. Ed. Engl.* **1986**, *25*, 1039-1134.
35. Izatt, R. M.; Paqlak, K.; Bradshaq, J. S.; Bruening, R. L. *Chem. Rev.* **1991**, *91*, 1721-2085.
36. Gokel, G. W. *Chemical Society Reviews*, **1992**, 39-47
37. Stetter, H.; Roos, E. -E. *Chem. Ber.* **1955**, *88*, 1390.
38. Hilgenfeld, R.; Saenger, W. *Angew. Chem., Int. Ed. Engl.* **1982**, *21*, 781.
39. Odashima, K.; Itai, A.; Itaka, Y.; Koga, K. J. *J. Amer. Chem. Soc.* **1980**, *102*, 2504.
40. Odashima, K.; Soga, T.; Koga, K. J. *Tetrahedron Lett.* **1981**, *22*, 5311.
41. Merz, T.; Wirtz, H.; Vogtle, F. *Angew. Chem., Int. Ed. Engl.* **1986**, *25*, 567.
42. Cowart, M. D.; Sucholeiki, I.; Bukownik, R. R.; Wilcox, C. S. *J. Amer. Chem. Soc.* **1988**, *110*, 6204.
43. Adrian, J. C.; Wilcox, C. S. *J. Amer. Chem. Soc.* **1992**, *114*, 1398-1403.
44. Petti, M. A.; Shepodd, T. J.; Barrans, R. E.; Dougherty, D. A. *J. Amer. Chem. Soc.* **1988**, *110*, 6825.
45. Kearney, P. C.; Mizouem L. S.; Kumpf, R. A.; Forman, J. E.; McCurdy, A.; Dougherty, D. A. *J. Amer. Chem. Soc.* **1993**, *115*, 9907-9919.
46. Schneider, H. -J. *Angew. Chem., Int. Ed. Engl.* **1991**, *30*, 1417-1436.
47. Diederich, F.; Dick, K. *Tetrahedron Lett.* **1982**, *23*, 3167.
48. Diederich, F. *Cyclophanes*, The Royal Society of Chemistry, Cambridge, **1991**, 246-263
49. Franck, H, S.; Evans, M. W. *J. Chem. Phys.* **1945**, *13*, 507.
50. Jorgensen, W. L.; Severance, D. L. *J. Amer. Chem. Soc.* **1990**, *112*, 4768.
51. Cochran, J. E.; Parrott, T. J.; Whitlock, B. J.; Whitlock, H. W. *J. Amer. Chem. Soc.* **1992**, *114*, 2269-2270.

52. Whitlock, B. J.; Whitlock, H. W. *J. Amer. Chem. Soc.* **1994**, *116*, 2301-2311.
53. Rebek, J. Jr.; Roberts, S. M. Eds. *Molecular recognition: chemical and biochemical problems II*, Royal society of chemistry, Cambridge, **1992**, 65-74.
54. Dixon, R. P.; Jubian, V.; Vincent, C.; Fan, E.; Garcia Tellado, F.; Hirst, S. C.; Hamilton, A. D. *ibid.* 75-82.
55. Still, C. W.; Erickson, S.; Wang, X.; Li, G.; Armstrong, A.; Hong, J. -I.; Namgoong, S. K.; Liu, R. *ibid.* 171-182.
56. Wilcox, C. S.; Adrian, J. C. Jr.; Webb, T. H.; Zaqacki, F. J. *J. Amer. Chem. Soc.* **1992**, *114*, 10189-10197.
57. Kikuchi, Y.; Tanaka, Y.; Sutarto, S.; Kobayashi, K.; Toi, H.; Aoyama, Y. *J. Amer. Chem. Soc.* **1992**, *114*, 10302-10306.
58. Huang, C. -Y.; Cabell, L. A.; Anslyn, E. V. *J. Amer. Chem. Soc.* **1994**, *116*, 2778-2792.
59. Diederich, F. *Angew. Chem., Int. Ed. Engl.* **1988**, *27*, 362-386.
60. Winkler, J.; Coutouli-Argyropoulou, E.; Leppkes, R.; Breslow, R. *J. Amer. Chem. Soc.* **1983**, *105*, 7198.
61. Schneider, H. -J.; Sangwan, N. K. *J. Chem. Soc. Chem. Commun.* **1986**, 1787.
62. Murakami, Y.; Hisaeda, Y.; Kikuchi, J.; Ohno, T.; Suzuki, M.; Matsuda, Y.; Matsuuram T. *J. Chem. Soc. Perkin Trans. 2.* **1988**, 1237.
63. Parraga, G.; Horvath, S. J.; Eisen, A.; Taylor, W. E.; Hood, L.; Young, E. T.; Klevit, R. E. *Science*, 1988, 241, 1489.
64. Van Staveren, C. J.; Fentor, D. E.; Reinhoudt, D. N.; Van Eerden, J.; Harkema, S. *J. Amer. Chem. Soc.* **1987**, *109*, 3456.

65. Van Staveren, C. J.; Van Eerden, J.; Van Veggel, F. C. J. M.; Markema, S.; Reinhoudt, D. N. *J. Amer. Chem. Soc.* **1988**, *110*, 4994.
66. Nijenhuis, W. F.; Van Doorn, A. R.; Reichwein, A. M.; De Jong, F.; Reinhoudt, D. N. *J. Amer. Chem. Soc.* **1991**, *113*, 3607.
67. Rudkevich, D. M.; Verboom, W.; Brzozka, Z.; Palys, M. J.; Stauthamer, W. P. R. V.; van Hummer, G. J.; Franken, S. M.; Harkema, S.; Engbersen, J. F. J.; Reinhoudt, D. N. *J. Amer. Chem. Soc.* **1994**, *116*, 4341-4351.
68. Maverick, A. W.; Buckingham, S. C.; Yao, Q. J.; Bradbury, J. R.; Stanley, G. C. *J. Amer. Chem. Soc.* **1986**, *108*, 7403-7431.
69. Maverick, A. W.; Ivie, M. L.; Waggenpack, J. H.; Fronczek, F. R. *Inorg. Chem.* **1990**, *29*, 2403-2409.
70. Fujita, M.; Yazaki, J.; Ogura, K. *J. Amer. Chem. Soc.* **1990**, *112*, 5645-5647.
71. Fujita, M.; Yazaki, J.; Ogura, K. *Tetrahedron Lett.* **1991**, *32*, 5589-5592.
72. Schneider, H. -J.; Ruf, D. *Angew. Chem., Int. Ed. Engl.* **1990**, *29*, 1159-1160.
73. Cole, K.; Farran, M. A.; Deshayes, K. *Tetrahedron Lett.* **1992**, *33*, 599-602.
74. (a) Mathias, J. P.; Seto, C. T.; Zerkowski, J. A.; Whitesides, G. M.; Roberts, S. M. Eds. *Molecular recognition: chemical and biochemical problems II*, Royal society of chemistry, Cambridge, **1992**, 35-49. (b) Ashton, P. R.; Philp, D.; Spencer, N.; Stoddart, F. J. *ibid.*, 75-63.
75. (a) Ghadiri, M. R.; Choi, C. *J. Amer. Chem. Soc.* **1990**, *112*, 1630-1632. (b) Ghadiri, M. R.; Fernholz, A. K. *J. Amer. Chem. Soc.* **1990**, *112*, 9633-9635.
76. Handel, T.; DeGrado, W. F. *J. Amer. Chem. Soc.* **1990**, *112*, 6710-6711.
77. Ruan, F.; Chen, Y.; Hopkins, P. B. *J. Amer. Chem. Soc.* **1990**, *112*, 9403-9404.

78. Lieberman, M.; Sasaki, T. *J. Amer. Chem. Soc.* **1991**, *113*, 1470-1471.
79. (a) Schepartz, A.; McDevitt, J. P. *J. Amer. Chem. Soc.* **1989**, *111*, 5977-5978. (b) Jones, M. W.; Gupta, N.; Schepartz, A.; Thrope, H. H. *Inorg. Chem.* **1992**, *31*, 1308-1310.
80. Baxter, P.; Lehn, J. -M.; DeCian, A.; Fischer, J. *Angew. Chem., Int. Ed. Engl.* **1993**, *32*, 69-72.
81. Wyler, R.; de Mendoza, J.; Rebek, J. Jr. *Angew. Chem., Int. Ed. Engl.* **1993**, *32*, 1699-1701.
82. Jeong, K. -S.; Tjivikua, T.; Muehldorf, A.; Deslongchamps, G.; Famuloc, M.; Rebeck, J. Jr. *J. Amer. Chem. Soc.* **1991**, *113*, 201.
83. Galan, A.; Andreu, D.; Echavarren, A. M.; Prados, P.; de Mendoza, J. *J. Amer. Chem. Soc.* **1992**, *114*, 1511-1512.
84. Takahashi, I.; Odashima, K.; Koga, K. *Tetrahedron Lett.* **1984**, *25*, 973-976.
85. Takahashi, I.; Odashima, K.; Koga, K. *Chem. Phar. Bull.* **1985**, *33*, 3571
86. Castro, P. P.; Georgiadis, T. M.; Diederich, F. *J. Org. Chem.* **1989**, *54*, 5835.
87. Lei, H.; Stoakes, M. S.; Schwabacher, A. W. *Synthesis*, **1992**, 1255-1260.
88. Lei, Grady, H. Doctoral Dissertation, Iowa State University, Iowa, USA.
89. Schwabacher, A. W.; Lee, J.; Lei, H. *J. Amer. Chem. Soc.* **1992**, *114*, 7597-7598.
90. Schwabacher, A. W.; Zhang, S.; Davy, W. *J. Amer. Chem. Soc.* **1993**, *115*, 6995-6996.
91. Gallagher, M. J.; Honegger, H. *Tetrahedron Lett.* **1977**, 2987-2990.
92. Diederich, F.; Dick, K. *J. Amer. Chem. Soc.* **1984**, *106*, 8024-8036.
93. Vogtle, F.; Muller, W. M.; Werner, U.; Losensky, H. -W. *Angew. Chem. Int. Ed. Engl.* **1987**, *26*, 901.



94. Murakami, Y.; Kikuchi, J. -I.; Ohno, T.; Hirayama, T.; Hisaeda, Y.; Nishimura, H.; Snyder, J. P.; Steliou, K. *J. Amer. Chem. Soc.* **1991**, *113*, 8229-8242.
95. Burger, K. Eds. *Biocoordination Chemistry: Coordination Equilibria in Biologically Active Systems*, Ellis Horwood, New York, **1990**.
96. Martell, A. E.; Motekaitis, R. J. *Determination and Use of Stability Constants*, 2nd Ed. VCH, New York, **1992**.
97. Martell, A.E.; Smith, R. M. *Critical Stability Constants*, Plenum Press, New York, **1974**, Vol. 1: Amino Acids.
98. Perrin, D. D. *Stability Constants of Metal-Ion Complexes*, Pergamon Press, New York, **1979**, Part B: Organic Ligands.
99. Kirby, A.J. *Adv. Phys. Org. Chem.* **1980**, *17*, 183-278.
100. Jencks, W. P. *Proc. Natl. Acad. Sci. USA* **1981**, *78*, 4046-4050.
101. Billo, E.J. *Inorg. Nucl. Chem. Lett.* **1975**, *11*, 491-496
102. Maret, W.; Zeppezauer, M. *Biochemistry.* **1986**, *25*, 1584-1588.
103. Evans, D. F. *J. Chem. Soc.* **1959**, 2003.
104. Deutsch, J.L.; Poling, S. M. *J. Chem. Educ.* **1969**, *46*, 167.
105. Loliger, J.; Scheffold, R. *J. Chem. Educ.* **1972**, *49*, 646.
106. Banci, L.; Bencini, A.; Benelli, C.; Gatteschi, D.; Zanchini, C. "Spectral-Structural Correlation in High-Spin Cobalt(II) Complexes " in *Structure and Bonding* Vol 52, Springer-Verlag, Berlin, **1982**, pp-37-86.
107. Spacu, P.; Marculescu, C.; Patron, L. *Rev. Roum. de Chimie*, **1979**, *24*, 191-195.
108. Ciampolini, M.; Nardi, N. *Inorg. Chem.* **1966**, *5*, 41.
109. Averill, D. F.; Legg, J. E.; Smith, D. L. *Inorg. Chem.* **1972**, *11*, 2344-2349.

110. McDonald, C. C.; Phillips, W. D. *J. Amer. Chem. Soc.* **1963**, *85*, 3736-3742.
111. Connors, K. A. *Binding Constants*, John Wiley & Son, New York, **1987**, pp 189-215
112. Wilcox, C. S. in Schneider, H. -J.; Durr, H. Eds. *Frontiers in Supramolecular Organic Chemistry and Photochemistry*, VCH, Weinheim, 1991, 121-143.
113. Bertini, I.; Luchinat, C. *NMR of Paramagnetic Molecules in Biological Systems*, Benjamin/Cummings, Menlo Park, **1986**.
114. Kroll, H. *J. Amer. Chem. Soc.* **1952**, *74*, 2036-2039.
115. Zimmerman, S. C. *Topics in current chemistry*, Springer-Verlag, Berlin, **1993**, Vol. 165, pp 71-102.
116. Mallik, S.; Johnson, R. D.; Arnold, F. H. *J. Amer. Chem. Soc.* **1993**, *115*, 2518-2520.
117. Sutton, P. A.; Buckingham, D. A. *Acc. Chem. Res.* **1987**, *20*, 357-364.
118. Chin, J. *Acc. Chem. Res.* **1991**, *24*, 145-152.
119. Schneider, H. -J; Schneider, U. *J Org. Chem.* **1987**, *52*, 1613-1615.
120. Still, W. C.; Kahn, M.; Mitra, A. *J Org. Chem.* **1978**, *43*, 2923.
121. Webber, G. *Biochem. J.* **1952**, *51*, 155.
122. Castellan, G. W. *Physical Chemistry*, 2nd Ed. Eddison-Wesley Reading, Massachusetts, **1971**, p301.
123. *CRC Handbook of Chemistry and Physics*, 70th Ed. The chemical Rubber Co. **1990**.
124. Heumann, A.; Faure, R. *J. Org. Chem.* **1993**, *58*, 1276-1279.

## ACKNOWLEDGMENTS

I would like to express deep appreciation to my major professor and mentor, Dr. Alan W. Schwabacher, for his enduring support and guidance in the projects which I have undertaken. Through his valuable advice, enthusiasm, and vast repertoire of scientific knowledge, he taught me a nature of scientific research.

I would also like to thank the fellow members of Dr. Schwabacher's research group, particularly to James Lane and Haiyan Lei Grady for their encouragement, friendship, and their 'being' during the completion of my projects.

I would like to express my thanks and love for my parents, siblings and my parents-in-law for their love, support and encouragement. Most importantly, I would like to thank my wife, Eunkyung. Her love, support, and patience was always there when I needed it. Finally, I would like to thank the Lord for always being there for me.